Effects of Entrained-air Size Distribution and Fly Ash on Self-compactability and Air Volumetric-stability of Fresh Concrete

by

PUTHIPAD Nipat

Student ID Number: 1196013

A dissertation submitted to the
Engineering Course, Department of Engineering,
Graduate School of Engineering,
Kochi University of Technology,
Kochi, Japan

in partial fulfillment of the requirements for the degree of
Doctor of Engineering

Assessment Committee:
      Supervisor: OUCHI Masahiro
      Co-Supervisor: TAKAGI Masataka
      Co-Supervisor: TAJIMA Masaki
      NASU Seigo
      SHIMA Hiroshi
      TANGTERMSIRIKUL Somnuk, Sirindhorn Internaltional Institute of Technology

March 2018

ABSTRACT

Self-compacting concrete (SCC) generally requires a higher proportion of cement in the mix, as compared to conventional concrete, in order to maintain adequate compactability characteristics. This leads to higher cost as well as greater impact on the environment. Considerable efforts have been made by a number of researchers to find ways of reducing the cement content of SCC.

One of the main approaches to reduce the cement content is to include fly ash in the mix. By enhancing the flowability of the concrete and encouraging the pozzolanic reaction, fly ash is useful as a replacement for cement in SCC. An alternative approach is air entrainment, which is beneficial because it reduces the cement content as a proportion of the total volume of concrete, which is increased by the inclusion of air. If the entrained air bubbles have suitable characteristics, they too can help to improve the flowability of the fresh concrete.

These understandings highlight the potential for combining fly ash with entrained air bubbles for a further reduction in cement content in self-compacting concrete. However, fly ash can have a significant influence on air entrainment in the fresh concrete, which points to the need for an investigation into the combined effects of fly ash and entrained air bubbles on the self-compactability of fresh concrete. Furthermore, the disturbance to air entrainment caused by fly ash can also affect the volumetric stability of the entrained air. Volumetric stability is another characteristic that is essential to SCC, since it affects flowability retention and certain properties of the hardened concrete.

The efficiency of the entrained air bubbles on the reduction in friction between mortar and model coarse aggregate is found to be mainly depended on the air size distribution, owing to the

fine air bubbles (<450μm) acting as compressible bearings and deformation of large air bubbles (>450μm). However, the combined effects of fly ash and fine entrained air bubbles have been found to promote the reduction in friction between mortar and model coarse aggregate. This leads to the enhancement in self-compactability of the fresh concrete. Besides, a higher aggregate content is also made possible through the combined effects of fly ash and fine entrained air bubbles.

The employment of fly ash has been found to reduce the volumetric stability of entrained air bubbles in fresh mortar, through higher content of large and unstable air bubbles being produced. The spherical shape of fly ash has also been suggested to easier movement, coalescence and escape of fine air bubbles. Nonetheless, the enhanced entrainment of fine air bubbles can improve the volumetric stability of entrained air in fresh mortar of SCC with fly ash.

ACKNOWLEDGEMENT

TABLE OF CONTENTS

LIST OF FIGURES

LIST OF TABLES

CHAPTER 1. INTRODUCTION

1.1 STUDY IMPORTANCE

The production of durable concrete relies on compaction being correctly carried out by skilled labourers. However, the availability of labourers with such skills has gradually fallen. To address the problem of producing durable concrete without the requirement for skilled labour, self-compacting concrete (SCC) was first developed in 1988.

Self-compacting concrete is a concrete with the ability to flow throughout the formwork for a structure without the need for compaction and without segregation or bleeding. To achieve adequate self-compactability, SCC must have suitable characteristics including filling ability, passing ability and stability. Typically, these characteristics are given to fresh concrete by limiting the aggregate content, using a low water-to-powder ratio and employing superplasticisers. As a result, SCC usually requires a higher cement content as compared with conventional concrete (**Fig. 1.1**). This leads to significantly higher costs and poorer sustainability in terms of the environment.

At the present time, many approaches to reduce the amount of cement used in SCC are being studied with the aim of reducing its cost and environmental impact. One commonly used method is to employ fly ash as partial replacement for cement in SCC. Since fly ash is a by-product of coal-burning power plants, its use as cement replacement is known to be beneficial in environmental terms. Besides, fly ash, through its spherical shape, is known to improve the flowability of the fresh concrete. This suggests the potential of fly ash to enhance the self-compactability of fresh concrete with higher fine aggregate contents.

Alternatively, air-entrainment has been found to be an effective way to reduce the usage of cement in SCC. Since entrained air bubbles increase the total volume of the SCC, the volume of

all other components, including cement, can be reduced by an equivalent amount. Moreover, the fine aggregate content can be increased if air bubbles with suitable characteristics can be entrained; this can further reduce cement usage. It has been suggested that suitable entrained air characteristics are mainly related to how fine the air bubbles are. Therefore, to reduce the cement content of SCC by this means there is a need to investigate methods of enhancing the entrainment of fine air bubbles. This also suggests the necessity of further work to evaluate the effects of the size distribution of the entrained air bubbles on the self-compactability of fresh concrete.

These two methods for enhancing the self-compactability of fresh concrete, by air entrainment and the use of fly ash, also suggest the potential for further reducing the amount of cement required by combining both approaches.

Furthermore, to ensure that the fresh self-compacting concrete retains its flowability, as well as to yield certain desirable properties of the hardened concrete, the volumetric stability of the entrained air bubbles is important. The volumetric stability of the entrained air has been found to be influenced by various factors including the concrete mix proportion and the characteristics of the entrained air. The presence of fly ash, as well as influencing air entrainment, can also affect the volumetric stability of the entrained air. Therefore, the effects of enhanced entrainment of fine air bubbles on the volumetric stability of the entrained air should also requires study.
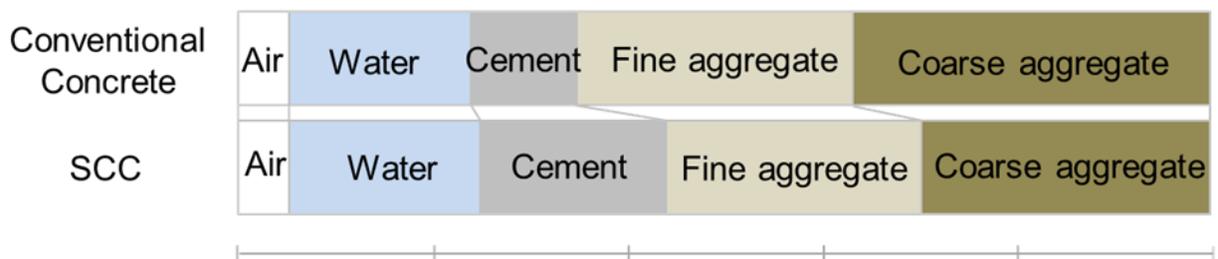
Fig. 1.1 Comparison of volumetric mix proportions of self-compacting concrete (SCC) and normal concrete

1.2 OBJECTIVE OF THE STUDY

The objective of this research is to investigate the combined effects of fly ash and entrained air bubbles for enhancement in the self-compactability of fresh concrete. This is expected to increase the aggregate content and, hence, reduce the proportion of cement in SCC.

In order to effectively improve the self-compactability of fresh concrete by air entrainment, the effects of entrained-air size distribution on friction between mortar and model coarse aggregate (Fmb) are studied. Various methods for enhancing the entrainment of fine air bubbles are investigated.

The research also includes a study into the influence of fly ash on the self-compactability of non-air-entrained concrete. The purpose of this is to investigate the potential of fly ash to reduce the required cement content in SCC. Additionally, this helps with the investigation of the combined effects of fly ash and entrained air on the self-compactability of fresh concrete.

Additionally, the effects of air size distribution on the volumetric stability of entrained air bubbles in fresh SCC mortar are studied, since stability is essential to the retention of flowability by fresh SCC as well as certain properties of the hardened concrete. The effects of fly ash on reducing the volumetric stability of the entrained air are also clarified. Besides, the enhanced entrainment of fine air bubbles for improvement in volumetric stability of entrained air in fresh concrete is also examined.

1.3 TESTING METHOD AND INDICES FOR THE EFFECTS OF FLY ASH AND SIZE OF ENTRAINED AIR BUBBLES ON THE SELF-COMPACTABILITY AND AIR VOLUMETRIC-STABILITY OF FRESH CONCRETE

1.3.1 METHOD AND INDICES FOR SELF-COMPACTABILITY OF FRESH CONCRETE THROUGH MORTAR TESTING

1.3.1.1 Indices for controlling flowability of fresh mortar

The literature suggests that the self-compactability of fresh concretes with the same coarse aggregate content depends mainly on the flowability of the fresh mortar (Nagamoto and Ozawa, 1997). Hence, in order to investigate the effects of fly ash and entrained air on the self-compactability of fresh concrete, the flowability of the mortar in each set of experiments is controlled to the same value by altering the superplasticiser (SP/P) dose and the water-to-powder volumetric ratio (*w/p*). Mortar flowability is assumed to be determined by deformability and viscosity. In this research, the deformability of fresh mortar is quantified in terms of relative flow area (Γm) in a mortar flow cone test, while fresh mortar viscosity is determined by the funnel test in terms relative funnel speed (Rm), as illustrated in **Fig. 1.2**. These indices are used to investigate and control the effect of fly ash and entrained air bubbles on the flowability of fresh mortar.
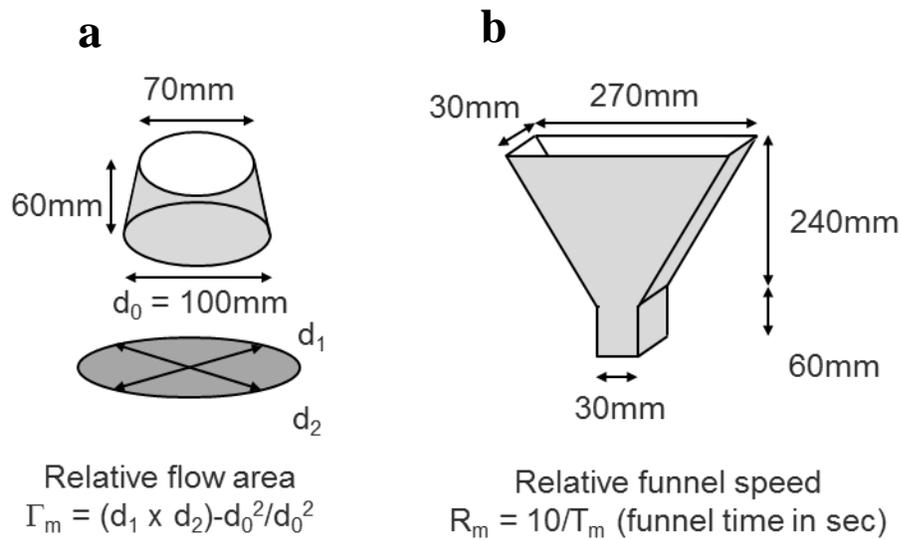
Fig. 1.2 Mortar flow cone test (a) and mortar funnel test (b)

1.3.1.2 Simple evaluation method for effects of fly ash and entrained air on friction between mortar and model coarse aggregate (Fmb)

As previously noted, in order for concrete to be self-compactable, it must have adequate flowability, passing ability and stability. These properties can be measured through a variety of concrete tests. However, such tests can cost significant amounts of time, materials and operators. The work of Nagamoto and Ozawa (1997) indicated that, for a certain coarse aggregate content, the self-compactability of fresh concrete mainly depends on the flowability of its mortar. Thereafter, methods of achieving adequate self-compactability through mortar testing were proposed (Nagamoto and Ozawa, 1997, and Ouchi et al, 1999). Nagamoto and Ozawa (1997) suggested suitable mortar flowability values in terms of mortar relative flow area and funnel speed for producing self-compacting concrete. Ouchi et al (1999) carried out further investigations and proposed a simple evaluation method for the interaction between coarse aggregate and mortar. This interaction between coarse aggregate and mortar was found to have a unique relationship with

5

the concrete Box-test. Hence, this unique relationship is assumed in this study and only certain results are selected for verification through concrete tests.

Ouchi et al.'s method involves adding glass beads to the fresh mortar as a model coarse aggregate for testing the mortar-coarse aggregate interaction. They indicated that the appropriate diameter and volume of glass beads is 10mm and 20% by total volume of mortar, respectively. The self-compactability of fresh concrete can then be quantified in terms of the relative funnel speed of the fresh mortar, Rm, and the fresh mortar with glass beads, Rmb. They also suggested that the self-compactability of the fresh concrete without air-entrainment can be quantified in terms of the degree of reduction in mortar flowability with the addition of the glass beads, 1-Rmb/Rm.

In this research, however, the intent is to investigate the effects of fly ash and entrained air on the self-compactability of fresh concrete. To quantify these effects, slightly different indices are used (**Fig. 1.3**). The effects of fly ash and entrained air on fresh concrete self-compactability can be quantified in terms of the change in the degree of flowability reduction of the mortar due to the addition of the model coarse aggregate. The actual index used depends on the factor being considered. For an example, the index $1-\Delta Rm_a/\Delta Rm_c$ is used to investigate the effects of entrained air on the self-compactability of fresh concrete without fly ash (**Fig. 1.3**).
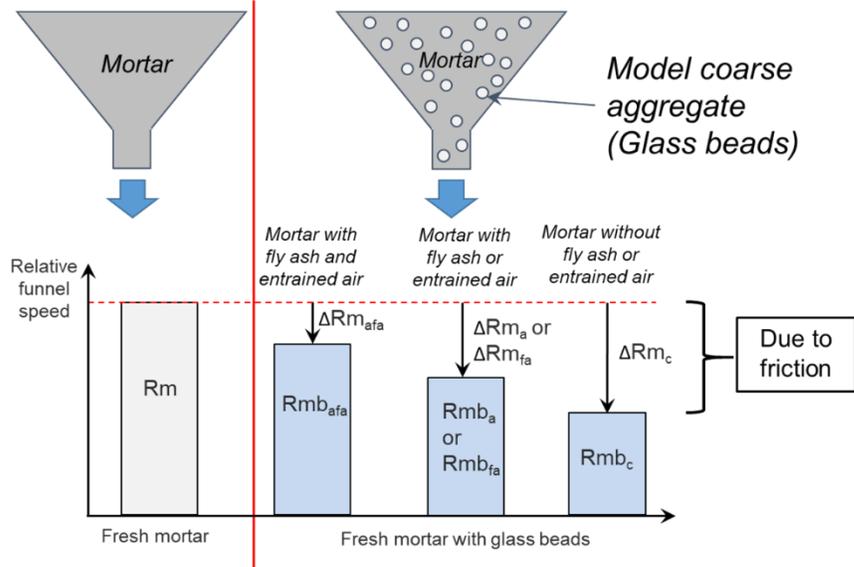
Fig. 1.3 Indices used to evaluate friction between model coarse aggregate and mortar matrix (Fmb)

1.3.2 METHOD FOR INVESTINGATING VOLUMETRIC STABILITY OF ENTRAINED AIR IN SCC THROUGH MORTAR TESTING

In this study, the change in air content of SCC fresh mortar during the first two hours after mixing is determined to quantify the volumetric stability of the entrained air bubbles in SCC. The dosage of air-entraining agents is adjusted so that the air content of every mortar sample with air-entrainment fell within the same range.

The air content of the fresh mortar is measured by the gravimetric method described in ASTM 138. The weight of the fresh mortar is measured in a container of known volume to determine its actual density. The actual density is then compared with the density as calculated from the designed mix proportion. The air content of the fresh mortar can then be obtained using the following equation:

$$A = \frac{D_C - D_A}{D_C} \qquad (1.1)$$

Where A is the air content of the fresh mortar (%), D_C is the density of the mortar as calculated from designed mix proportions (kg/m^3) and D_A is the actual density of the mortar obtained from its weight (kg/m^3).

1.3.3 MEASUREMENT OF ENTRAINED AIR SIZE DISTRIBUTION BY AIR VOID ANALYSIS (AVA)

In order to clarify the effects of entrained air size distribution on the volumetric stability of the air and the self-compactability of the fresh concrete, the size distribution of the entrained air bubbles was obtained in the fresh state. An instrument known as an Air Void Analyser (AVA) has been developed for measuring the air-void characteristics of concrete in the fresh state (AASHTO TP75); this was used to obtain the size distribution of the entrained air.

The AVA determines the air void characteristics of fresh mortar and concrete using 20cm^3 mortar samples. The air bubbles in the 20cm^3 sample are released into a viscous release liquid in the AVA apparatus set up, as illustrated in **Fig 1.4**. This release liquid allows the air bubbles to retain their original size. The air bubbles then rise through the release liquid and the water column, and are collected under the buoyancy pan.

According to Stokes' law, the larger bubbles tend to rise faster than the smaller ones. The viscous release liquid slows down the initial rise of the bubbles, providing a larger gap in the time required for bubbles of different sizes to reach the top of the column. This makes it easier to distinguish bubbles with different sizes. As the rising bubbles rise into the buoyancy pan, the change in buoyancy, or weight, of the pan as a function of time can be used to determine the size distribution of the bubbles in the sample. The air void characteristics obtained are based on ASTM C457.
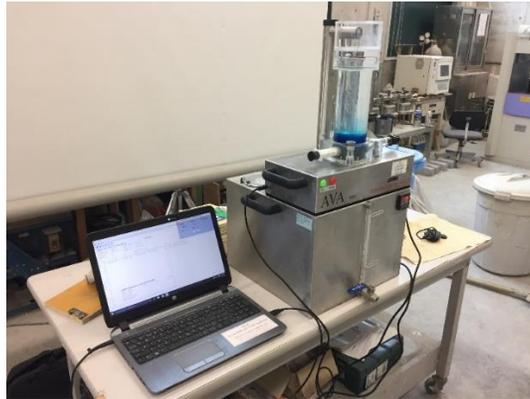
Fig. 1.4 Setup of air void analysis (AVA) instrument

1.3.4 TESTS FOR VERIFYING THE EFFECTS OF FLY ASH AND ENTRAINED AIR ON SELF-COMPACTABILITY OF FRESH CONCRETE

In this study, certain mortar mix proportions are selected for verification through concrete tests as noted in section 1.3.1.2. These concrete tests include the slump flow test, the V-funnel test, air measurements and the box test. The slump flow area of every concrete mix is controlled to be in the same range by adjusting the dosage of the superplasticiser (SP/P). The air content of every concrete mix with air entrainment, measured by the gravimetric method, is also controlled by altering the dosage of the air-entraining agent (AEA). The fill height of the fresh concrete, obtained from the box test, is used to quantify the self-compactability of the mix. The box test is conducted using concrete with a coarse aggregate content (g/c), including air, of 0.30 and obstacle R_1 (consisting of five deformed rebars of 10mm nominal diameter), as illustrated in **Fig. 1.5**.
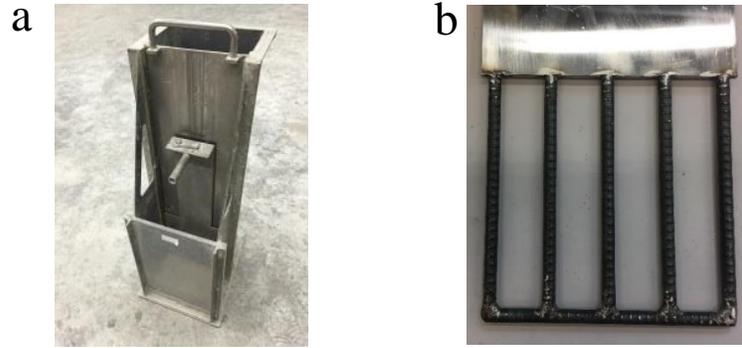
Fig. 1.5 Concrete box test (a) and obstacle R₁ (b)

1.3.5 MATERIALS AND MIXING METHODS FOR MORTAR AND CONCRETE

1.3.5.1 Materials

The properties of the materials used in this series of experiments are shown in **Table 1.1**. The powder materials used are ordinary Portland cement (OPC) and class-1 fly ash as specified by the Japanese Industrial Standards (JIS R5210 and JIS A6201), as shown in **Table 1.2**. **Figure 1.6** verifies that the particles of the class-1 fly ash have a spherical shape. The superplasticiser (SP) used consists of a polycarboxylate base blended with a viscosity-modifying agent (VMA) to enhance SCC stability. Four types of air-entraining agent (AEA) are used. These are designated AEA1, AEA2, AEA3 and AEA4 and are based on modified rosin, long-chain akylcarpxylate, an akyl-aryl sulfonate compound and a vinsol resin, respectively. AEA2 is also specified as preventing the carbon on the fly ash surface from affecting air-entrainment. A defoaming agent (DA) is also used to enhance the entrainment of fine air bubbles; a polyalkyleneglycol derivative is selected for this purpose. The fine aggregate (S), model coarse aggregate (MCA) and coarse aggregate (G) used are limestone (LS), glass beads and crushed stone (CS), respectively.

Table 1.1
Properties of materials used

Material	Type	Specific gravity (g/cm^3)	Fineness (cm^2/g)	LOI (%)	F.M.	CaO (%)	SiO$_2$ (%)	Al$_2$O$_3$ (%)	Fe$_2$O$_3$ (%)	SO$_3$ (%)	MgO (%)	Cl$^-$ (%)	Alkali (%)
Powder materials	OPC (JIS R5210)	3.15	3490	1.96	-	64.82	20.26	5.42	2.92	2.08	0.91	0.01	0.55
	Fly ash I (JIS A6201)	2.40	5500	1.90	-	-	59.10	-	-	-	-	-	-
S	Limestone	2.68	-	-	2.70-2.90	-	-	-	-	-	-	-	-
G	Crushed stone (max. size: 20mm)	2.70	-	-	6.70	-	-	-	-	-	-	-	-
MCA	Glass beads	2.54	Diameter: 10mm										
SP	Polycarboxylate base blended with VMA												
AEA1	Modified rosin based anionic surface active agent												
AEA2	Long-chain alkylcarboxylate based anionic surface active and non-ionic surface active agent												
AEA3	Akyl-aryl sulfonate compound based anionic surface active agent												
AEA4	Vinsol resin												
DA	Polyalkyleneglycol derivative												

Table 1.2
Specifications of powder materials used (JIS R5210 and JIS A6201)

Properties		Material	
		OPC	Fly ash class I
Specific gravity (g/cm^3)		-	≥ 1.95
Fineness	Blaine (cm^2/g)	≥ 2500	≥ 5000
	45 mm retained (%)	-	≤ 10
Setting time	Initial (min)	≥ 60	-
	Final (h)	≤ 10	-
Soundness	Pat method	Good	-
	Le Chatelier flask method (mm)	≤ 10	-
Compressive strength (N/mm^2)	1 d	-	-
	3 d	≥ 12.5	-
	7 d	≥ 22.5	-
	28 d	≥ 42.5	-
Heat of hydration (J/g)	7 d	-	-
	28 d	-	-
Chemical composition (%)	MgO	≤ 5.0	-
	SO$_3$	≤ 3.5	-
	LOI	≤ 5.0	≤ 3.0
	Alkali	≤ 0.75	-
	Cl$^-$	≤ 0.035	-
	SiO$_2$	-	≥ 45
Flow value ratio (%)		-	≥ 105
Strength activity index (%)	28 d	-	≥ 90
	91 d	-	≥ 100
Moisture		-	≤ 1.0

30μm
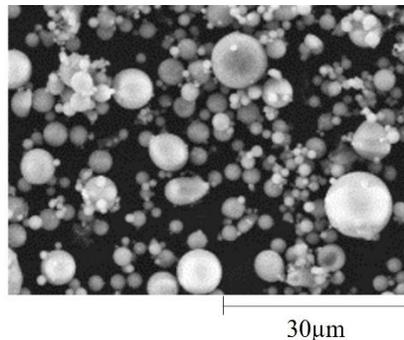
Fig. 1.6 SEM image of fly ash particles at 2500x magnification showing spherical shape

1.3.5.2 Mixing methods of mortar and concrete

Various mixing processes are used in this study to obtain various size distributions of entrained air bubbles in the SCC. These mixing processes are specified in **Table 1.3.** The mixers used for mortar and concrete mixing complied with the Japanese Industrial Standards (JIS R5201 and JIS A8603-1). The batch sizes for mortar and concrete mixing were 1.68 and 25 litres, respectively.

Table 1.3
Mixing methods and details

Method	Material	Mixing process
A	Mortar	Powder + Aggregate ⟶(30 sec) Water 1 (63% of powder volume) + SP ⟶(60 sec) AEA + Water 2 (Rest of water) ⟶(60 sec) End
	Concrete	Powder + Aggregate ⟶(30 sec) Water 1 (63% of powder volume) + SP ⟶(90 sec) AEA + Water 2 (Rest of water) ⟶(90 sec) End
B	Mortar	Powder + Aggregate ⟶(30 sec) Water 1 (Rest of water) + SP + AEA ⟶(60 sec) DA + Water 2 (15% of powder volume) ⟶(60 sec) End
	Concrete	Powder + Aggregate ⟶(30 sec) Water 1 (Rest of water) + SP + AEA ⟶(90 sec) DA + Water 2 (15% of powder volume) ⟶(90 sec) End
C	Mortar	Powder + Aggregate ⟶(30 sec) Water 1 (63% of powder volume) + SP ⟶(60 sec) AEA + Water 2 (Rest of water) ⟶(60 sec) DA ⟶(60 sec) End

1.3.6 POSSIBLE EFFECTS OF ENTRAINED AIR BUBBLES ON REDUCTION IN FRICTION BETWEEN MODEL COARSE AGGREGATE AND MORTAR MATRIX

In order to clarify the effects of entrained air bubbles on the friction between the model coarse aggregate and the mortar matrix in SCC, the experiments are set up in a certain way. As

mentioned in section 1.3.1.2, this friction is quantified in terms of $(Rm_{ba}-Rm_{bc})/Rm$. However, it has been suggested that air entrainment influences the relative funnel speed of mortar with model coarse aggregate (Rmb_a) through various mechanisms (**Fig. 1.7**).

One of the main effects of air entrainment on Rmb_a may be attributed to the increase in total volume of the mortar (Attachaiyawuth and Ouchi, 2014). This can lead to the replacement of fine and model coarse aggregate by entrained air bubbles. Consequently, the aggregate spacing increases, resulting in lower stress on the mortar matrix. Thus, in this study, in order to investigate other effects of air entrainment, the designed contents of fine and model coarse aggregate in mortar with entrained air are initially higher than in mortar without entrained air. This leads to an equal content of fine and model coarse aggregate in finished mortars both with and without air entrainment, as illustrated in **Fig. 1.8**.

The water retention of entrained air bubbles is different from that of cement particles, and this may also influence Rmb_a through changes in the deformability (Γm) and plastic viscosity (Rm) of the mortar. Besides, certain air-entraining agents may reduce the surface tension of water (Powers, 1968) and, therefore, may affect Rm (Schonhorn, 1967). However, in this study, the Γm and Rm of every mortar mix proportion in each set of experiments are controlled to be in the same range by altering the dosage of superplasticiser (SP/P) and the water-to-powder volumetric ratio (*w/p*), respectively.

Subsequently, owing to the experimental setup used in this research, $(Rm_{ba}-Rm_{bc})/Rm$ is expected to depend mainly on the action of entrained air bubbles within fresh mortar containing model coarse aggregate. Some authors have attributed enhancement flowability of the concrete to the ball-bearing effects of the entrained air bubbles (Attachaiyawuth et al, 2016, Paillere, 1995 and Aïtcin and Flatt, 2016). Besides, Edmeades and Hewlett (1998) have suggested that aggregate-air-

cement-air-aggregate type of system can permit relatively free motion in shear with the stabilised entrained air bubbles acting as compressible bearings. These effects of entrained air bubbles have been found to be influenced by the bubble characteristics (Attachaiyawuth et al, 2016). Furthermore, Muncaster (1993) has indicated that pressure is lower inside larger air bubbles, as compared to smaller ones. These larger air bubbles may subjected to larger deformation and destabilised under compression by the model coarse aggregate during mortar flowability testing. Thus, the distance between the aggregate, acting as restraint to the mortar matrix, may be reduced
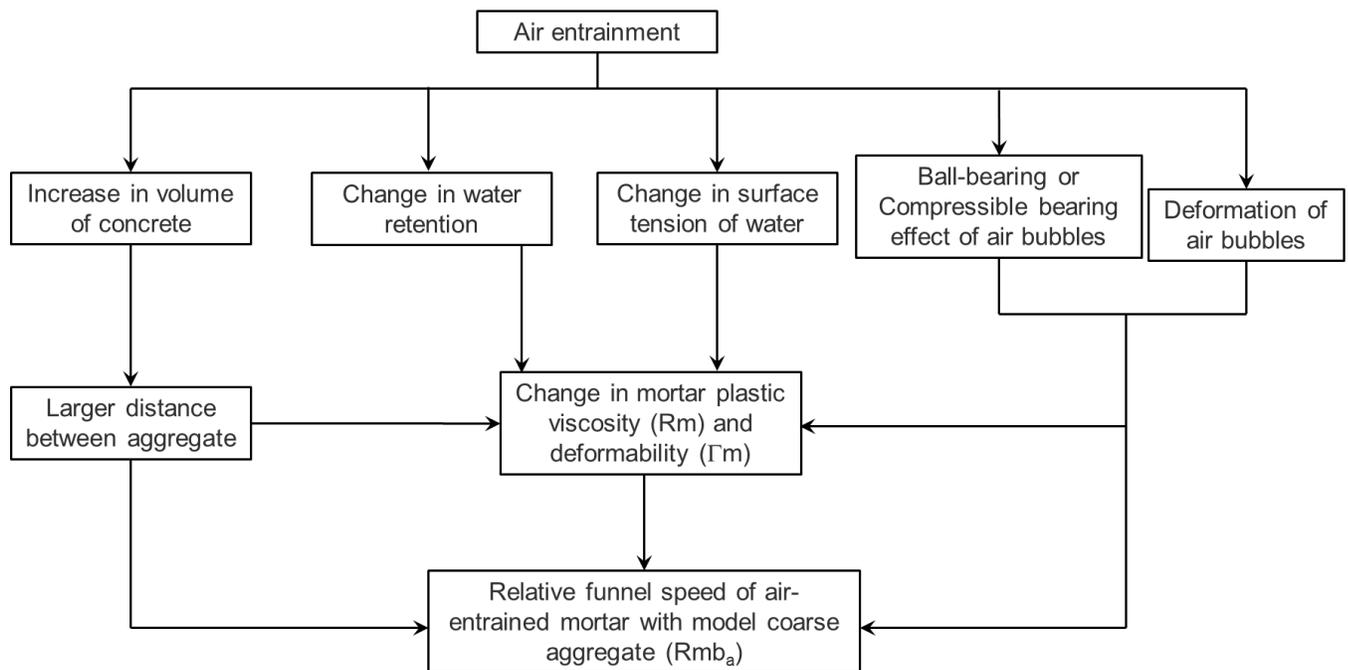
Fig. 1.7 Possible effects of air entrainment on relative funnel speed of air-entrained mortar with model coarse aggregate
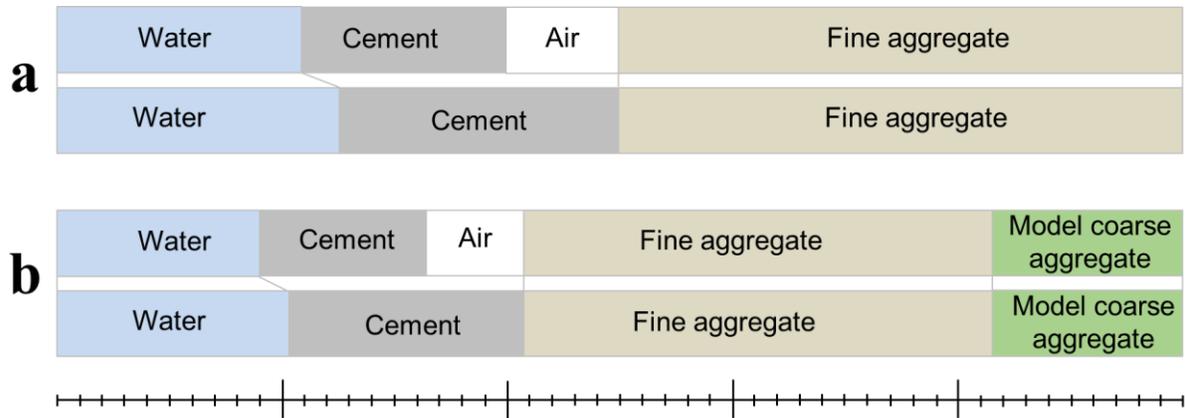
Fig. 1.8 Mix proportions of mortar for analysing the effects of entrained air bubbles in mortar without (a) and with (b) model coarse aggregate

1.4 DETAILS OF STUDY

This report on the study is divided into a number of chapters. A brief explanation of each chapter follows below.

Chapter 2 discusses adjustments to the entrained-air size distributions in the fresh mortar as measured by the Air Void Analysis (AVA). Measurements by the AVA tend to be lower than those obtained by the gravimetric method. Therefore, adjustments are necessary to evaluate the effects of fine entrained air bubbles for improvement in volumetric stability of the entrained air and reduction in friction between mortar and model coarse aggregate (Fmb).

Chapter 3 introduces the investigation into the effects of entrained air bubbles on the reduction in Fmb to reflect the enhancement in self-compactability of fresh concrete. In this chapter, various methods for enhancing the entrainment of fine air bubbles are presented. These methods include the selection of suitable air-entraining agents and mixing methods, as well as the

employment of a defoaming agent. Moreover, the effects of entrained air size distribution on friction between mortar and coarse aggregate in fresh mortar are discussed.

Chapter 4 deals with the combined effects of fine entrained air bubbles and fly ash for further reduction in friction between model coarse aggregate and the mortar matrix. The effects of fly ash and fine entrained air bubbles are compared. A defoaming agent is used to enhance the entrainment of fine air bubbles in these mortars with fly ash. The combined effects of fly ash and fine entrained air bubbles on the self-compactability of fresh concrete are also investigated with the aim of increasing the aggregate content in SCC.

The effects of entrained air size distribution on the volumetric stability of the entrained air in fresh SCC mortar are studied in Chapter 5. The reduced volumetric stability of the entrained air associated with the use of fly ash is also clarified. Methods of enhancing the entrainment of fine air bubbles for improved volumetric stability of entrained air in fresh SCC mortar are also presented.

The general conclusions of this study are summarised and listed in the final chapter, Chapter 6.

The main structure of the research is illustrated in **Fig. 1.9**.
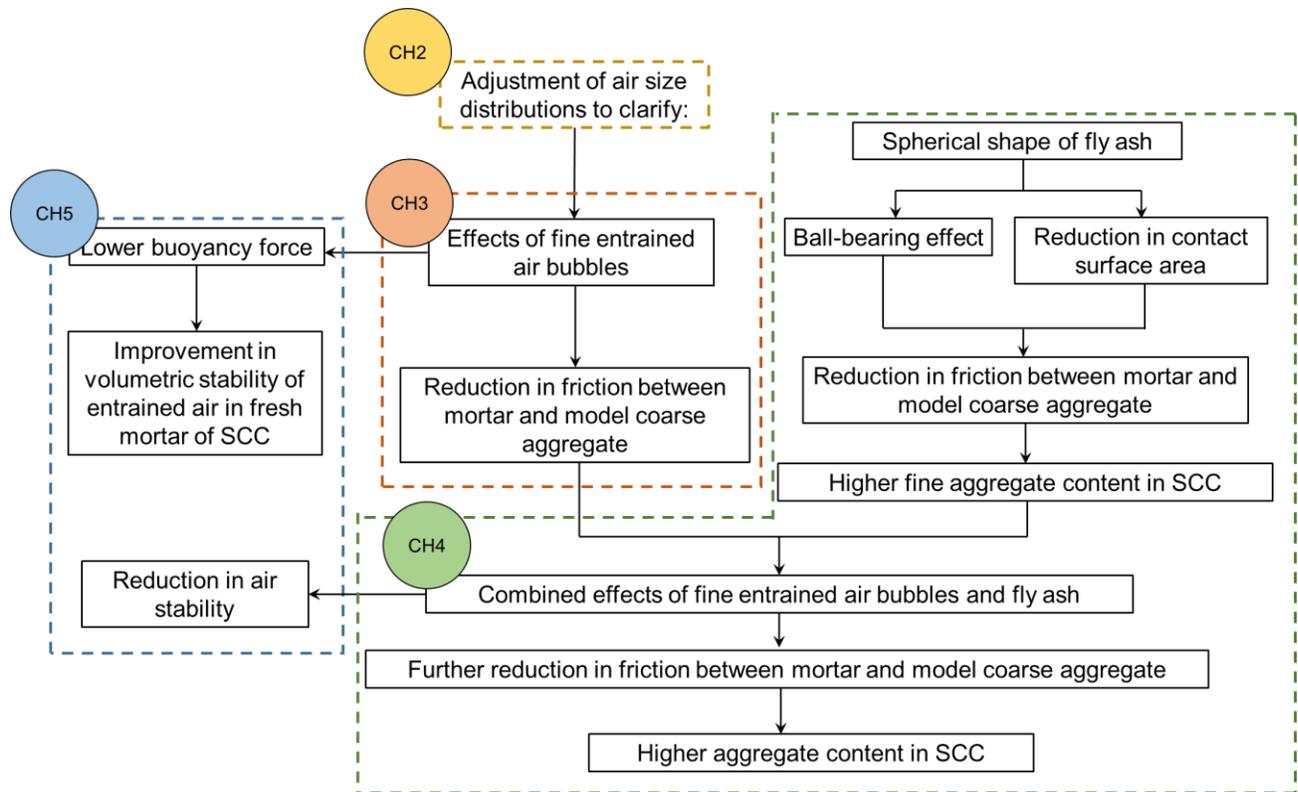
Fig. 1.9 Structure of the research

REFERENCES

AASHTO TP75. *Provisional standard test method for air-void characteristics of freshly mixed concrete by buoyancy change*. American Association of State Highway and Transportation Officials, 2008.

ASTM C138. Standard test method for density (unit weight), yield and air content (gravimetric) of concrete. American society of testing and materials, 2001.

ASTM 457. Standard test method for microscopical determination of parameters of the air-void system in hardened concrete. American society of testing and materials, 2009.

Aïtcin, P. and Flatt, R.J. (2016) *Science and technology of concrete admixtures*. Elsevier, UK.

Attachaiyawuth, A. and Ouchi, M. (2014) Effect of entrained air on mitigation of reduction in interaction between coarse aggregate and mortar during deformation of self-compacting concrete at fresh state. *Proceedings of the Japan Concrete Institute*. 36: 1444-1449.

Attachaiyawuth, A., Rath, S., Tanaka, K. and Ouchi, M. (2016) Improvement of self-compactability of air-enhanced self-compacting concrete with fine entrained air. *Journal of Advanced Concrete Technology*. 14: 55-69.

Edmeades, R.M. and Hewlett, P.C. (1998) 15 cement admixtures. *Lea's Chemistry of Cement and Concrete*. 841-905.

JIS A6201. *Fly ash for use in concrete.* Japanese Industrial Standards, 2015.

JIS R5201. *Physical testing methods for cement.* Japanese Industrial Standards, 2015. (Equivalent to ISO 697. *Cement-Test methods-Determination of strength*. International Organization for Standardization, 2009.)

JIS R5210. *Portland cement.* Japanese Industrial Standards, 2009.

JIS A8603-1. *Concrete mixers – Part 1: Terms and commercial specifications*. Japanese Industrial Standards, 2010. (Equivalent to ISO 18650-1. *Building construction machinery and equipment – Concrete mixers – Part 1: Vocabulary and general specifications (MOD)*. International Organization for Standardization, 2004.)

Nagamoto, N. and Ozawa, K. (1997) Mixture proportions of self-compacting high-performance concrete. *American Concrete Institute*. ACI SP-172. 623-636.

Ouchi, M., Edamatsu, Y., Ozawa, K. and Okamura, H. (1999) Simple evaluation method for interaction between coarse aggregate and mortar particles in self-compacting concrete. *Transaction of the Japan Concrete Institute*. 21: 121-130.

Paillere, A.M. (1995) *Application of admixtures in concrete*. Rilem report 10. Rilem, UK.

Powers, T.C. (1968) *The properties of fresh concrete*. John Wiley & Sons, Inc., New York.

Schonhorn, H. (1967) Surface tension-viscosity relationship of liquids. *Journal of Chemical and Engineering Data*. 4(12): 524-525.

CHAPTER 2 ADJUSTMENT OF AIR SIZE DISTRIBUTIONS OBTAINED FROM AIR

VOID ANALYSIS

2.1 INTRODUCTION

As mentioned in section 1.3.3, Air Void Analysis (AVA) is used in this research to measure the air size distribution of fresh mortar. The experiments carried out, however, demonstrated that the air content obtained by AVA tends to be lower than that obtained by the gravimetric method (**Fig. 2.1**). This might be attributable to air bubbles that go undetected due to limitations of the AVA technique or loss of air bubbles during sampling. Given that these air bubbles may influence the friction between mortar and model coarse aggregate (Fmb), as well as the volumetric stability of the entrained air, it is important to this research that AVA air size distributions can be corrected.

Two methods for correcting the AVA air size distributions of fresh mortar are proposed in this chapter. In the first method, it is assumed that the difference in air content between the two measurement methods is accounted for by large air bubbles (>1500µm). The second method aims to adjust the air size distributions obtained from AVA towards those obtained with the Linear Transverse Method (LTM) as compiled in ASTM C457.
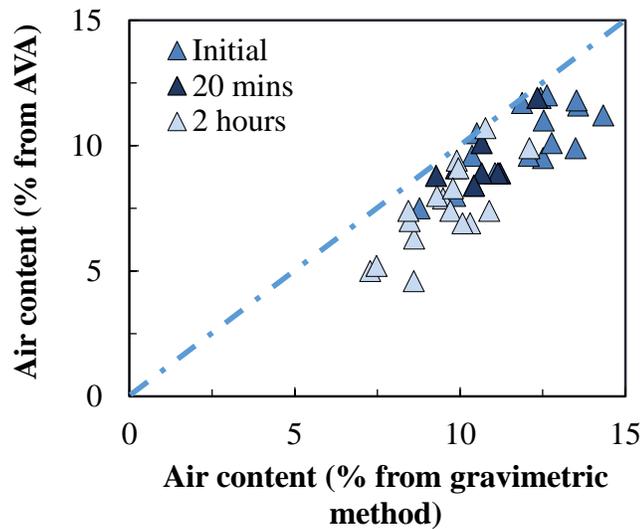
Fig. 2.1 Lower air content measured by AVA than gravimetric method

2.2 TEST PROCEDURES, MIX PRPORTIONS AND FRESH PROPERTIES FOR AIR DISTRIBUTION CORRECTION

2.2.1 MORTAR TEST PROCEDURES

The test procedures used in this chapter are shown in **Table 2.1**. Since AVA was conducted at 120 minutes after mixing and fresh mortar at 120 minutes tends to be quite stiff, only a slight movement of bubbles is likely to occur thereafter until the mortar reaches its hardened state. Thus the change in air size distributions in the period from 120 minutes until the hardened state will be minimal. This means that the air size distributions obtained from AVA and LTM (which is carried out in the hardened state) in this chapter can be compared.

22

Table 2.1
Test procedures

Type	Test procedure	
	Fresh state	Hardened State
	120 minutes	
Mortar	Air measurement (gravimetric method and AVA)	Air measurement (LTM)

2.2.2 MORTAR MIX PROPORTIONS AND AIR CONTENT

All of the mix proportions of mortar that were tested to evaluate differences in measurements of air content by AVA and the gravimetric method are presented in **Table 2.2**. The air content measurements obtained by the gravimetric method, AVA and LTM are shown in **Table 2.3**.

Table 2.2
Mortar mix proportions

Mix	Mix proportion (kg/m^3)								SP/P (%)	F.M.* of S	s/m* including air	Mixing method
	C*	Water	S*	AEA1	AEA2	AEA3	AEA4	DA				
MA2	636	248	1474	0.04	-	-	-	-	1.30			
MA3	641	246	1474	-	0.39	-	-	-	1.22			
MA4	633	249	1474	-	-	0.10	-	-	1.24			B
MA5	619	253	1474	-	-	-	0.173	-	1.27	2.80	0.50	
MA6	627	251	1474	-	6.77	-	-	0.63	1.15			
MA7	636	248	1474	0.07	-	-	-	-	1.35			A
MA8	644	245	1474	-	-	0.26	-	-	1.35			
MA9	653	243	1474	-	-	2.29	-	0.65	1.30			C

*C: cement; S: fine aggregate; F.M.: fineness modulus; *s/m*: ratio of fine aggregate to mortar by volume

Table 2.3
Measured air content of mortar

Mix	Air content by gravimetric method (%)	Air content by AVA (%)	Air content by LTM (%)
MA2	9.70	7.40	10.46
MA3	10.30	6.90	9.87
MA4	8.43	7.40	11.29
MA5	10.07	6.90	11.94
MA6	10.88	7.40	11.31
MA7	9.30	8.00	9.81
MA8	9.78	8.30	10.84
MA9	12.09	9.90	11.06

2.3 CORRECTION OF ENTRAINED AIR BUBBLE DISTRIBUTION IN CONSIDERATION OF DISCREPANCY BETWEEN AVA AND GRAVIMETRIC RESULTS

2.3.1 ASSUMPTION THAT DISCREPANCY IS DUE TO LARGE AIR BUBBLES

Magura (1996) reported similar results to those obtained in experiments in this study, with air contents obtained using AVA tending to be lower than those from the gravimetric method. It was suggested that the discrepancy resulted from a limitation of AVA, in which large air bubbles with a size exceeding 3000μm are not measured (Magura, 1996). There is also an increased chance of large entrapped air bubbles escaping during preparation of the smaller samples used for AVA than for the gravimetric method. Therefore, all size distributions obtained by AVA were corrected by adding the difference between the air contents obtained by the two methods to the volume of large air bubbles (those with a diameter exceeding 1500μm), as illustrated by **Fig. 2.2**.
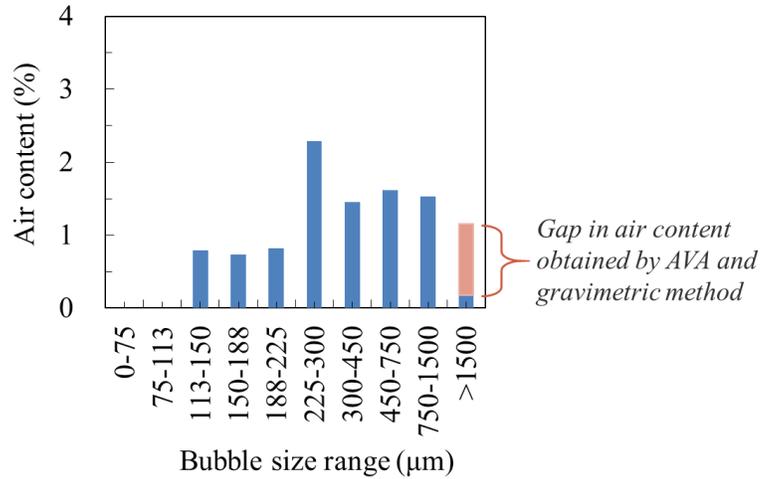
Fig. 2.2 Correction of air size distribution based on assumption that air content discrepancy results from large air bubbles (>1500μm)

2.3.2 CORRECTION TOWARDS RESULTS FROM LINEAR TRANSVERSE METHOD

Entrained-air size distributions of mortars MA2, MA3, MA4, MA5, MA6, MA7, MA8 and MA9 at a time 120 minutes after mixing, as obtained using AVA, were compared with those in the hardened state obtained using LTM. The results suggest that a complicated correction is required (**Figs. 2.3**, **2.4**, **2.5**, **2.6**, **2.7**, **2.8**, **2.9**, **and 2.10**). This correction includes shifting AVA results down by one size range. The difference in the air content obtained by AVA and gravimetric method was also added content of bubbles in all size ranges, over 75μm, evenly. This correction was verified with the actual data obtained from LTM. The verification was carried out by comparing fine to coarse air bubbles ratio (*fb/cb*) obtained from the corrected air size distribution with the actual data from LTM. The boundary that distinguish between fine and coarse air bubbles in the adjusted air size distributions towards LTM is 300μm, as suggested in **Appendix A**. Similar

25

results between the corrected and actual air size distributions (**Fig. 2.11**). This suggests the satisfaction of this correction.
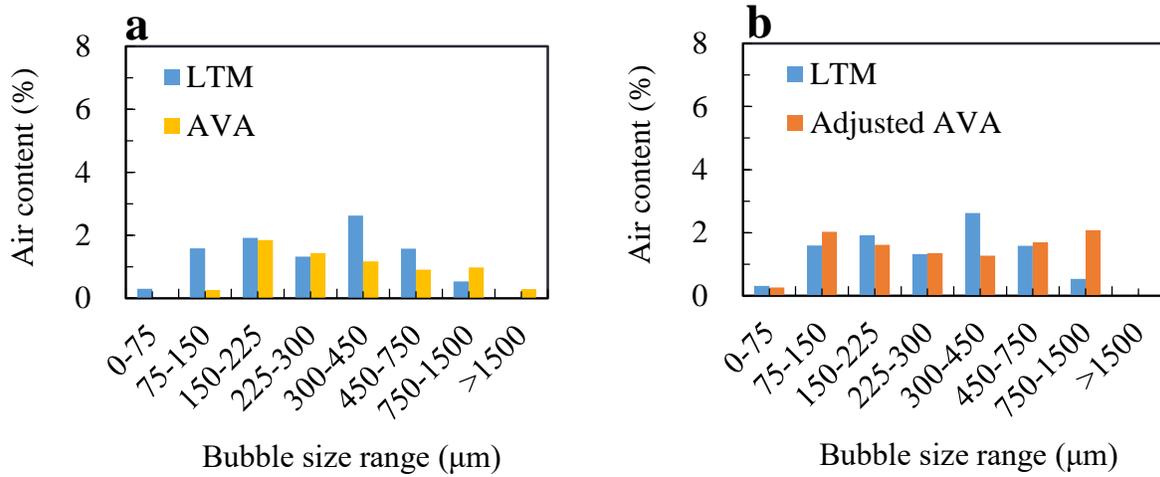
Fig. 2.3 Comparison between air size distributions of mortar MA2 obtained from LTM and AVA before (a) and after (b) correction
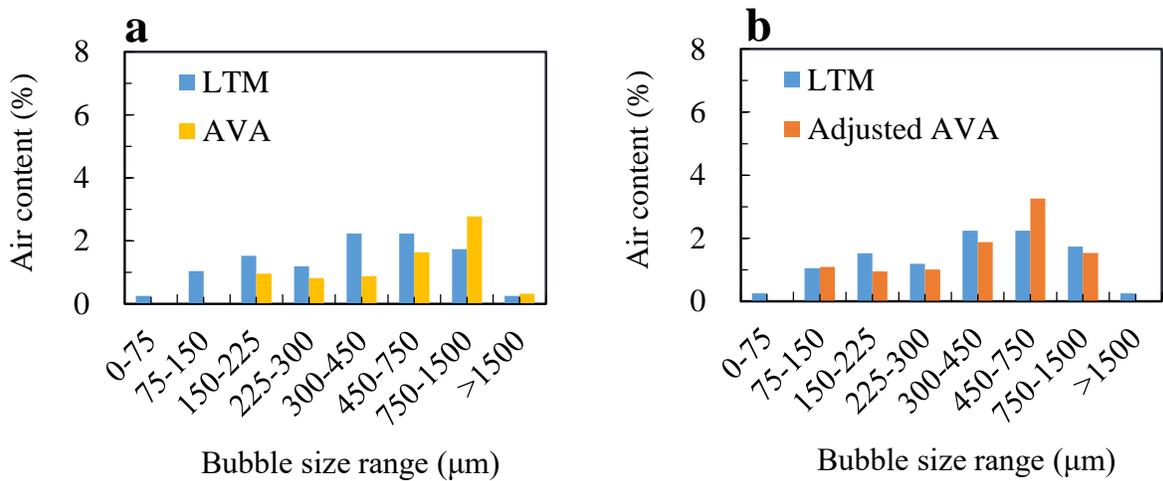
Fig. 2.4 Comparison between air size distributions of mortar MA3 obtained from LTM and AVA before (a) and after (b) correction
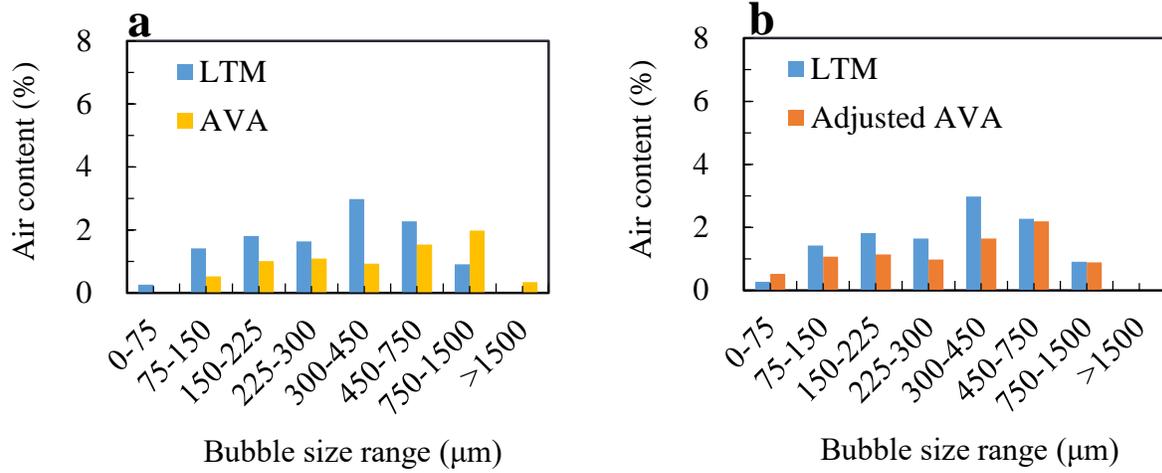
Fig. 2.5 Comparison between air size distributions of mortar MA4 obtained from LTM and AVA before (a) and after (b) correction
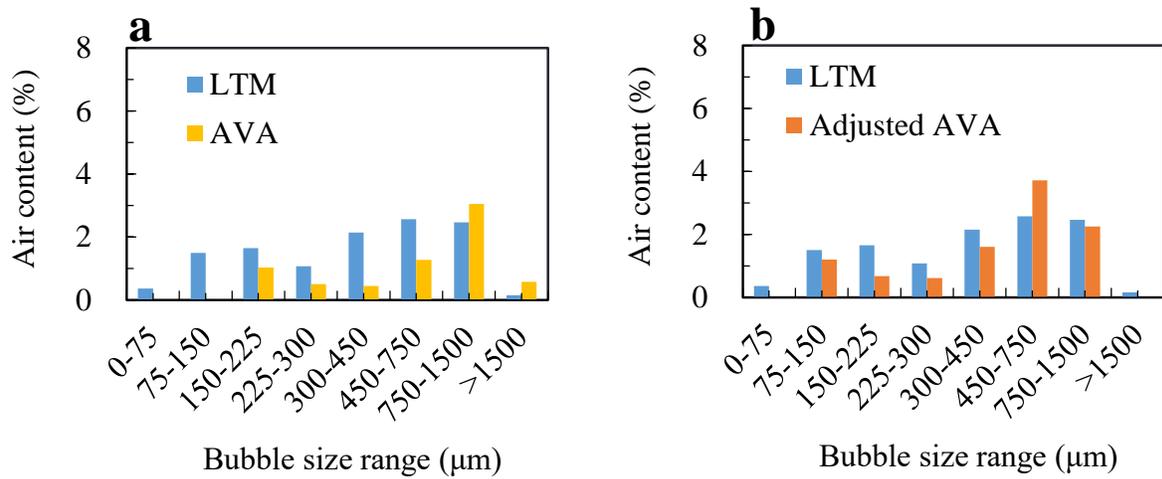
Fig. 2.6 Comparison between air size distributions of mortar MA5 obtained from LTM and AVA before (a) and after (b) correction
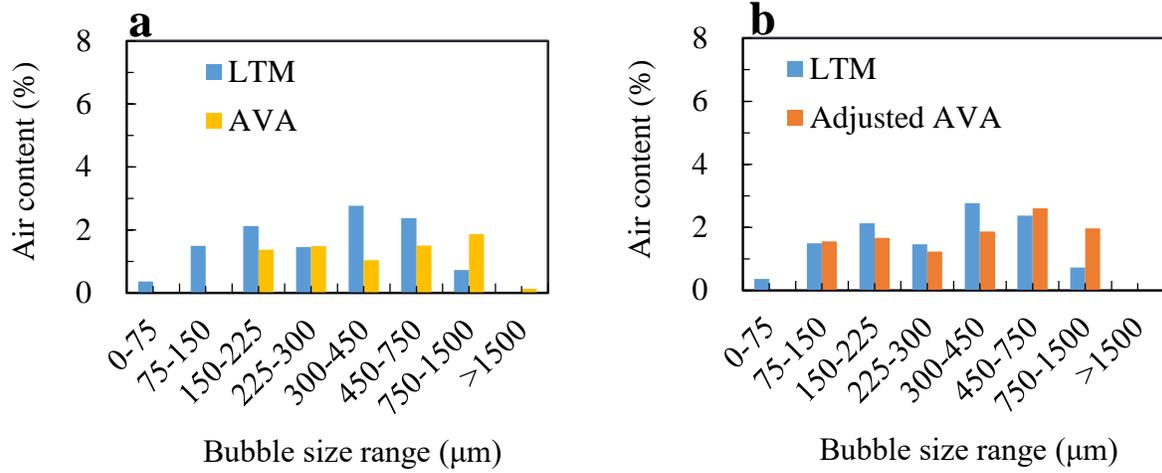
Fig. 2.7 Comparison between air size distributions of mortar MA6 obtained from LTM and AVA before (a) and after (b) correction
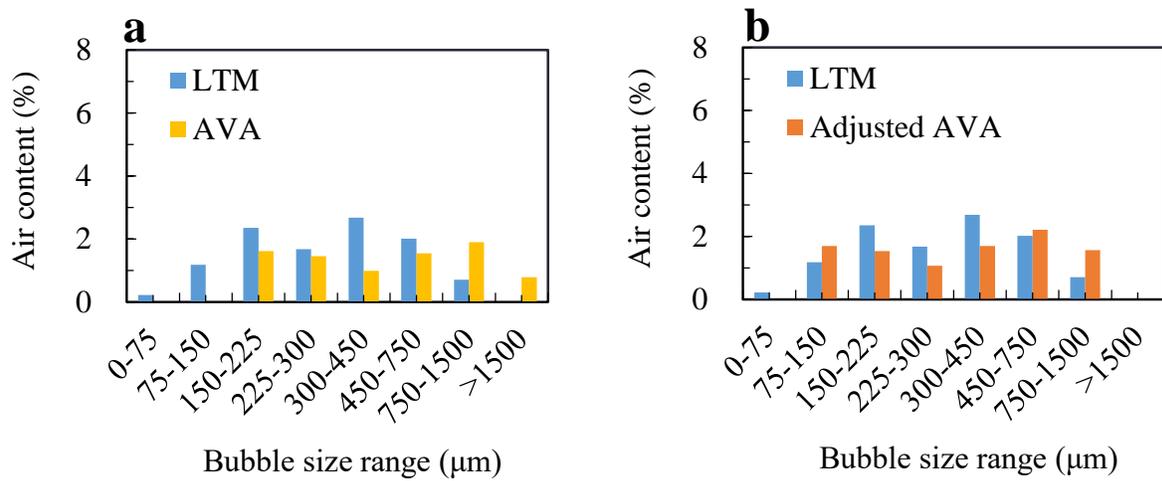
Fig. 2.8 Comparison between air size distributions of mortar MA7 obtained from LTM and AVA before (a) and after (b) correction
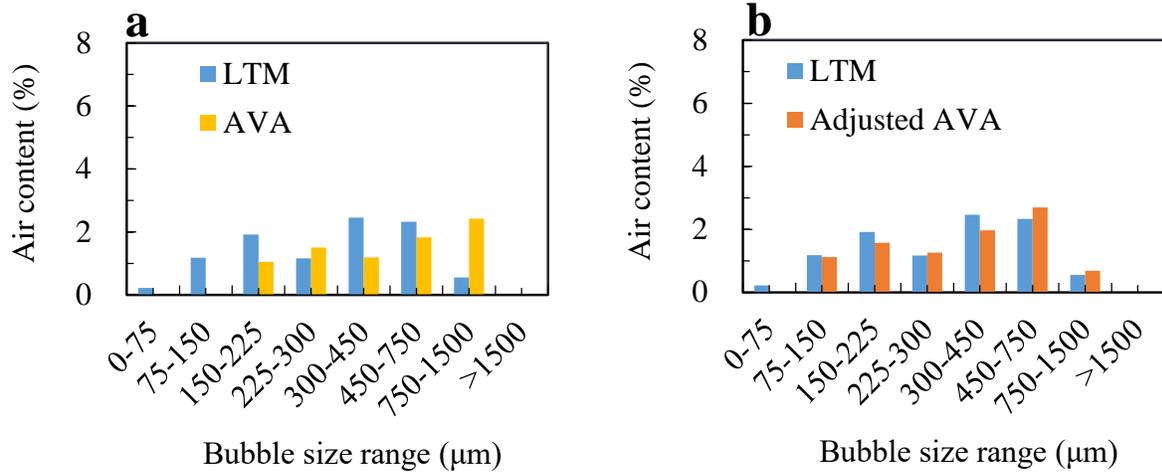
Fig. 2.9 Comparison between air size distributions of mortar MA8 obtained from LTM and AVA before (a) and after (b) correction
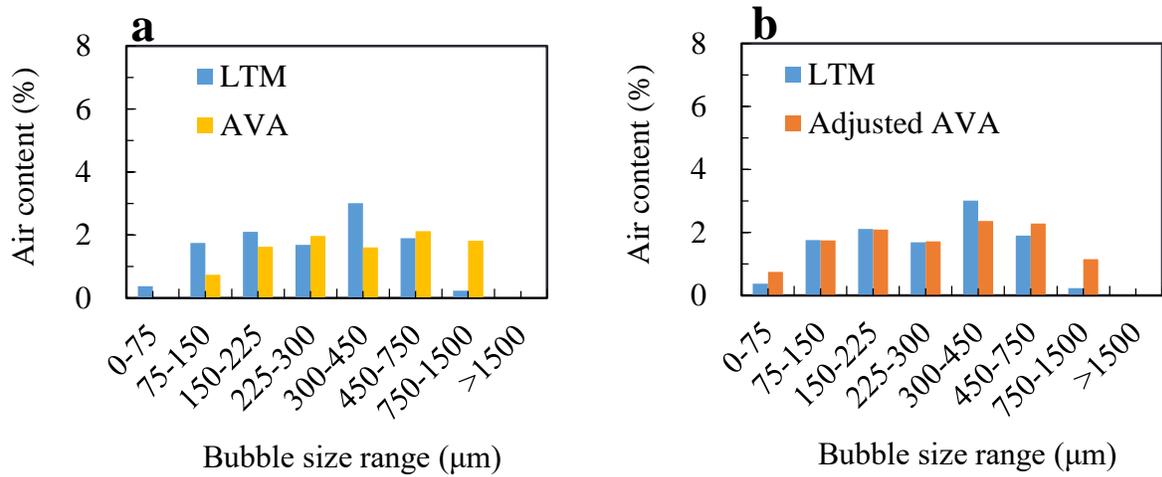
Fig. 2.10 Comparison between air size distributions of mortar MA9 obtained from LTM and AVA before (a) and after (b) correction
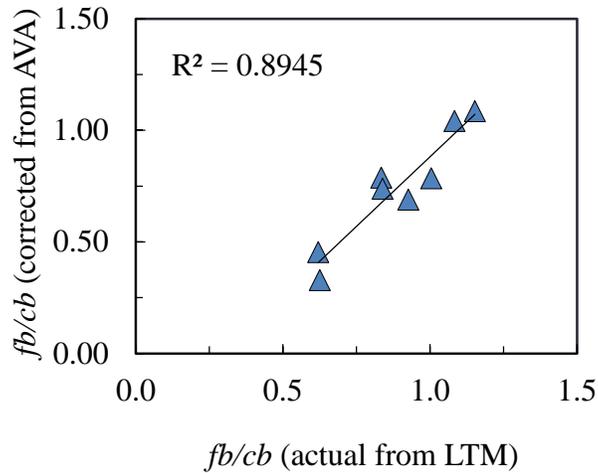
Fig. 2.11 Satisfactory relationship between ratios of fine to coarse air bubbles obtained

from corrected AVA air size distributions and actual data from LTM

2.3.3 COMPARING TWO METHODS OF CORRECTION

The results from the correction made by adjusting values towards the LTM data are seen to be similar to those obtained by assuming the discrepancy is caused by large air bubbles (>1500μm). This is illustrated by comparing the fine to coarse air bubble ratio (*fb/cb*), as in **Fig. 2.12**. The boundary that distinguish between fine and coarse air bubbles in the adjusted air size distributions towards LTM is 300μm (**Appendix A**). Besides, 450μm is suggested to be the critical size in the corrected air size distribution t by assuming the discrepancy is caused by large air bubbles (>1500μm), as explained in **Chapter 3**. However, similar conclusions can be drawn from the further evaluation of the air size distributions adjusted by both methods (**Appendix A**).
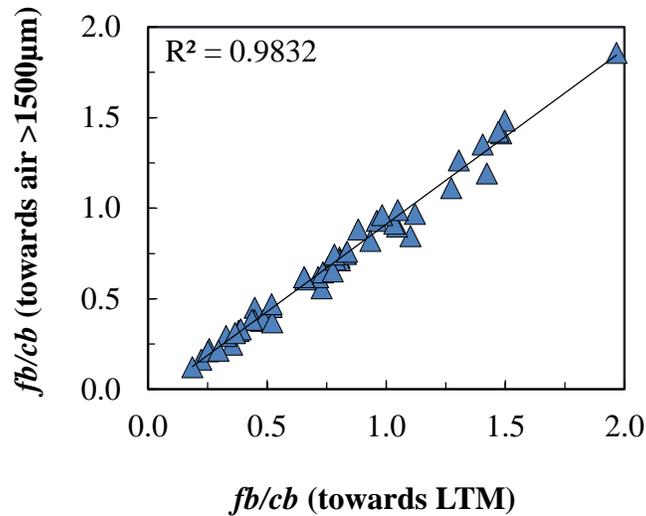
Fig. 2.12 Comparison of fine to coarse air bubble ratio obtained using the two corrections

2.4 CONCLUDING REMARKS

In this chapter, two methods for correcting the air size distributions obtained using Air Void Analysis (AVA) are investigated. Correction is necessary because of a discrepancy observed between air content obtained by AVA and that by the gravimetric method. The following conclusions can be drawn:

1) A simple correction can be carried out by assuming that the discrepancy in the air content obtained by AVA and the gravimetric method arises because of large air bubbles (>1500μm).

2) A more complicated correction is suggested by comparing the air size distributions obtained by AVA with those from the Linear Transverse Method (LTM), which takes measurements from hardened mortar. The correction involves shifting the entrained-air size distribution obtained using AVA down by one size range. The undetected air bubbles by AVA has found to be the bubbles in all size ranges evenly.

3) The results obtained by these two methods of correction are shown to follow similar trends.

31

These two methods for correcting the air size distributions obtained using AVA are simply explained by the summaries given in **Fig. 2.13**. Since both methods of correction lead to the same conclusion (**Appendix A**), for simplification of this research, the correction method used is the simpler one, where it is assumed that the discrepancy between AVA and the gravimetric method arises because of large air bubbles (>1500µm).
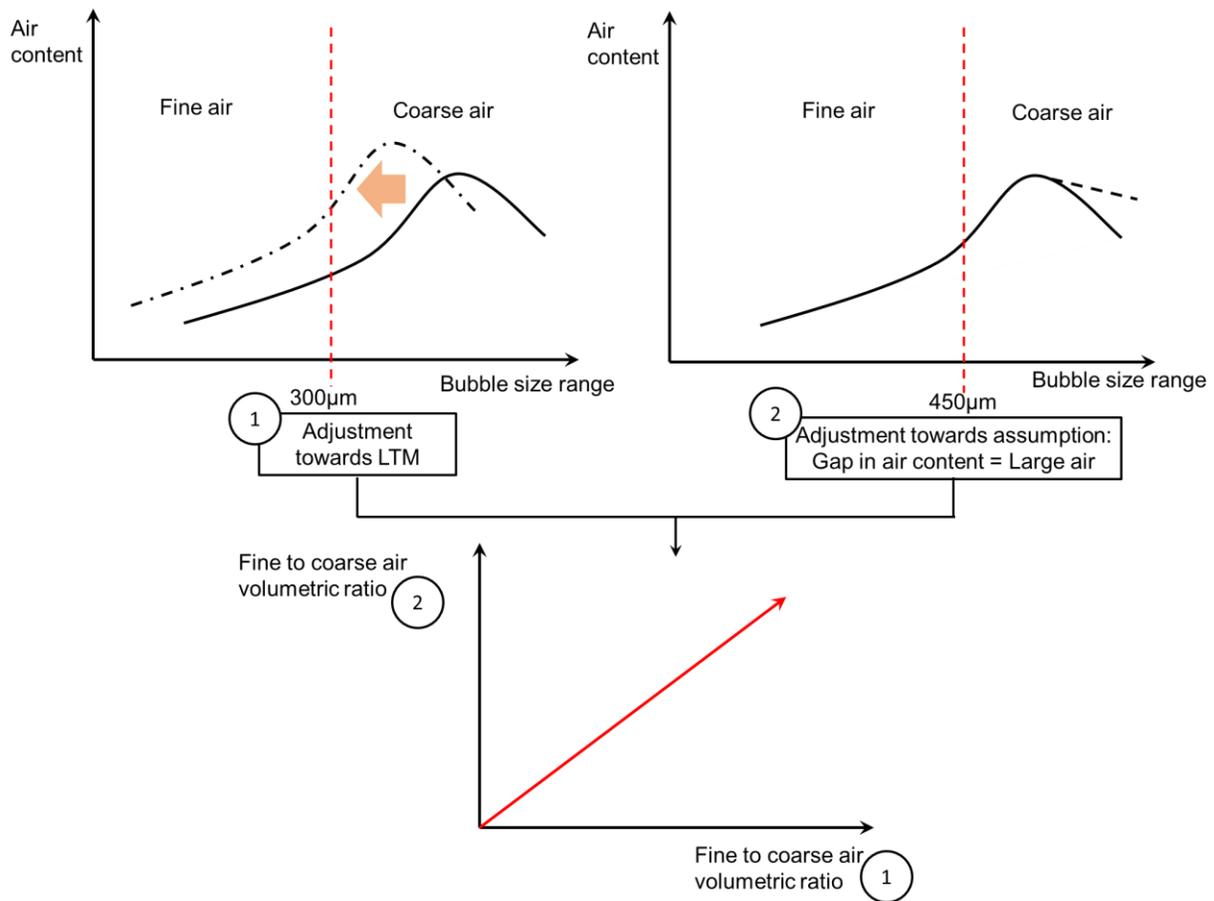
Fig. 2.13 Proposed procedures for correcting air size distributions obtained from AVA

REFERENCES

ASTM 457. Standard test method for microscopical determination of parameters of the air-void system in hardened concrete. American society of testing and materials, 2009.

Magura, D.D. (1996) Air void analyzer evaluation. *U.S. Department of Transportation*. Report no. FHWA-SA-96-062.

CHAPTER 3 EFFECTS OF ENTRAINED AIR BUBBLES ON MITIGATION OF FRICTION BETWEEN MORTAR AND MODEL COARSE AGGREGATE

3.1 INTRODUCTION

Air entrainment is known to offer the potential for reducing the cement content in self-compacting concrete (SCC). Since entrained air bubbles replace a certain portion of the SCC volume, the total volume of all other components, including cement, can be reduced by an equivalent amount. The effects of entrained air bubbles on the self-compactability of fresh concrete have also been studied (Attachaiyawuth and Ouchi, 2014, Attachaiyawuth et al, 2015 and 2016) with the aim of allowing further increase in the aggregate content and therefore reducing the cement content in SCC.

In their recent work, Attachaiyawuth et al, 2016 investigated how entraining air bubbles can enhance the self-compactability of fresh concrete, as measured in terms of concrete fill height. Fresh concretes with various dosages of air entraining agent (AEA) and mixing methods was tested. The investigation revealed that the fill height tends to increase as the total surface area of all entrained air bubbles rises. In their work, however, the size distributions of entrained air used in the evaluation were obtained by the Linear Transverse Method (LTM), which is an analytical method in which trapped bubbles are measured in the hardened state. Air distributions obtained using this method might differ from those measured during tests of the self-compactability of the fresh concrete.

In this chapter, various methods for enhancing the entrainment of fine air bubbles are investigated. These methods include the choice of air-entraining agent and mixing methods, as well as using a defoaming agent (Ouchi et al, 2017). The effects of entrained air size distribution

on friction between mortar and model coarse aggregate (Fmb) are studied. The air size distributions of the fresh mortar for the evaluation were obtained from AVA and corrected as discussed in **Chapter 2**.

3.2 MORTAR TEST PROCEDURES, MIX PROPORTIONS AND FRESH PROPERTIES

3.2.1 MORTAR TEST PROCEDURES

The tests carried out on fresh SCC mortar to evaluate entrained-air volumetric-stability and friction between mortar and model coarse aggregate (Fmb) are shown in **Table 3.1**. Size distributions of the entrained air bubbles in the fresh mortar were obtained by Air Void Analysis (AVA). Samples were evaluated by AVA at 5 and 20 minutes after mortar mixing with the aim of investigating the effects of entrained air size distribution on Fmb. All mortar tests except AVA were repeated three times and an average obtained for each mix proportion; in the literature (Rath et al, 2017a) it is suggested that AVA has satisfactory repeatability so only one test was required. Every batch of mortar was rested prior the tests at 5 minutes and 20 minutes**.** During these periods, the mortar was covered with a moist towel to prevent loss of moisture.

Table 3.1
Test procedure

Type	Procedure	
	5 minutes	20 minutes
Mortar	- Mortar flow test - Mortar funnel test - Air measurement (gravimetric method and AVA*)	- Remix for 5 sec. - Mortar flow test - Mortar funnel test - Air measurement (gravimetric method and AVA*) - V-funnel test on mortar with glass beads

*Only for mortar with air-entrainment

3.2.2 MORTAR MIX PROPORTIONS AND FRESH PROPERTIES

The mix proportions of mortars that were tested to investigate the effects of entrained air bubbles on the Fmb are all listed in **Table 3.2**. The water-to-powder ratio (w/p) was adjusted so that the relative funnel speed (Rm) of every batch of mortar was in the range of 1.30 to 1.40 (**Table 3.3**). The relative flow area (Γm) of every batch of mortar was also controlled, by altering the dosage of the superplasticiser (SP/P), to be in the range 5.5 to 6.6. Furthermore, the target was to achieve an air content in entrained-air mortars of 10% to 12% by changing the dosage of AEA. Thus, for all mix proportions with entrained air, s/m (where the mortar quantity includes the air) was between 0.49 and 0.50. As discussed in **Section 1.3.6**, by controlling these parameters, the effects of entrained air bubbles on the friction between model and coarse aggregate can be evaluated.

Various types of AEA were used: AEA1, AEA2, AEA3 and AEA4 (**Table 3.2**). Several mixing methods were tested for their ability to enhance the entrainment of fine air bubbles. The differences in these mixing methods mainly consist of different sequences of admixture additions. A defoaming agent (DA) was also employed in mortar mixes MA6 and MA9. The dosage of DA tested in the experiment was 0.10% by total weight of powder. Besides, this series of mortar mix proportions was used to analyse the improvement in volumetric stability of entrained air in fresh SCC mortar resulting from the enhanced entrainment of fine air bubbles.

Table 3.2
Mortar mix proportions

Mix	Mix proportion (kg/m³)								SP/P (%)	F.M.* of S	*s/m* including air	Mixing method
	C*	Water	S*	AEA1	AEA2	AEA3	AEA4	DA				
MA1	746	263	1340	-	-	-	-	-	1.20			
MA2	636	248	1474	0.044	-	-	-	-	1.30			
MA3	641	246	1474	-	0.385	-	-	-	1.22			B
MA4	633	249	1474	-	-	0.095	-	-	1.24			
MA5	619	253	1474	-	-	-	0.173	-	1.27	2.80	0.50	
MA6	627	251	1474	-	6.774	-	-	0.627	1.15			
MA7	636	248	1474	0.070	-	-	-	-	1.35			A
MA8	644	245	1474	-	-	0.258	-	-	1.35			
MA9	653	243	1474	-	-	2.286	-	0.653	1.30			C

* C: cement; S: fine aggregate; F.M.: fineness modulus; *s/m*: ratio of fine aggregate to mortar by volume

Table 3.3
Measured properties of mortar

Mix	Air content by gravimetric method (%)	Γm	Rm	Rm$_{avg}$	Rmb$_c$	Rmb$_a$
MA1	0.21	5.6	1.33		0.82	-
MA2	11.22	6.0	1.36		-	OBS*
MA3	10.39	5.9	1.37		-	0.81
MA4	11.24	5.8	1.32		-	0.77
MA5	10.82	5.8	1.37	1.36	-	OBS*
MA6	10.35	6.4	1.36		-	0.86
MA7	10.16	6.1	1.35		-	0.79
MA8	10.01	5.71	1.40		-	0.91
MA9	10.31	5.73	1.39		-	0.93

*OBS: obstructed (mortar with glass beads was unable to flow through the funnel)

3.3 ENHANCED FINE AIR ENTRAINMENT TO MITIGATE FRICTION BETWEEN MORTAR AND MODEL COARSE AGGREGATE

3.3.1 EFFECT OF AEA TYPE ON FRICTION BETWEEN AIR-ENTRAINED MORTAR AND MODEL COARSE AGGREGATE

Mortars made with the four different types of AEA were tested to investigate the effects of air size distribution in the mortar on friction between mortar and model coarse aggregate (Fmb). The tests entailed measuring the relative funnel speed of mortar with glass beads representing the coarse aggregate, both with air entrainment (Rmb_a) and without (Rmb_c), as well as the relative funnel speed of mortar without glass beads (Rm). Since Rm of all mortar mix proportions was controlled to be in the same range, the average Rm (Rm_{avg}) was used in the evaluation. The effects of entrained air on friction between mortar and coarse aggregate was quantified using the index $1-\Delta Rm_a/\Delta Rm_c$. The size distributions of the entrained air bubbles in the fresh mortar samples were determined by AVA.

Figure 3.1 shows that index $1-\Delta Rm_a/\Delta Rm_c$ was negative in mortars with AEA2 and AEA3. This suggests that the air bubbles entrained in the fresh mortar by AEA2 and AEA3 tend to increase the Fmb. After the addition of glass beads, the fresh mortars with AEA1 and AEA4 were unable to pass through the funnel during testing (**Table 3.2**). However, comparing only AEA type, this indicates that air bubbles entrained by AEA1 and AEA4 tend to reduce the flowability of the fresh mortar even more than AEA2 and AEA3. These effects may be attributed to the difference in characteristics of the air bubbles entrained by different types of AEA. **Figure 3.2** presents the size distributions of the entrained air bubbles in fresh mortar with the various AEA types. The results suggest that the reduced flowability obtained with AEA1 and AEA4, as compared to AEA2 and AEA3, may mainly result from the higher proportion of large entrained air bubbles with size over

450µm. As discussed in **Section 1.3.6**, due to the lower pressure inside larger bubbles (Muncaster, 1993), these larger entrained air bubbles may subject to larger deformation than the smaller ones. This may lead to less distance between model aggregate particles, acting as restraints to the mortar matrix, as the bubbles are compressed by the aggregate and.
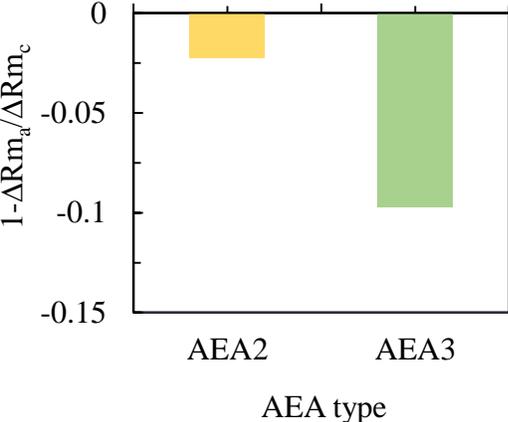
Fig. 3.1 Negative effects of entrained air bubbles on friction between model coarse aggregate, in terms of 1-ΔRm$_a$/ΔRm$_c$, in mortars with AEA2 and AEA3
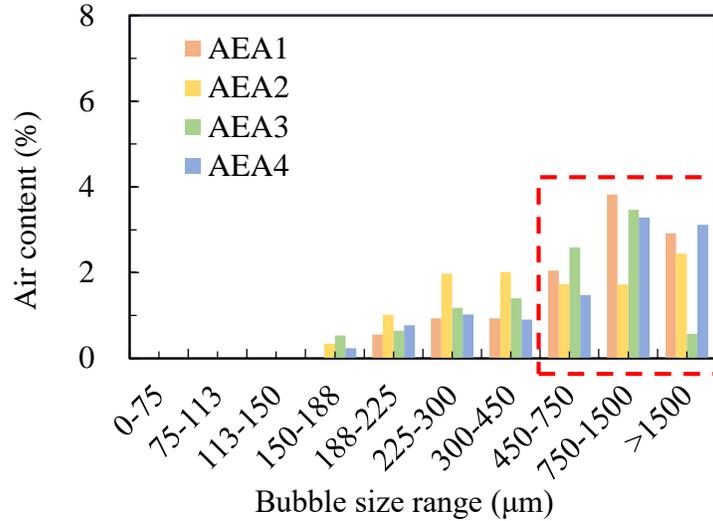
Fig. 3.2 Lower proportion of large entrained air bubbles (>450μm) in fresh mortars with AEA2 and AEA3 than with AEA1 and AEA4 at the time of glass bead addition

3.3.2 EFFECT OF MIXING METHOD ON FRICTION BETWEEN AIR-ENTRAINED MORTAR AND MODEL COARSE AGGREGATE

Mortar mix proportions MA1, MA2, MA4, MA7 and MA8 were tested to evaluate the effects of different mixing methods on entrained air bubbles in the fresh mortar and hence on the friction between mortar and coarse aggregate. The differences between the various mixing methods are mainly in the sequence of admixture addition, as indicated in **Table 1.3**. With mixing method B, both superplasticiser (SP) and AEA were added to the mortar at the same time, while with method A the SP was added to the mortar prior to the addition of the AEA. Rath et al (2017b) have suggested that mixing method A will increase the fineness of the entrained air bubbles by reducing the viscosity of the mortar prior to AEA addition. This sequence may also prevent the SP from interfering with air entrainment. The effects of entrained air bubbles on Fmb were quantified in terms of $1-\Delta Rm_a/\Delta Rm_c$.

The results indicate that method A yields a higher $1-\Delta Rm_a/\Delta Rm_c$ whatever the type of AEA. **Figure 3.3** suggests that, with this method, fresh mortar with AEA1 containing glass beads was able to flow through the funnel (in contrast with the findings in **Section 3.3.1**), owing to the change in mixing method. Further, the air bubbles entrained with AEA3 when using mixing method A reduce the Fmb (**Fig. 3.3**). The higher $1-\Delta Rm_a/\Delta Rm_c$ with this mixing procedure may be attributed to the higher content of fine entrained air bubbles of size smaller than 450μm (**Fig. 3.4**). These fine air bubbles may act as compressible bearings, as discussed in **Section 1.3.6**, and lead to reduced shear force between mortar and model coarse aggregate (Edmeades and Hewlett, 1998). Moreover, **Fig. 3.4** indicates that the proportion of large air bubbles (>450μm), which may subjected to large deformation, is reduced in fresh mortar mixed using method A, as compared to that mixed with method B. This suggests that, under compression, the model coarse aggregate spacing during funnel testing is reduced with method B as compared to with method A.
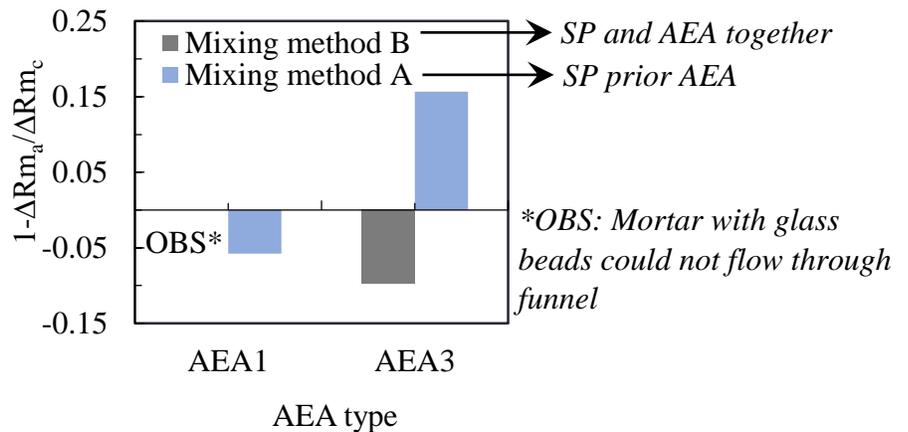
Fig. 3.3 Higher values of $1-\Delta Rm_a/\Delta Rm_c$, in mortar with mixing method A as compared to that with mixing method B for any type of AEA
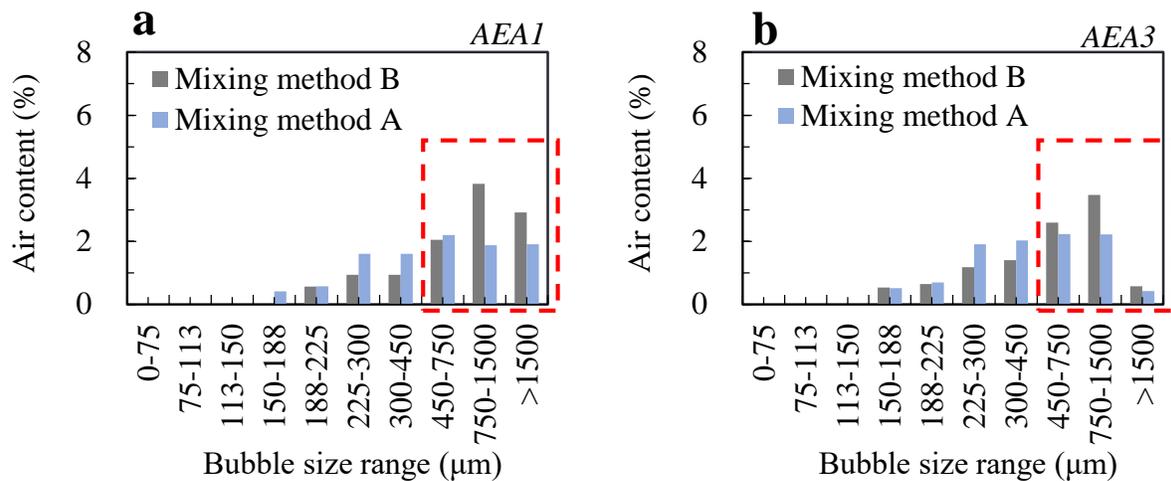
Fig. 3.4 Higher content of fine entrained air bubbles (<450μm) in mortar at time of glass bead addition with mixing method A, as compared to that with mixing method B, for both AEA1 (a) and AEA3 (b)

3.3.3 USE OF DEFOAMING AGENT TO REDUCE FRICTION BETWEEN AIR-ENTRAINED MORTAR AND MODEL COARSE AGGREGATE

Ouchi et al (2017) indicated that the addition of a defoaming agent (DA) can eliminate large entrained air bubbles, so DA has the potential to enhance the entrainment of fine air. A DA was included in mortar mix MA6. Mortar mix proportions MA1, MA3 and MA6 were tested. The results were analysed to investigate whether defoaming enhances the ability of entrained air bubbles to reduce the Fmb. In this analysis also, the effects were quantified in terms of $1-\Delta Rm_a/\Delta Rm_c$.

Figure 3.5 illustrates how $1-\Delta Rm_a/\Delta Rm_c$ was higher in mortar with AEA2 when the DA was employed. **Figure 3.6** shows that, in the fresh mortar with the DA, there was a higher content of fine entrained air bubbles (<450μm), which can act as compressible bearings, and a lower

42

content of large and easily deformed bubbles (>450μm). This may be mainly attributed to the

ability of DA to eliminate large air bubbles and enhance the entrainment of fine air bubbles.
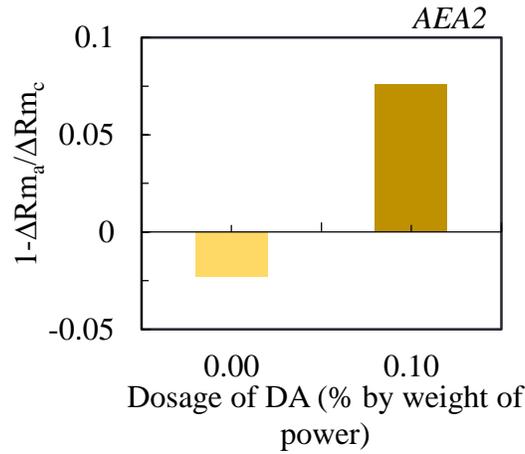
Fig. 3.5 Reduced friction between mortar and model coarse aggregate in terms of 1-

ΔRm$_a$/ΔRm$_c$ with use of DA
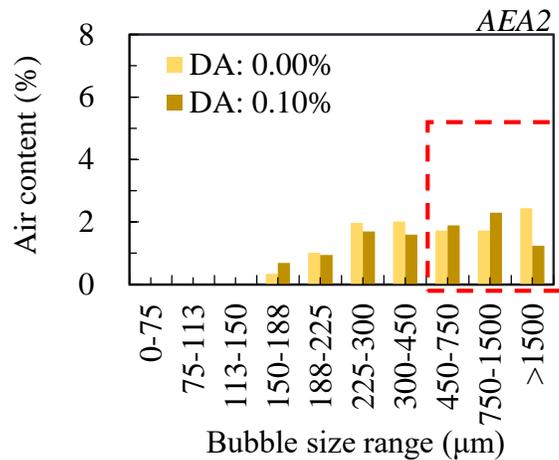
Fig. 3.6 Higher proportion of fine entrained air bubbles (<450μm) at the time of glass bead

addition when a DA is used

3.3.4 RELATIONSHIP BETWEEN DISTRIBUTION OF ENTRAINED BUBBLE SIZE AND FRICTION BETWEEN MORTAR AND MODEL COARSE AGGREGATE

With the aim of clarifying the relationship between entrained air bubble size distribution and Fmb in terms of $1-\Delta Rm_a/\Delta Rm_c$, the experimental results from all mortar mix proportions, MA1, MA2 MA3, MA4, MA5, MA6, MA7, MA8 and MA9, were analysed. The results of this analysis suggest that fine entrained air bubbles, of size smaller than 450μm, have a positive effect, with a higher proportion of such bubbles corresponding to an increase in $1-\Delta Rm_a/\Delta Rm_c$, as shown in **Fig. 3.7**.

Since the air content of all mortars in this series of experiments was controlled to be in the same range, a higher fine air bubble content also suggests a lower proportion of large bubbles. The negative effects of large air bubbles, of size over 450μm, on $1-\Delta Rm_a/\Delta Rm_c$ are illustrated in **Fig. 3.8**. These results suggest that 450μm may be the critical size, with smaller sizes enhancing the mortar-aggregate friction-reducing effects of entrained air bubbles. The results also suggest that, while fine entrained air bubbles can have a positive effect, large ones may be detrimental and increase friction between mortar and coarse aggregate. There is a proportional relationship between rising volumetric ratio of fine to coarse air bubbles (*fb/cb*) when the critical size is set to 450μm and enhanced $1-\Delta Rm_a/\Delta Rm_c$, as presented in **Fig. 3.9**. Further, the results for mixes MA2 and MA5 suggested that, with *fb/cb* below 0.34, fresh mortar with glass beads may be unable to flow through the funnel (**Fig. 3.9**). The mortar-aggregate friction-reducing effects of fine entrained air bubbles are simply illustrated in **Fig. 3.10 (a)**, with the deformation of large air bubbles shown in **(b)**.
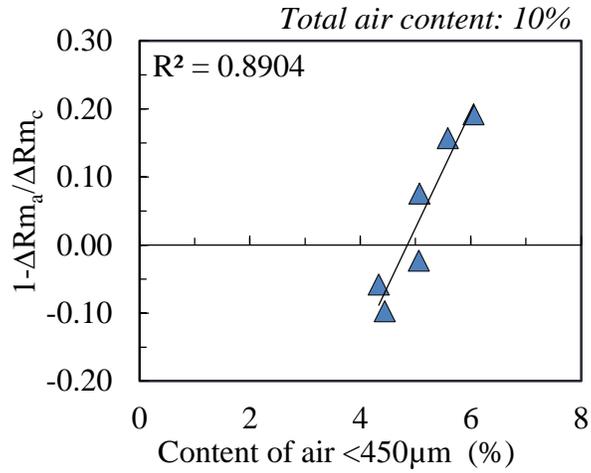
Fig. 3.7 Positive effects of fine entrained air bubbles (<450μm) on 1-ΔRm$_a$/ΔRm$_c$
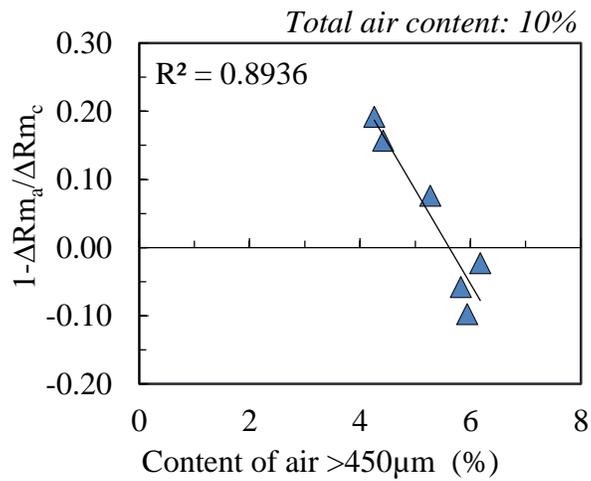
Fig. 3.8 Negative effects of large entrained air bubbles (>450μm) on 1-ΔRm$_a$/ΔRm$_c$
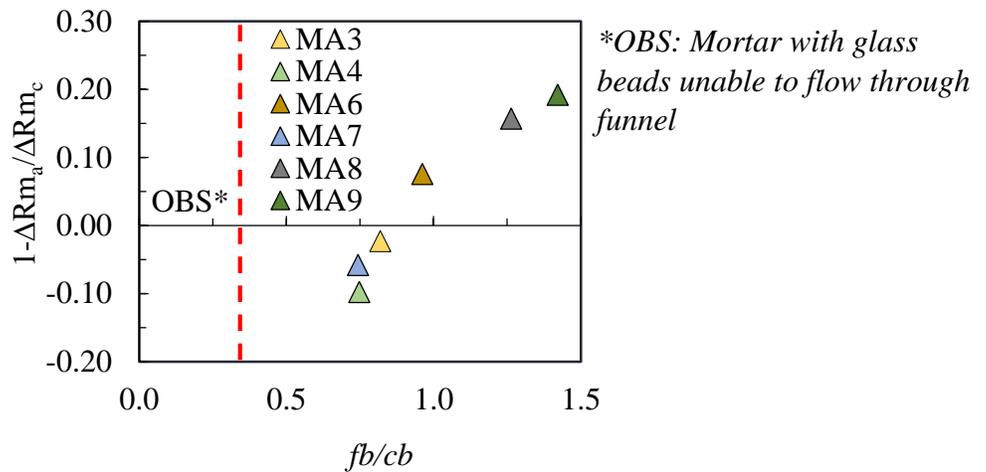
Fig. 3.9 Proportional Relationship between friction-reducing effects of entrained air bubbles (1-ΔRm_a/ΔRm_c) and volumetric ratio of fine to coarse air bubbles (*fb/cb*) with critical size of 450μm
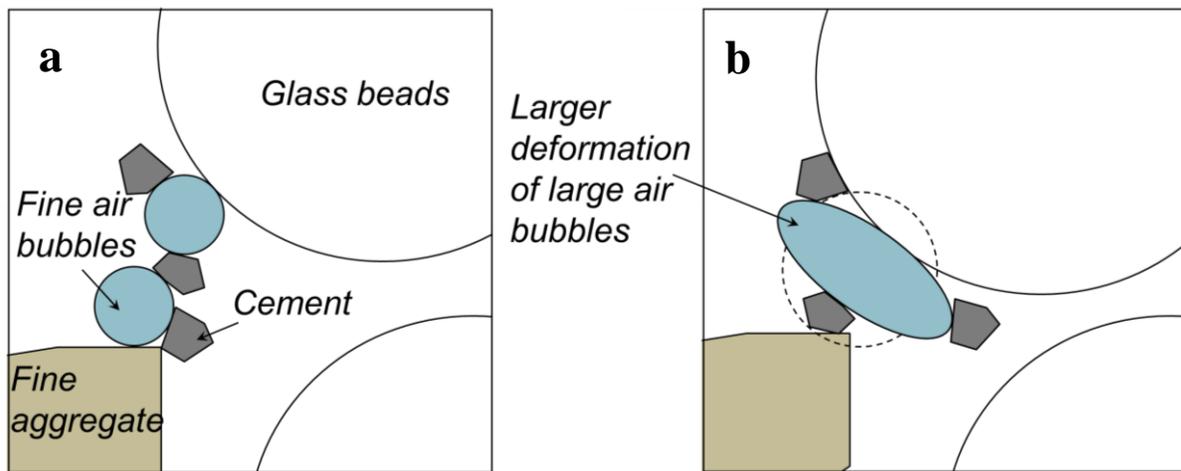
Fig. 3.10 Fine entrained air bubbles acting as compressible bearings (a) that reduce friction between mortar and model coarse aggregate (Edmeades and Hewlett, 1998) and reduced distance between aggregate particles due to large deformation of large air bubbles (b)

3.3.5 CONCEPTUAL EQUATION FOR EFFECTS OF ENTRAINED AIR BUBBLES ON

FRICION REDUCTION

As discussed in **Section 3.3.4**, the fine air bubbles with the size smaller than 450μm tends

to have positive effects on friction reduction, while large air bubbles with the size over 450μm

leads to negative effects. Therefore, a conceptual equation for the effects of entrained air bubbles

on friction reduction may be written in terms of:

$$1 - \frac{\Delta Rm_a}{\Delta Rm_c} = f(fb) + g(cb) \qquad (3.1)$$

Where $1-\Delta Rm_a/\Delta Rm_c$ is the net effects of entrained air on reduction in friction between mortar

and model coarse aggregate; *fb* and *cb* are the content fine and coarse air bubbles (%),

respectively, with 450 as a boundary size; functions *f* and *g* are functions of fine and coarse air

bubbles, respectively, on the friction reduction.

According to the results from **Section 3.3.4**, both function f and g should be linear at

certain content of fine and coarse air bubbles (**Fig. 3.11**). Therefore Eq. (3.1) can be simply

written as:

$$1 - \frac{\Delta Rm_a}{\Delta Rm_c} = (A \times fb) + (B \times cb) \qquad (3.2)$$

Where coefficients *A* and *B* are the effectiveness of fine and coarse air bubbles, respectively, on

the friction reduction.

In the case of the experimental results in this research, coefficients *A* and *B* can be

obtained by considering the content of fine and coarse air at no mitigation in friction (1-

$\Delta Rm_a/\Delta Rm_c = 0$). Consequently, by rearranging Eq. (3.2) B to A ratio can be attained through

the x-intersect of the relationship between content of fine and coarse air and $1-\Delta Rm_a/\Delta Rm_c$ (**Fig.**

3.7 and **Fig. 3.8**):

$$\frac{B}{A} = -\left(\frac{fb_0}{cb_0}\right) \qquad (3.3)$$

Where fb_0 and cb_0 are the content of fine and coarse air, respectively, at no mitigation in friction.

From **Fig. 3.7** and **Fig. 3.8**, B to A ratio, in this case, is around -0.87. Furthermore, Eq. (3.2) can rearranged into:

$$1 - \frac{\Delta Rm_a}{\Delta Rm_c} = A \times \left(fb + \left(\frac{B}{A} \times cb\right)\right) \qquad (3.4)$$

According to the above equation coefficient A is the inclination of the relationship shown in **Fig. 3.12**. After coefficient A has been obtained, coefficient B can be further calculated. In this research, coefficient A and B are around 0.089 and -0.077, respectively.
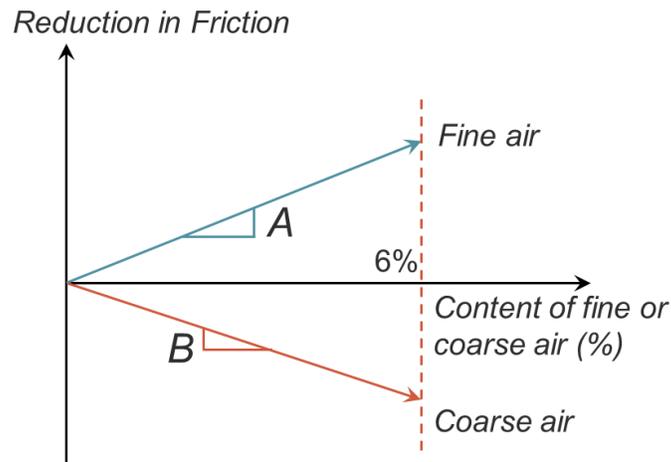
Fig. 3.11 Linear effects of fine and coarse air bubbles on reduction in friction between mortar and model coarse aggregate

Total air content: 10%

$y = 0.0888x$
$R^2 = 0.964$
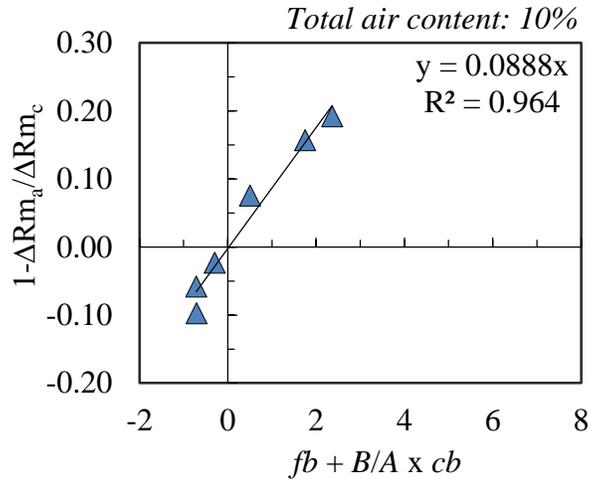
Fig. 3.11 Linear relationship between $1\text{-}\Delta Rm_a/\Delta Rm_c$ and *fb* + *B/A* x *cb*

3.5 CONCLUDING REMARKS

A series of mortar samples with different mix proportions were tested to investigate the effects of entrained air bubbles, and particularly the distribution of air bubble size, on Fmb. Various methods with potential to enhance the entrainment of fine air bubbles in the fresh mortar were used. The following conclusions can be drawn based on the evaluation of the results:

1) The entrainment of fine air bubbles in the fresh mortar of SCC can be enhanced through various methods including:

- Selection of a suitable air-entraining agent

- Adding the superplasticiser to the mortar during mixing prior to addition of the air-entraining agent

- Addition of a defoaming agent

2) Friction between mortar and model coarse aggregate tends to fall as the proportion of fine entrained air bubbles (<450μm) increases. This may attributed mainly to the relatively free

49

motion in shear between mortar and model coarse aggregate with fine air bubbles acting as compressible bearings.

3) Large air bubbles (>450μm) are found to increase the friction between mortar and model coarse aggregate. This may be because large bubbles may subjected to large deformation under compression between aggregate particles. This leads to reduced distance between aggregate particles acting as restraints to the mortar matrix.

4) A proportional relationship is demonstrated between a higher volumetric ratio of fine bubbles to coarse bubbles, when the critical size is set to 450μm, and falling friction between mortar and model coarse aggregate.

In summary, a higher entrained air content increases the total volume of self-compacting concrete, while a higher proportion of fine entrained air bubbles reduces the friction between mortar and coarse aggregate, as summarised in **Fig. 3.13**. This suggests that entraining suitable air bubbles has the potential to enhance the self-compactability of fresh concrete while also being very beneficial in reducing the cement content of self-compacting concrete.
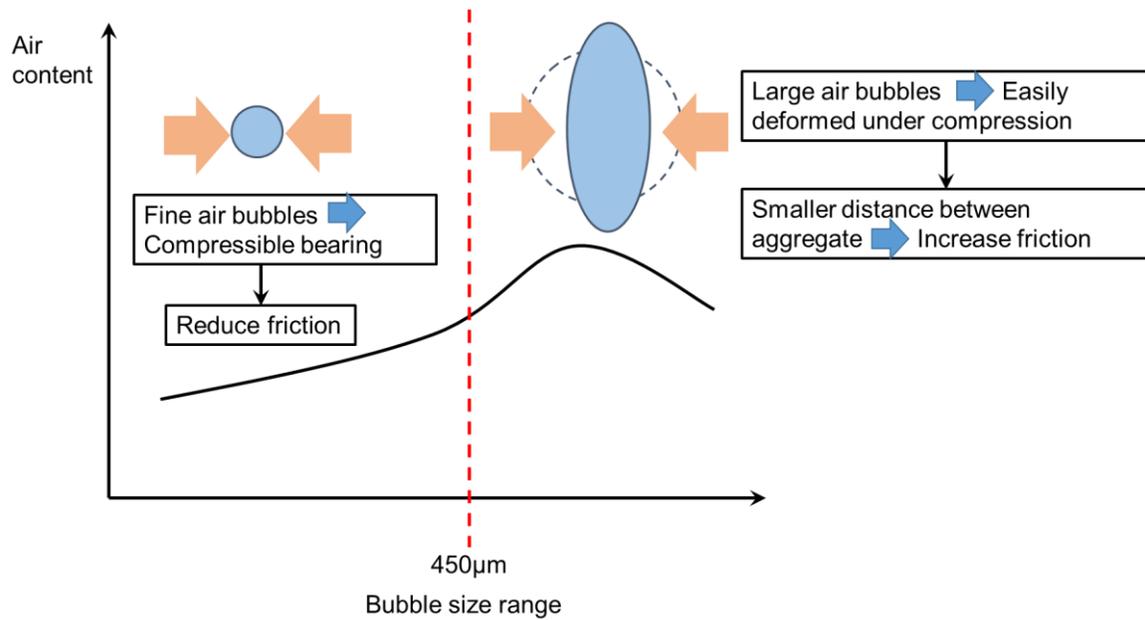
Fig. 3.13 Summarised effects of entrained air bubbles on friction between mortar and model coarse aggregate

REFERENCES

Attachaiyawuth, A. and Ouchi, M. (2014) Effect of entrained air on mitigation of reduction in interaction between coarse aggregate and mortar during deformation of self-compacting concrete at fresh state. *Proceedings of the Japan Concrete Institute*. 36: 1444-1449.

Attachaiyawuth, A., Tanaka, K., Rath, S. and Ouchi, M. (2015) Air-enhanced self-compactability of fresh concrete with effective mixing method. *Proceedings of the Japan Concrete Institute*. 37: 1069-1074.

Attachaiyawuth, A., Rath, S., Tanaka, K. and Ouchi, M. (2016). Improvement of self-compactability of air-enhanced self-compacting concrete with fine entrained air. *Journal of Advanced Concrete Technology*. 14: 55-69.

Edmeades, R.M. and Hewlett, P.C. (1998) 15 Cement admixtures. *Lea's Chemistry of Cement and Concrete*. 841-905.

Ley, M.T., Folliard, K.J. and Hover, K.C. (2009a) Observations of air-bubbles escaped from fresh cement paste. *Cement and Concrete Research*. 39 (5): 409-416.

Ley, M.T., Chancey, R., Juenger, M.C.G. and Folliard, K.J. (2009b) The physical and chemical characteristics of the shell of entrained air bubbles in cement paste, *Cement and Concrete Research*. 39 (5): 417-425.

Muncaster, R. (1993) *A-level physics*. Nelson Thornes, UK.

Ouchi, M., Kameshima, K. and Attachaiyawuth, A. (2017) Improvement in self-compacting properties of fresh concrete by eliminating large air bubbles using an antifoaming agent. *Journal of Advanced Concrete Technology*. 15: 29-37.

Rath, S., Puthipad, N., Attachaiyawuth, A. and Ouchi, M. (2017a) Critical size of entrained air to stability of air volume in mortar of self-compacting concrete at fresh state. *Journal of Advanced Concrete Technology*. 15: 29-37.

Rath, S., Ouchi, M., Puthipad, N. and Attachaiyawuth, A. (2017b) Improving the stability of entrained air in self-compacting concrete by optimizing the mix viscosity and air entraining agent dosage. *Construction and Building Materials*. 148: 531-537.

CHAPTER 4 COMBINED EFFECTS OF FINE ENTRAINED AIR BUBBLES AND FLY ASH ON IMPROVEMENT IN SELF-COMPACTABILITY OF FRESH CONCRETE

4.1 INTRODUCTION

Fly ash is in wide use as a replacement for cement to improve the environmental credentials of concrete. Since fly ash is a by-product of burning coal in electric power plants, it is abundant and there is a desire increase its re-use. Fly ash undergoes pozzolanic and hydration reactions similar to cement, so through these chemical reactions the required compressive strength of concrete can be maintained at an appropriate replacement ratio (Dhir et al, 1988, Tangtermsirikul, 2003 and Oner et al, 2005). Moreover, owing to the spherical shape of its particles, fly ash also enhances the flowability of the fresh concrete. Consequently, fly ash is a widely used ingredient in self-compacting concrete (SCC) due to its low cost and good performance as a cement replacement (Güneyisi et al, 2013).

The effects of fly ash on the fresh and rheological properties of SCC have been studied in depth (Tangtermsirikul, 2003, Wattanalarmlerd and Ouchi, 2005, and Liu, 2010, Zhao et al, 2015 and Güneyisi et al, 2015). In particular, Tangtermsirikul (2003) has intensely studied and clarified the influence of fly ash on workability of fresh concrete. The detailed method of mix design for concrete with fly ash was also proposed (Tangtermsirikul, 2003).

Wattanalarmlerd and Ouchi (2005) also investigated the influence of fly ash on the flowability of SCC in terms of mortar flow area and funnel speed. They concluded that fly ash acts as a form of lubricant due to its spherical shape. Fly ash can also prevent the formation of agglomerate cement particle lumps. This suggests the potential of fly ash to enhance the self-compactability of fresh concrete.

Furthermore, Naik et al (2012) reported on research in which cement was replaced with fly ash in SCC for reasons of economy. They suggested that the spherical particles of fly ash have a ball-bearing effect that reduces friction between paste and large aggregate particles. This can considerably reduce the dosage of superplasticiser required in SCC. Therefore, with a high volume of fly ash, a high-strength yet economical SCC can be developed (Naik et al, 2012).

In **Chapter 3**, it was determined that the friction between mortar and model coarse aggregate (Fmb) can also be reduced by entraining fine air bubbles. This suggests that there is a potential combined effect of fly ash and fine bubble entrainment in which the self-compactability of fresh concrete might be further enhanced. Until now, however, the combined effects of entrained air bubbles and fly ash on the self-compactability of fresh concrete have not been studied.

In this chapter, the effects of fly ash and fine entrained air bubbles on the Fmb are first compared. Then it is investigated whether the combined effects of fly ash and fine entrained air bubbles can further reduce the friction in the case of a higher aggregate content SCC.

4.2 MORTAR AND CONCRETE TEST PROCEDURES, MIX PRPORTIONS AND FRESH PROPERTIES

4.2.1 MORTAR AND CONCRETE TEST PROCEDURES

Table 4.1 shows all the tests carried out on the fresh properties of mortar and concrete with the aim of evaluating the volumetric stability of entrained air and the friction between mortar and model coarse aggregate (Fmb) in fresh SCC mortar. All tests on mortar except Air Void Analysis (AVA) were repeated three times for each mix and the results averaged; in the literature (Rath et al, 2017) it is suggested that AVA has satisfactory repeatability so only one test was required. After the tests at 5 minutes, every batch of mortar was rested. During these rest periods, the mortar was

covered with a moist towel to prevent loss of moisture. Tests on the finished concrete were performed once for each mix so as to verify the results obtained from mortar testing.

In order to reduce the time required for testing, the size distribution of entrained air bubbles in the fresh mortar obtained at 5 minutes was also used in investigating the effects of entrained air size distribution on the Fmb. Since this friction testing was carried out at 20 minutes, the distributions obtained at 5 minutes were corrected prior to the evaluation, as explained later in **Section 4.3**.

Table 4.1
Test procedure

Type	Procedure	
	5 minutes	20 minutes
Mortar	- Mortar flow test - Mortar funnel test - Air measurement (gravimetric method and AVA*)	- Remix for 5 sec. - Mortar flow test - Mortar funnel test - Air measurement (gravimetric method) - Mortar with glass beads V-funnel test
Concrete	- Concrete slump flow test - Air measurement (gravimetric and AVA) - Concrete V-funnel test - Concrete box test	

*Only for mortar with air-entrainment

4.2.2 MORTAR AND CONCRETE MIX PRPORTIONS AND FRESH PROPERTIES

Two sets of mortar mix proportions were tested, 'MF' and 'MAF', as shown in **Table 4.2**. Various ratios (fa/m) of fly ash to total mortar (including air) were considered in these two sets. The water-to-powder ratio (w/p) was adjusted such that the relative funnel speed (Rm) of every batch of mortar in each set, each of which had the same fine aggregate content (s/m), was in the same range (**Table 4.3**). Further, the Γm value of every batch was controlled to be in the range of 5.5 to 6.6 by altering the dosage of the superplasticiser (SP/P), so mortar with a similar Rm in each

case could be used to analyse the effects of fly ash and entrained air bubbles on the self-compactability of the fresh concrete. Furthermore, the target air content in the entrained-air mortars was 10% to 12%, which was achieved by changing the AEA dosage. Thus, for all mix proportions with entrained air, the value of s/m (where the mortar quantity includes the air) was between 0.49 and 0.50.

A defoaming agent (DA) was employed in mortar mix proportions MAF5, MAF6, MAF9 and MAF10 in order to evaluate the effects of entrained air size distribution on the Fmb in fresh concrete with fly ash. This series of mortars was also used to analyse the enhancement of entrained air bubble stability resulting from addition of the DA. The dosages of DA tested in the experiment were 0.05% and 0.10% by total weight of powder.

The average value of Rm (Rm_{avg}) used for the evaluation is shown in **Table 4.3**. The dosage of superplasticiser was also adjusted to control Γ_m of every batch of mortar to be in the same range of 5.5 to 6.6.

Certain mortar mixture proportions (MF1, MF3, MF4, MF5, MF6 and MF7) were chosen for verification by testing the concrete as well. These mixes are designated CF1, CF2, CF3, CF4, CF5 and CF6 and were also used for clarifying the effects of fly ash with a higher fine aggregate content in SCC (**Table 2.1**). Mortar mix proportions MAF2, MAF7 and MAF11 were also selected for verification by concrete testing; these concrete mixes are designated CAF1, CAF2 and CAF3. They are used to clarify the effects of fine entrained air bubbles on self-compactability in fresh concrete with fly ash (**Table 4.2**). The air content of the entrained air concrete was controlled within the range 7% to 9% by adjusting the dosage of AEA (**Table 4.3**). Subsequently, the ratio (g/c) of coarse aggregate to total concrete (including entrained air) was held constant in the range 0.29 to 0.30 in all concrete mix proportions. Also, s/m (where the mortar quantity includes the

entrained air) was controlled to between 0.49 and 0.50. Additionally, SP/P was altered to control

the slump flow of every concrete mix proportion in the range 600mm to 700mm.

Table 4.2
Mortar and concrete mix proportions

Mix	Mix proportion (kg/m³)								SP/P (%)	F.M. of S	*fa/m* including air	Mixing method	*s/m* including air
	C*	Fly ash	W*	S*	G*	AEA 1	AEA 2	DA					
MF1	749	-	262	1340	-	-	-	-	2.13		0.00		0.50
MF2	600	150	247	1340	-	-	-	-	1.34		0.06		0.50
MF3	430	299	239	1340	-	-	-	-	1.02		0.12		0.50
MF4	282	423	234	1340	-	-	-	-	0.88	2.7	0.17	B	0.50
MF5	674	-	236	1474	-	-	-	-	3.01		0.00		0.54
MF6	394	274	211	1474	-	-	-	-	1.16		0.11		0.55
MF7	258	387	207	1474	-	-	-	-	0.86		0.16		0.54
MAF1	776	-	254	1340	-	-	-	-	1.33		0.00		0.50
MAF2	493	240	244	1340	-	-	-	-	0.90		0.10		0.49
MAF3	672	-	237	1474	-	0.05	-	-	1.65		0.00		0.50
MAF4	562	107	227	1474	-	0.08	-	-	1.55		0.04		0.50
MAF5	355	267	226	1474	-	0.12	-	-	0.84		0.10		0.50
MAF6	338	267	242	1474	-	0.42	-	0.30	0.82	2.9	0.10	A	0.50
MAF7	341	267	230	1474	-	1.10	-	0.61	0.99		0.10		0.50
MAF8	656	-	242	1474	-	-	0.53	-	1.20		0.00		0.50
MAF9	341	267	230	1474	-	-	3.16	-	0.65		0.10		0.50
MAF10	331	267	234	1474	-	-	5.74	0.30	0.56		0.10		0.50
MAF11	338	267	232	1474	-	-	7.26	0.60	0.58		0.10		0.50
CF1	524	-	184	938	810	-	-	-	1.90		0.00		0.48
CF2	301	209	167	938	810	-	-	-	0.82		0.12		0.48
CF3	197	296	164	938	810	-	-	-	0.65	2.7	0.17	B	0.48
CF4	472	-	165	1032	810	-	-	-	2.81		0.00		0.54
CF5	276	192	148	1032	810	-	-	-	0.96		0.11		0.54
CF6	181	271	145	1032	810	-	-	-	0.80		0.16		0.54
CAF1	345	168	171	938	810	-	-	-	0.80		0.10		0.49
CAF2	232	181	157	1002	864	0.25	-	0.41	0.95	2.9	0.10	A	0.49
CAF3	230	181	157	1002	864	-	3.29	0.41	0.65		0.10		0.50

*C: Cement; W: Water; S: fine aggregate; G: coarse aggregate; *fa/m*: volume of fly ash in mortar; *s/m*: fine aggregate to mortar volumetric ratio

Table 4.3
Measured properties of mortar and concrete

Mix	Air content by gravimetric method (%)	Γm	Rm	Rm$_{avg}$	Rmb$_c$	Rmb$_a$	Rmb$_{fa}$	Rmb$_{afa}$	Slump flow (mm)	Funnel time (s)	Fill height (mm)
MF1	0.18	5.8	1.71		0.97	-	-	-	-	-	-
MF2	0.08	6.1	1.71	1.71	-	-	1.02	-	-	-	-
MF3	0.19	6.3	1.73		-	-	1.08	-	-	-	-
MF4	0.89	6.1	1.67		-	-	1.10	-	-	-	-
MF5	1.64	5.5	0.71		0.30	-	-	-	-	-	-
MF6	0.80	6.2	0.74	0.74	-	-	0.41	-	-	-	-
MF7	1.84	5.8	0.77		-	-	0.46	-	-	-	-
MAF1	0.00	5.7	1.36		0.79	-	-	-	-	-	-
MAF2	1.64	6.0	1.36		-	-	0.89	-	-	-	-
MAF3	10.70	5.7	1.36		-	0.80	-	-	-	-	-
MAF4	10.13	5.5	1.40		-	-	-	0.85	-	-	-
MAF5	10.94	5.7	1.36		-	-	-	0.90	-	-	-
MAF6	10.50	5.6	1.38	1.37	-	-	-	0.94	-	-	-
MAF7	10.67	5.5	1.36		-	-	-	0.97	-	-	-
MAF8	10.46	5.7	1.39		-	-	-	0.89	-	-	-
MAF9	10.86	5.8	1.39		-	-	-	0.97	-	-	-
MAF10	10.03	5.8	1.37		-	-	-	0.97	-	-	-
MAF11	10.73	6.1	1.35		-	-	-	1.02	-	-	-
CF1	3.39	-	-	-	-	-	-	-	640	10.8	87.5
CF2	1.71	-	-	-	-	-	-	-	685	6.0	290.0
CF3	2.72	-	-	-	-	-	-	-	620	11.1	255.0
CF4	1.56	-	-	-	-	-	-	-	605	35.6	0.0
CF5	0.98	-	-	-	-	-	-	-	610	17.0	75.0
CF6	0.85	-	-	-	-	-	-	-	600	11.1	135.0
CAF1	1.54	-	-	-	-	-	-	-	630	9.83	143
CAF2	8.84	-	-	-	-	-	-	-	670	6.90	150
CAF3	7.42	-	-	-	-	-	-	-	700	8.68	250

4.3 ESTIMATED ENTRAINED AIR SIZE DISTRIBUTIONS 20 MINUTES AFTER MORTAR MIXING

As mentioned in **Section 4.2.1**, in order to reduce the testing time, the entrained air size distributions obtained at 5 minutes were used to analyse the effects of entrained air on friction between mortar and model aggregate in the fresh mortar with fly ash at 20 minutes. However, the data obtained shows an apparent slight reduction in the air content of mortar from the initial value

over the period from 5 to 20 minutes after mixing (**Fig. 4.1**). Analysis of the results from **Chapter 3** suggested that this may result from the rapid escape of large (>450µm) entrained air bubbles (see **Appendix B**). With the tests for interaction between mortar and model coarse aggregate conducted at 20 minutes, this slight reduction in air content needs to be taken into consideration. For simplicity, all size distributions obtained by AVA at 5 minutes were adjusted based on the assumption that the proportion of larger (>450µm) bubbles falls proportionally with time. The results from **Chapter 3** were then used to verify this assumption. The results indicated that this assumption is satisfactory, with agreement between the ratios of fine to coarse air bubbles obtained from the calculated (estimated) and measured air size distributions (**Fig. 4.2**). The critical size delineating the fine and coarse air bubbles is 450µm as previously suggested in **Section 3.3.4**.
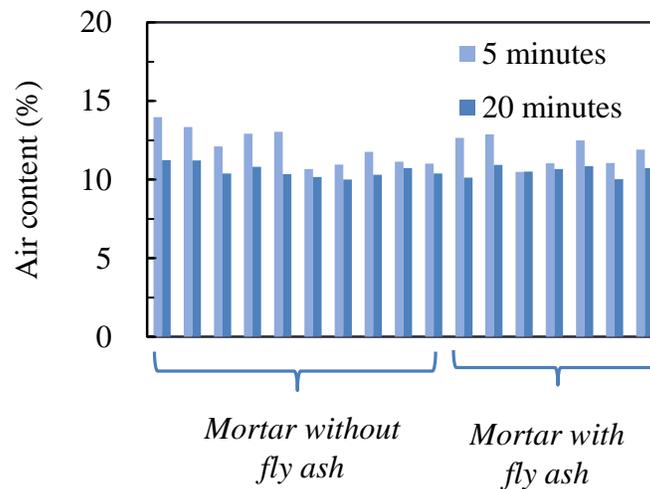
Fig. 4.1 Slight reduction in content of entrained air between 5 and 20 minutes
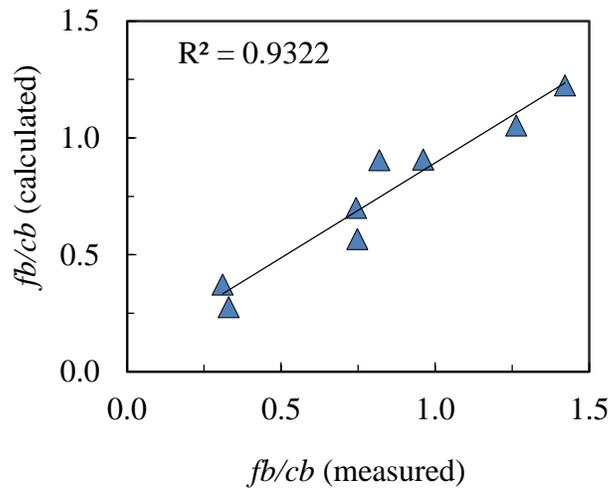
Fig. 4.2 Satisfactory agreement between measured and calculated (from values in fresh mortar at 5 minutes) ratios of fine to coarse air bubbles in fresh mortar at 20 minutes

4.4 COMPARISON BETWEEN THE EFFECTS OF FLY ASH AND FINE ENTRAINED AIR BUBBLES ON REDUCTION IN FRICTION BETWEEN MORTAR AND MODEL COARSE AGGREGATE

4.4.1 EFFECT OF FLY ASH ON REDUCTION IN FRICTION BETWEEN MORTAR AND MODEL COARSE AGGREGATE

Mortar mixes MF1, MF2, MF3, MF4, MF5, MF6 and MF7 were tested and analysed to clarify how effectively fly ash acts to reduce the Fmb. The effect of fly ash on reducing friction was quantified in terms of relative funnel speed of mortar containing glass beads in cases with (Rmb_{fa}) and without (Rmb_c) fly ash, and the relative funnel speed of mortar without glass beads (Rm). Since Rm was held in the same range in every mortar mix proportion, the Rm value used in the evaluation was the average Rm (Rm_{avg}). That is, as explained in **Section 1.3.1.2**, the effect of fly ash on the Fmb was analysed in terms of the index $1-\Delta Rm_{fa}/\Delta Rm_c$.

Table 4.2 shows that the required water content was reduced at higher fly ash to powder ratios (*fa/p*) in order to obtain a mortar with the same Rm. Additionally, in spite of the lower *w/p*, fly ash was found to reduce the required dosage of superplasticiser to achieve an equal mortar relative flow area (Γm).

The results indicate that the index $1-\Delta Rm_{fa}/\Delta Rm_c$ increased with respect to higher *fa/p* (**Fig. 4.3**). Since the relative funnel speed (Rm) of every mix in this series of experiments was controlled to the same range, this increase in $1-\Delta Rm_{fa}/\Delta Rm_c$ may be explainable in terms of a reduction in shear force between the paste and both the fine aggregate particles and the model coarse aggregate particles, owing to the spherical shape of the fly ash particles (**Fig. 4.4**). The reasons for this reduced shear force include the ball-bearing effect and the reduced contact area between solid particles when spherical fly ash is present.

The effect of fly ash on the self-compactability of fresh concrete with a higher *s/m* of 0.55 was also quantified. The results indicate lower funnel speeds, Rm, in fresh mortar with higher proportion of fine aggregate (**Fig. 4.3**). This may result from the stress on the paste phase, which derives from the fine aggregate, being higher when *s/m* is higher. This higher stress can be attributed to the smaller separation between fine aggregate particles as *s/m* in the fresh mortar increases. However, **Fig. 4.3** shows a greater increase in $1-\Delta Rm_{fa}/\Delta Rm_c$ in the fresh mortar with higher *s/m* as the proportion of fly ash is increased. With a higher proportion of fine aggregate, the distance between aggregate particles is smaller and there is a higher chance of interaction between fly ash and fine aggregate. Hence, fly ash may be more effective in mortars with higher *s/m*.
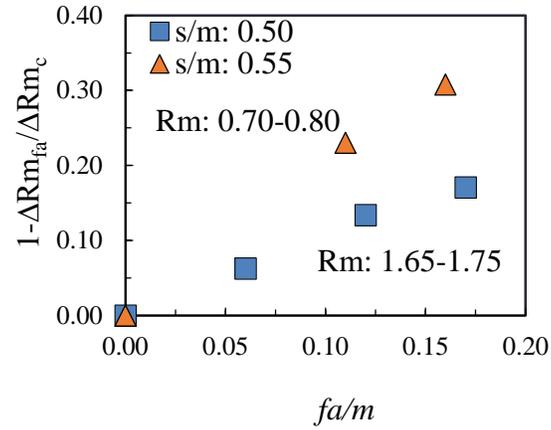
Fig. 4.3 Effects of fly ash on reduction in friction between mortar and model coarse aggregate in terms of 1-$\Delta Rm_{fa}/\Delta Rm_c$ with respect to higher fly ash content in fresh mortar for two fine aggregate ratios
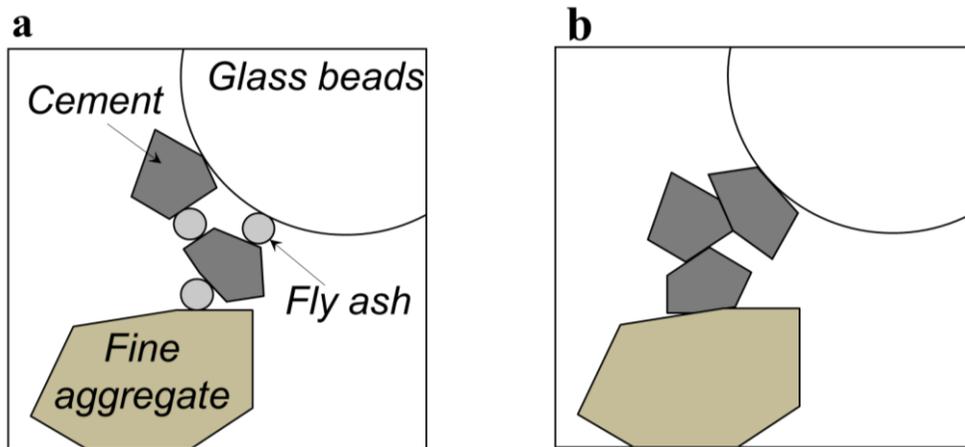
Fig. 4.4 Reduction in shear force between mortar and model aggregate owing to spherical shape of fly ash particles (a), as compared to that in mortar without fly ash (b)

4.4.2 COMPARING THE EFFECTS OF FLY ASH AND ENTRAINED AIR BUBBLES ON

REDUCTION IN FRICTION BETWEEN MORTAR AND MODEL COARSE AGGREGATE

The effect of fine entrained air bubbles on the Fmb was investigated in **Chapter 3** (**Fig. 4.5**). Here, those results are compared with the effect of fly ash on reducing the friction. The effects of fly ash and fine entrained air bubbles are quantified in terms of $1-\Delta Rm_{fa}/\Delta Rm_c$ and $1-\Delta Rm_a/\Delta Rm_c$, respectively. However, since the total air content in every mortar mix proportion is around 10%, any effect of fine air on $1-\Delta Rm_a/\Delta Rm_c$ may affected also by the content of large air bubbles (**Fig. 4.6**).

Fig. 4.5 has suggested a linear relationship in $1-\Delta Rm_{fa}/\Delta Rm_c$ with respect to higher content of fly ash in mortar with Rm of 1.65-1.75. Therefore, with lower range of Rm (by lower water to powder volumetric ratio), $1-\Delta Rm_{fa}/\Delta Rm_c$ tends to increase more dramatically due to the closer distance between solid particles.

However, the results showed that, with the same range of Rm, $1-\Delta Rm_a/\Delta Rm_c$ tends to increase dramatically as the fine air bubble content rises, whereas $1-\Delta Rm_{fa}/\Delta Rm_c$ rises more gradually with respect to higher fly ash contents (**Fig. 4.5**). This suggests that $1-\Delta Rm_a/\Delta Rm_c$ is very sensitive to the size distribution of the entrained air. **Figure 4.5** also illustrates that, when there is a high content of fine air bubbles, the entrained air is more effective in reducing Fmb than fly ash. This may be attributed to relatively free motion in shear between mortar and the model coarse aggregate with the entrained air bubbles acting as compressible bearings (Edmeades and Hewlett, 1998), while fly ash may lead to adhesion between mortar and model coarse aggregate. On the other hand, **Fig. 4.5** suggests that, with a lower content of fine air, the entrained air bubbles less effectively reduce Fmb than fly ash. This may be because larger air bubbles may subject to

larger deformation, resulting in smaller distances between aggregate particles, as discussed in

Section 1.3.6.
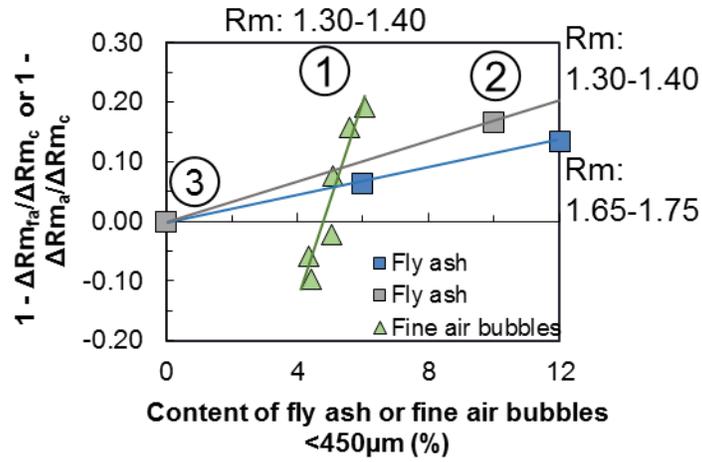
Fig. 4.5 Comparison of effects of fly ash and entrained air bubbles on friction between

model coarse aggregate and mortar in terms of 1-$\Delta Rm_{fa}/\Delta Rm_c$ and 1-$\Delta Rm_a/\Delta Rm_c$,

respectively
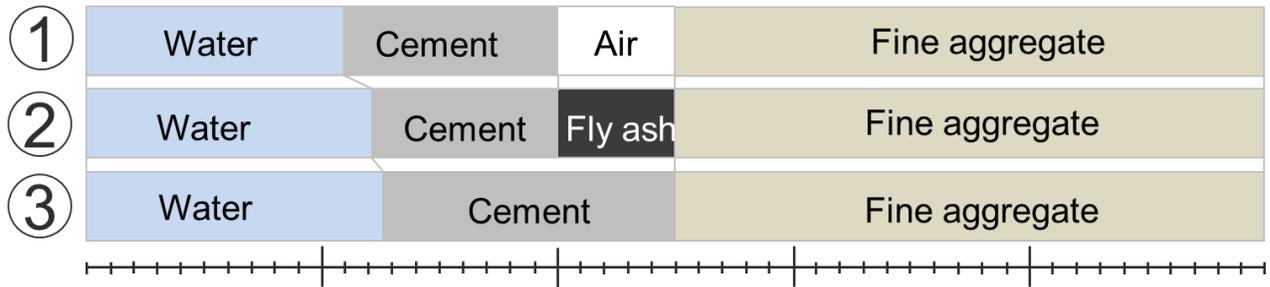
Fig. 4.6 Equal total content of fly ash and entrained air in the mortar mix proportions used

for comparison

4.5 COMBINED EFFECTS OF FINE AIR BUBBLES AND FLY ASH ON FRICTION BETWEEN MODEL COARSE AGGREGATE AND MORTAR

4.5.1 ADDITION OF DEFOAMING AGENT TO REDUCE FRICTION BETWEEN MODEL COARSE AGGREGATE AND AIR-ENTRAINED MORTAR WITH FLY ASH

The flowability of mortar mixes MAF1, MAF4 and MAF8 was tested and evaluated to clarify the effects of entrained air bubbles on the Fmb in mortar with fly ash. The DA was included in mortar mixes MAF5, MAF6, MAF9 and MAF10 and these mortars were used to investigate how fine entrained air bubbles act to reduce Fmb in mortar with fly ash. The effect of entrained air on the Fmb was measured in terms of relative funnel speed of fly ash mortar containing glass beads with (Rmb_{afa}) and without (Rmb_{fa}) air entrainment, and the relative funnel speed of mortar without glass beads (Rm). Since Rm was held in the same range in every mortar mix proportion, the Rm value used in the evaluation was the average Rm (Rm_{avg}). Thus the index used to evaluate friction was $1-\Delta Rm_{afa}/\Delta Rm_{fa}$. The size distributions of entrained air bubbles in the fresh mortar were determined by AVA.

As mentioned in **Section 4.2.2**, two dosages of DA were tested (0.05% and 0.10% by total weight of powder). In practice, the AEA1 and AEA2 also had to be increased in line with the higher dosage of DA. This suggests that the DA removes air from the mortar matrix, requiring a higher dosage of AEA to achieve the target air content.

The results indicate that $1-\Delta Rm_{afa}/\Delta Rm_{fa}$ was positive in mortars with both AEA1 and AEA2 (**Fig. 4.7**). This suggests that, in addition to fly ash, entrained air bubbles also help to reduce the Fmb. However, $1-\Delta Rm_{afa}/\Delta Rm_{fa}$ was found to be higher in mortar with AEA2 as compared to

that with AEA1. As with the **Chapter 3** results, this may be attributed to the lower content of large

air bubbles (>450μm) and higher content of fine air bubbles (<450μm) in mortar with AEA2.

  Figure 4.7 also shows that the Fmb in mortar with fly ash was further reduced, whatever

the type of AEA, in the case of mortars containing DA. This may be attributable to the ability of

DA to eliminate large air bubbles (>450μm). Thus, the entrainment of fine air bubbles (<450μm)

was enhanced when DA was added to mortars with both AEA1 and AEA2 (**Fig. 4.8**).
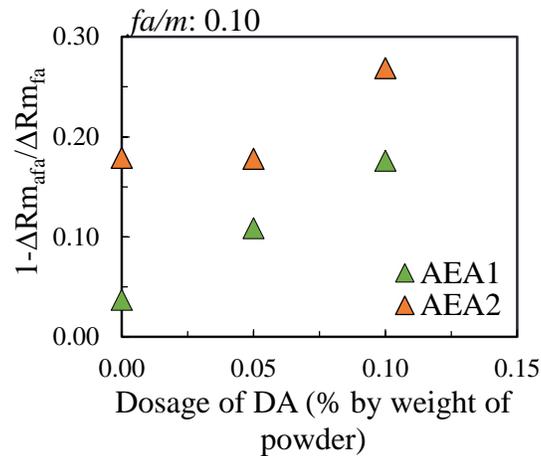
Fig. 4.7 Reduction in friction between model coarse aggregate and mortar with fly ash

owing to the effects of entrained air bubbles with increasing dosage of DA
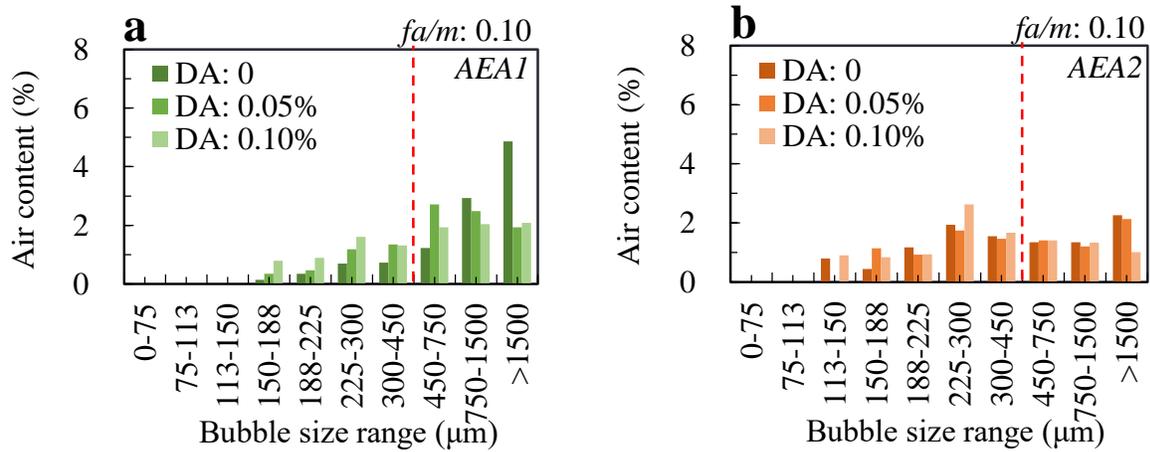
Fig. 4.8 Reduced entrainment of large air bubbles (>450μm) and enhanced entrainment of fine bubbles (<450μm) in fresh mortar with fly ash, both with AEA1 (a) and AEA2 (b), with addition of defoaming agent

4.5.2 RELATIONSHIP BETWEEN ENTRAINED AIR BUBBLE SIZE DISTRIBUTION AND FRICTION BETWEEN MODEL COARSE AGGREGATE AND MORTAR WITH FLY ASH

Mortar mixes MAF1, MAF4, MAF5, MAF6, MAF8, MAF9 and MAF10 were further evaluated to investigate the effects of entrained air size distribution on the Fmb in mortar with fly ash. The results demonstrate that fine air bubbles (<450μm) have a positive effect in reducing the Fmb in mortar with fly ash (**Fig. 4.9**). Since the air content of every mortar mix in this series of experiments was held in the same range, a higher content of fine air bubbles implies that there are fewer large bubbles. Therefore, it is clear that large air bubbles (>450μm) have a negative effect on $1-\Delta Rm_{afa}/\Delta Rm_{fa}$, as seen in **Fig. 4.9**. These results suggest that 450μm may be the critical size of entrained air bubbles, with bubbles below the critical size reducing the Fmb in mortar with fly ash. Furthermore, there is a proportional relationship between the volumetric ratio of fine to coarse air bubbles (*fb/cb*) when the critical size is set to 450μm and $1-\Delta Rm_{afa}/\Delta Rm_{fa}$, as shown in **Fig. 4.10**.

One of the main ways that entrained air bubbles act on $1-\Delta Rm_{afa}/\Delta Rm_{fa}$ might be explained by fine entrained air bubbles (>450µm) acting as compressible bearings, as discussed in **Section 1.3.6**. Besides, larger entrained air bubbles possibly subject to larger deformation than finer ones due to the lower excess pressure across the bubble boundary (Muncaster, 1993); this may cause the spacing between aggregate, acting as restraints to the mortar matrix, reduced.
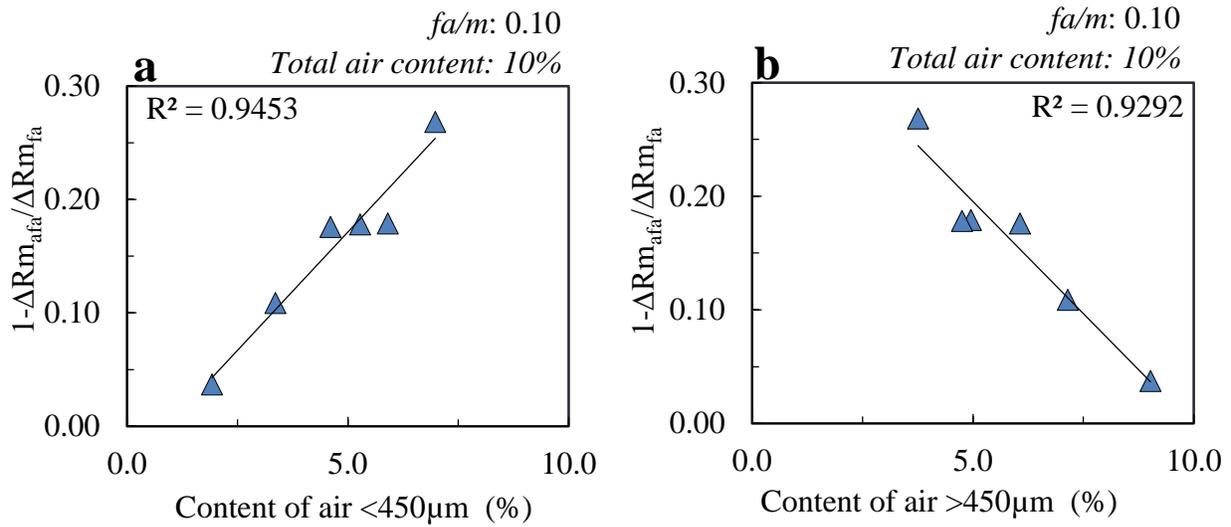
Fig. 4.9 Positive (a) and negative correlation (b) of fine (<450µm) and large (>450µm) air bubbles with $1-\Delta Rm_{afa}/\Delta Rm_{fa}$
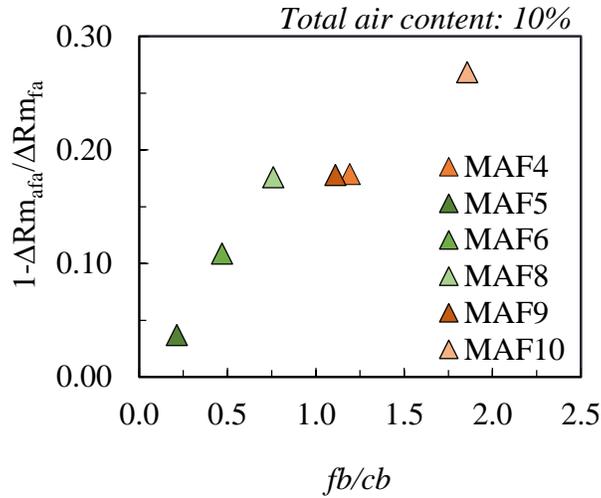
Fig. 4.10 Proportional relationship between volumetric ratio of fine to coarse air bubbles (fb/cb) when the critical size is set to 450µm and 1-$\Delta Rm_{afa}/\Delta Rm_{fa}$

4.5.3 COMPARISON OF EFFECTS OF AIR SIZE DISTRUTION ON FRICTION BETWEEN MODEL COARSE AGGREGATE AND MORTARS WITH AND WITHOUT FLY ASH

The effects of air size distributions in mortars with and without fly ash on the Fmb were compared (**Fig. 4.11**). The effects of entrained air bubbles on friction were quantified in terms of 1-$\Delta Rm_{afa}/\Delta Rm_{fa}$ and 1-$\Delta Rm_{a}/\Delta Rm_{c}$, respectively, for mortars with and without fly ash. Taking the critical bubble size to be 450µm, the results demonstrate that 1-$\Delta Rm_{a}/\Delta Rm_{c}$ tends to increase more dramatically as the volumetric ratio of fine to coarse air bubbles (fb/cb) rises than 1-$\Delta Rm_{afa}/\Delta Rm_{fa}$. Apparently, cement particles are coarser than fly ash, resulting in higher friction between solid particles in fresh mortar without fly ash, as compared to that with fly ash. Consequently, higher fa/cb suggests higher amount of fine air bubbles acting as compressible bearings, which might be more effective in reducing friction between coarser particles of cement, as compared to fly ash, and other solid particles. However, in spite of lower fa/cb, the entrained air bubbles tend to be more efficient in reducing the Fmb in mortar with fly ash, as compared to that without fly ash (**Fig.**

69

4.11). This might be owed to the lower increase in friction as coarse aggregate moved towards each other as larger air bubbles undergo larger deformation, leading to smaller distance between aggregate.

Besides, by applying Eq. (3.2) to the effects of entrained air in mortar with fly ash, the effectiveness of fine air (A) and coarse air (B) on the friction reduction between model coarse aggregate and mortar with fly ash can be obtained as discussed in **Section 3.3.5**. Coefficients A and B can be attained by using Fig. 4.9 and Fig. 4.12. The experimental results have suggested that the magnitude of both coefficients A and B in mortar with fly ash (0.038 and -0.003) are lower than that in mortar without fly ash (0.89 and -0.077). This suggests the lower effectiveness of both fine and large air bubbles on friction in mortar with fly ash, as compared to that without fly ash.
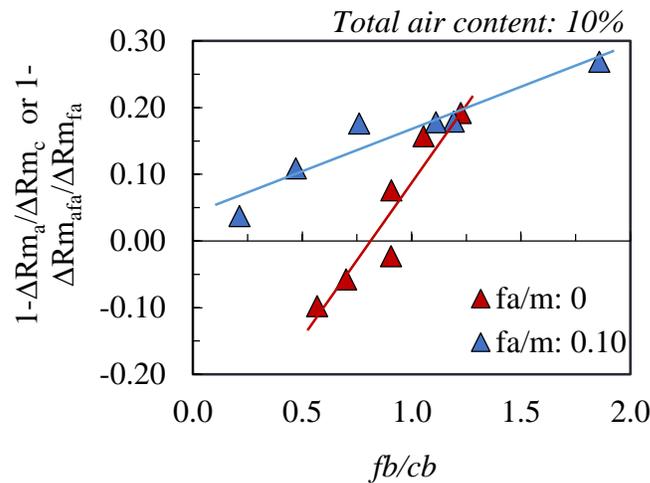
Fig. 4.11 Relationships between air size distributions in mortars with and without fly ash and the friction between model coarse aggregate and mortar in terms of $1\text{-}\Delta Rm_{afa}/\Delta Rm_{fa}$ and $1\text{-}\Delta Rm_a/\Delta Rm_c$, respectively
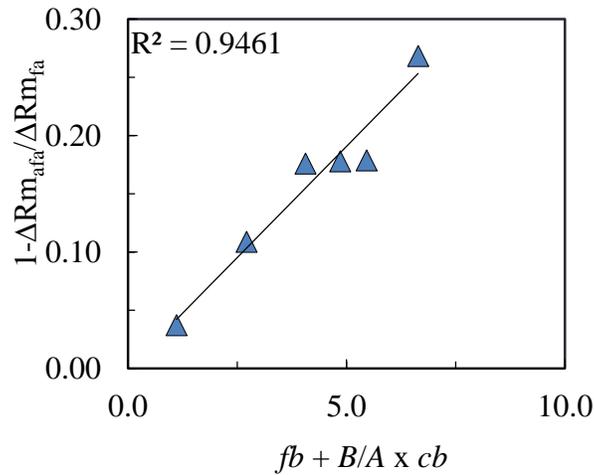
Fig. 4.12 Linear relationship between 1-ΔRm_a/ΔRm_c and *fb* + *B*/*A* x *cb* in mortar with fly ash (*fa/m*: 0.10)

4.6 COMBINED EFFECTS OF FINE ENTRAINED AIR BUBBLES AND FLY ASH ON SELF-COMPACTABILITY OF FRESH CONCRETE

4.6.1 EFFECTS OF FLY ASH ON SELF-COMPACTABILITY OF FRESH CONCRETE

The concrete mixes CF1, CF2, CF3, CF4, CF5 and CF6, were tested to verify how fly ash enhances the self-compactability of fresh concrete. Self-compactability was quantified in terms of concrete fill height. Corresponding to mortar mixes proportions MF1, MF3, MF4, MF5, MF6 and MF7, these concrete mixtures were designed to analyse how fly ash leads to reduced friction between mortar and coarse aggregate and thereby enhances the self-compactability of fresh concrete. The coarse aggregate content (*g/c*) of every mix was kept constant at 0.30. Further, as found in the case of the mortar tests, fresh concrete with fly ash tends to require a lower dosage of superplasticiser to achieve an equal concrete slump flow compared with fresh concrete without fly ash (**Table 4.2**).

The results suggest that fly ash can considerably enhance the self-compactability of fresh concrete with *s/m* of both 0.50 and 0.55 (**Fig. 4.13**). This figure also suggests that, with *fa/p* of 0.48, the fill height of the fresh concrete can be increased to a similar level as that of the fresh concrete without fly ash with lower *s/m*. Besides, with the effects of fly ash, the fill height of fresh concrete with an *s/m* of 0.50 can be enhanced to over 250mm. That is, the results indicate that fly ash can potentially allow a higher *s/m* in SCC. Thus, in addition to the replacement of cement with fly ash, the amount of cement needed in SCC can be further reduced by increasing the proportion of fine aggregate content.
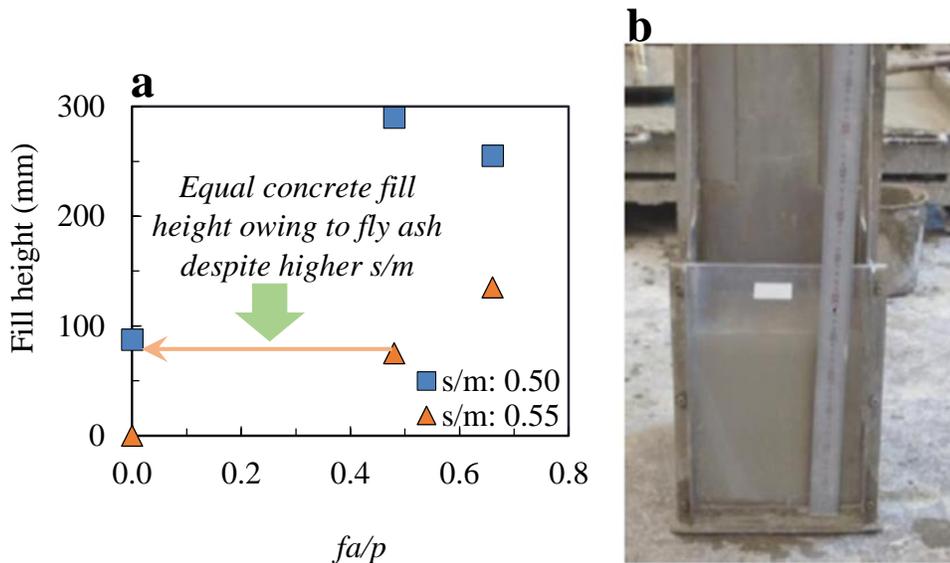
Fig. 4.13 Enhancement in self-compactability of fresh concrete, in terms of fill height, owing to the reduced friction between mortar and coarse aggregate in fly ash concrete with an *s/m* of both 0.50 and 0.55 (a) and an example of concrete box test (b)

4.6.2 EFFECTS OF FINE ENTRAINED AIR BUBBLES ON SELF-COMPACTABILITY OF FRESH CONCRETE WITH FLY ASH

Tests were conducted using concrete mixes CAF1, CAF2 and CAF3 to evaluate the effects of fine entrained air bubbles on the self-compactability of fresh concrete. Self-compactability was quantified in terms of concrete fill height, as obtained using the box test. By investigating the correspondence with mortar mixes MAF1, MAF6 and MAF10, the results from these tests were used to analyse the effects of fine entrained air bubbles. Since the proportions of fly ash and aggregate to total volume (including air) were controlled to be similar in all concrete mix proportions, any enhancement in self-compactability can be attributed to the effects of the entrained air bubbles.

Lower dosages of AEA1 and AEA2 were required to achieve the target air content in the fresh concrete as compared to the mortar cases. This might be attributable to the presence of coarse aggregate, which can generate higher amount of energy during mixing and stabilise a larger amount of air.

The results for fresh concrete with AEA1 indicate a slight increase in fill height resulting from the effects of fine entrained air bubbles (**Fig. 4.14**). This suggests that the self-compactability of fresh concrete can be maintained while employing a higher aggregate content. At the same time, the effect of fine entrained air bubbles entrained with AEA2 is to increase the fill height up to 250mm (**Fig. 4.14**). This indicates the potential increasing the aggregate content in SCC with fly ash if a higher proportion of fine air bubbles are entrained. As in the results from mortar testing, this improvement may be attributable to a lower proportion of large entrained air bubbles (>450µm) in concrete with AEA2, as compared to that with AEA1 (**Fig. 4.15**). Large entrained air bubbles may be more easily deformed, leading to reduced aggregate spacing in fresh concrete with

73

AEA1, as compared to that in concrete with AEA2. **Figure 4.15** also shows a similar proportion of small entrained air bubbles in concrete with AEA1 as in concrete with AEA2. This suggests that large air bubbles with a size over 450µm might also contribute to reducing the self-compactability of the fresh concrete.
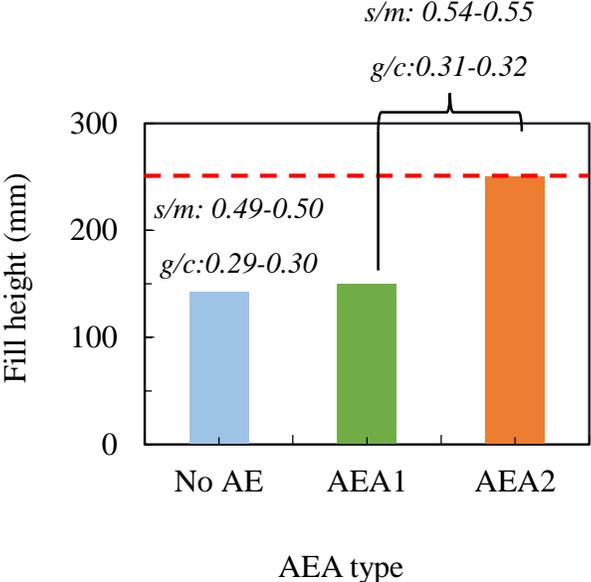
Fig. 4.14 Enhancement in self-compactability of fresh concrete with fly ash to mortar ratio (*fa/m*) of 0.10, in terms of fill height in the concrete box test, resulting from the effects of fine entrained air bubbles with AEA2
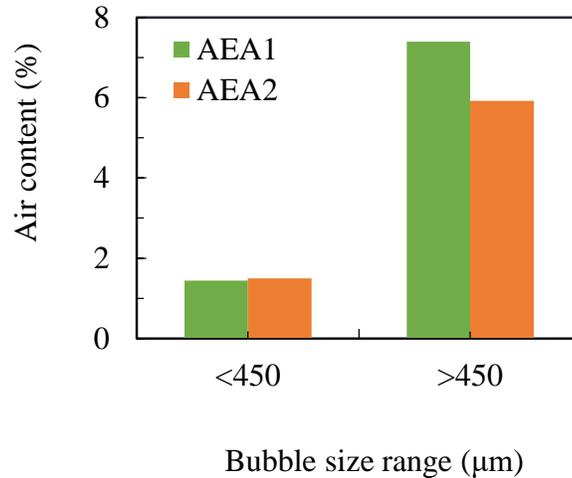
Fig. 4.15 Larger proportion of large air bubbles (>450μm) in fresh concrete with AEA1 as compared to that in concrete with AEA2

4.7 CONCLUDING REMARKS

Various mortar mixes were tested to investigate the combined effects of fine entrained air bubbles and fly ash on the Fmb. A defoaming agent was also used to enhance the entrainment of fine air bubbles in the fresh mortars that included with fly ash. Additionally, some concrete mixes were also tested to investigate the combined effects on the self-compactability of fresh concrete and confirm the possibility of increasing the aggregate content in self-compacting concrete. Based on the results of these tests, the following conclusions can be drawn:

1) Fly ash was found to reduce the friction between mortar and model coarse aggregate. This may be attributable to the spherical shape of fly ash particles, which contributes to the ball-bearing effect and reduction in contact area between other solid particles.

2) Friction between mortar and model coarse aggregate tended to be more sensitive to air bubble size distribution than to fly ash content. This may be attributed to relatively free motion in shear of between mortar and model coarse aggregate with fine entrained air bubbles acting as

75

compressible bearings, while fly ash may lead to adhesion between mortar and aggregate.. Furthermore, large air bubbles may subject to large deformation, resulting in shorter distance between aggregate acting as restraints to the mortar matrix, whereas fly ash is solid and does not deform.

3) The combined effects of fly ash and fine entrained air bubbles promote further reductions in friction between mortar and model coarse aggregate.

4) The effects of entrained air bubbles on reduction in friction between model coarse aggregate and mortar with fly ash tends to be less sensitive to air size distribution, as compared to that in mortar without fly ash. Owing to the spherical shape of fly ash, lower stress and friction are created between fly ash, as compared to cement, and other solid particles. This may result in lower effectiveness of fine entrained air bubbles, acting as compressible bearings for reducing friction between finer particles of fly ash, as compared to cement, with other solid particles. Besides, lower friction of mortar with fly ash may lead to lower increase in friction as aggregate moves towards each other due to the large deformation of large air bubbles.

5) The reduction in friction between mortar and model coarse aggregate enhances the self-compactability of fresh concrete, as measured in terms of fill height.

6). The concrete box test also suggested that, if a defoaming agent is used, the self-compactability of fresh concrete with a high volume of fly ash can be maintained while using a higher aggregate content owing to the effects of fine entrained air bubbles. It appears that, with a certain type of air-entraining agent, a higher aggregate content can be employed in self-compacting concrete as a result of the low proportion of large air bubbles (>450µm).

The effects of fly ash and entrained air bubbles on friction between mortar and model coarse aggregate, as well as their combined effects, are simply summarised in **Fig. 4.16** and

Fig. 4.17. The addition of fly ash is found to enable use of a higher fine aggregate content in self-compacting concrete. Besides, it is suggested that the effects of fine entrained air bubbles allow a higher aggregate content in self-compacting concrete containing fly ash. These results imply that the combined effects of fly ash and fine entrained air bubbles can potentially reduce the amount of cement required, and thereby improve the environmental sustainability of SCC.
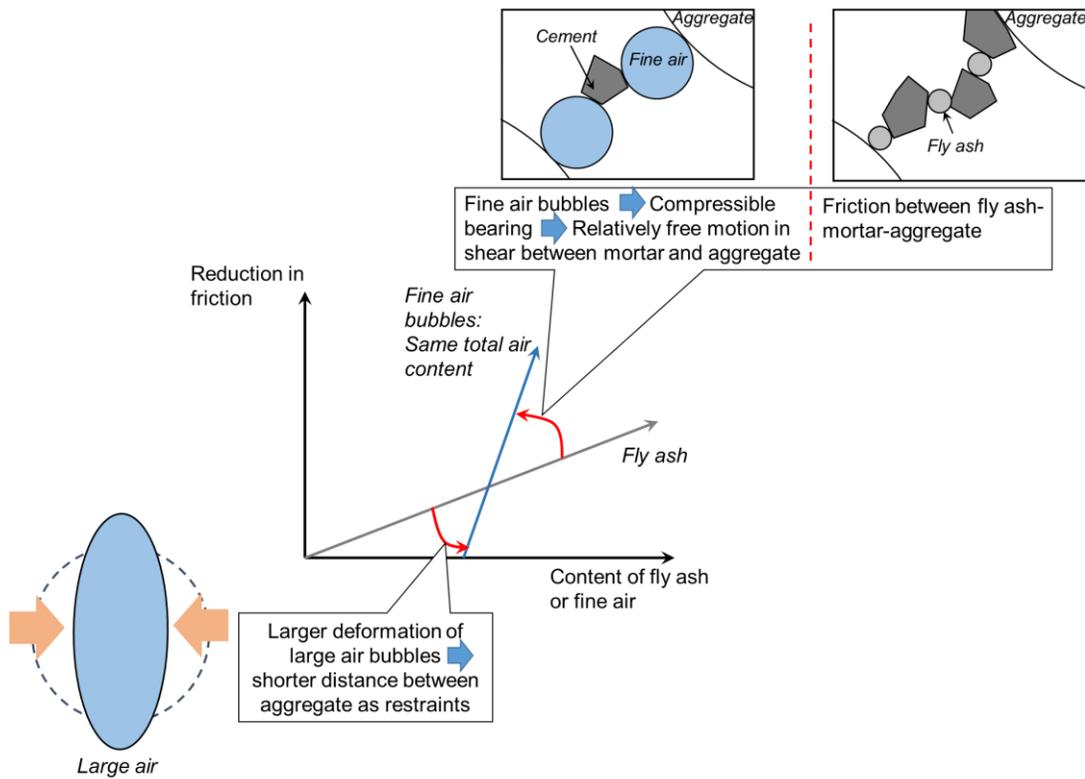
Fig. 4.16 Summary on the comparison of effects of entrained air bubbles and fly ash with possible explanatory mechanisms
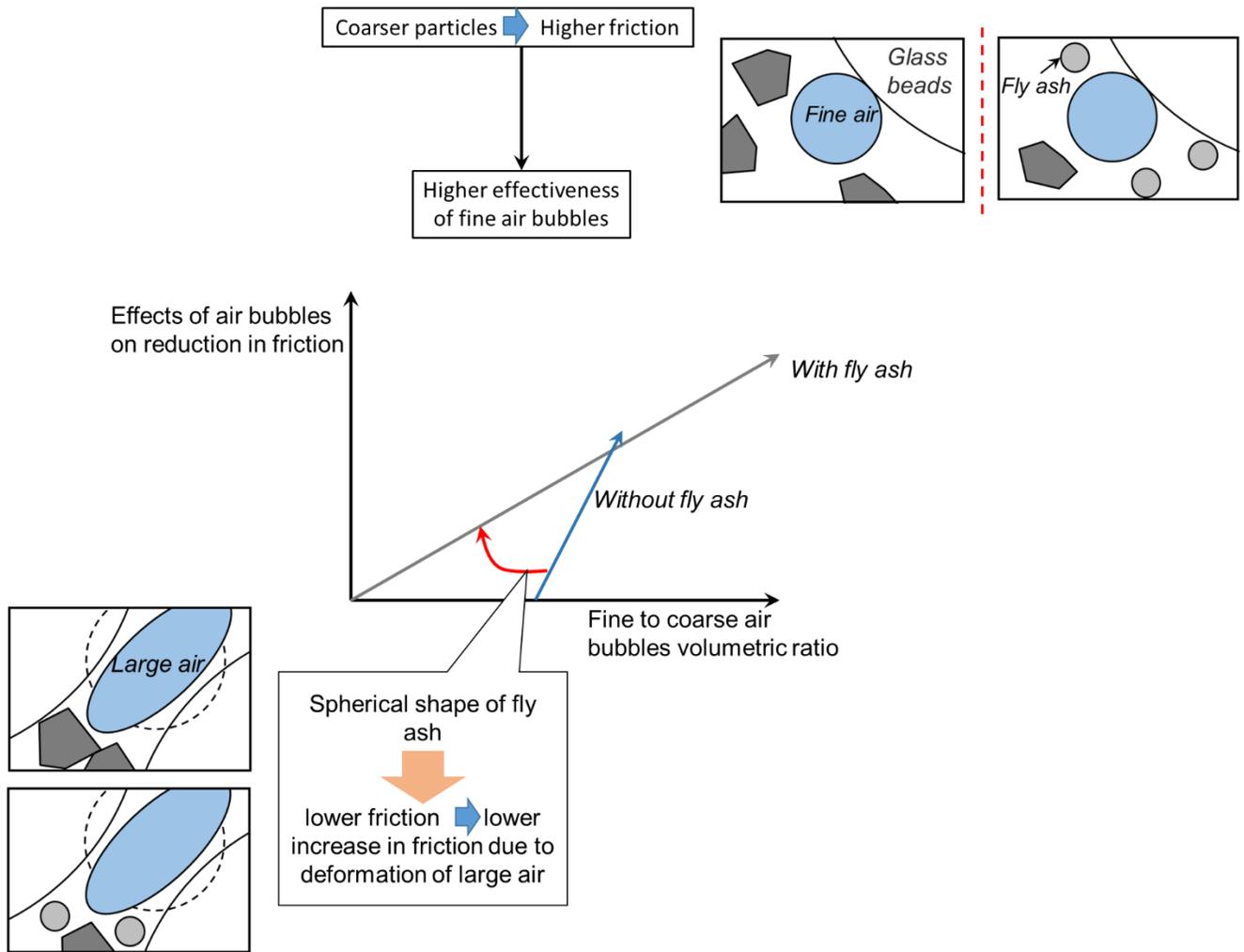
Fig. 4.17 Summary on the interaction between entrained air bubbles and fly ash with possible explanatory mechanisms

REFERENCES

Dhir, R.K., Munday, J.G.L. and Ho, N.Y. (1988) PFA in structural precast concrete: Engineering properties. *Journal of Cement and Concrete Research*. 18 (6): 852-862.

Edmeades, R.M. and Hewlett, P.C. (1998) 15 Cement admixtures. *Lea's Chemistry of Cement and Concrete*. 841-905.

Güneyisi, E., Gesoğlu, M. and Algin, Z. (2013) 9 – Performance of self-compacting concrete (SCC) with high-volume supplementary cementitious materials (SCMs). *Journal of Eco-Efficient Concrete*. 198-217.

Liu, M. (2010) Self-compacting concrete with different levels of pulverized fuel ash. *Journal of Construction and Building Materials*. 24 (7): 1245-1252.

Muncaster, R. (1993) *A-level physics*. Nelson Thornes, UK.

Naik, T.R., Kumar, R., Ramme, B.W. and Canpolat, F. (2012) Development of high-strength, economical self-consolidating concrete. *Journal of Construction and Building Materials*. 30: 463-469.

Oner, A., Akyuz, S. and Yildiz, R. (2005) An experimental study on strength development of concrete containing fly ash and optimum usage of fly ash in concrete. *Journal of Cement and Concrete Research*. 35 (6): 1165-1171.

Rath, S., Puthipad, N., Attachaiyawuth, A. and Ouchi, M. (2017) Critical size of entrained air to stability of air volume in mortar of self-compacting concrete at fresh state, *Journal of Advanced Concrete Technology*. 15: 29-37.

Tangtermsirikul, S. (2003) *Durability and mix design of concrete*. Thailand: Printing House of Thammasat.

Zhao, H., Sun, W., Wu, X. and Gao, B. (2015) The properties of the self-compacting concrete with fly ash and ground granulated blast furnace slag mineral admixtures. *Journal of Cleaner Production*. 95: 66-74.

CHAPTER 5 ENTRAINMENT OF FINE AIR BUBBLES FOR ENHANCEMENT IN VOLUMETRIC STABILITY OF ENTRAINED AIR

5.1 INTRODUCTION

Chapter 3 and 4 have suggested that the effects of fly ash and entrained air bubbles can potentially enhance the self-compactability of fresh concrete. However, the flowability of self-compacting concrete (SCC) as well as certain properties of the hardened concrete is known to depend on the volumetric stability of entrained air bubbles in the fresh concrete. The volumetric stability of the entrained air has been found to be influenced by various factors including the concrete mix proportion and certain characteristics of the entrained air itself (Rath et al, 2015, 2016, 2017a and 2017b).

Rath et al (2017b) suggested a critical size for entrained air bubbles which essentially reduces the air volumetric-stability in SCC. In this work, they also considered the coalescence of entrained air bubbles over time. Nonetheless, they arrived at this conclusion by assuming that a fraction of air bubbles of a certain size coalesce, instead of analysing actual changes in air bubble size distribution over time.

Furthermore, fly ash has been found to disturb air entrainment and air void stability in fresh concrete (Gebler and Klieger, 1983). This has been attributed to adsorption of air-entraining agent by carbon on the surface of the fly ash (Freeman et al, 1997, Hill et al, 1997 and Pederson et al, 2008). Although the fly ash used in this research has a rather low loss on ignition (LOI) (**Table 1.1**), it may influence the entrained air bubble size distribution and stability through other physical properties, such as its spherical shape. Any influence of fly ash on the volumetric stability of

80

entrained air bubbles can affect the flowability of the SCC over time, as well as certain hardened properties.

In this chapter, the volumetric stability of entrained air bubbles in the fresh mortar of SCC is investigated by analysing the change in air bubble size distribution over time. Various methods for enhancing the entrainment of fine air bubbles to improve the volumetric stability of entrained air are also studied. Furthermore, the reduction in volumetric stability of entrained air in fresh mortar of SCC resulting from the use of fly ash is clarified. Finally in this chapter, the use of a defoaming agent to improve volumetric stability of the entrained air is considered.

5.2 MORTAR TEST PROCEDURES, MIX PRPORTIONS AND FRESH PROPERTIES

5.2.1 MORTAR TEST PROCEDURES

Table 5.1 shows all the tests carried out on the fresh properties of mortar to evaluate the volumetric stability of entrained air bubbles in fresh SCC mortar. As described in earlier chapters, all tests on mortar in the at 5 minutes and 20 minutes except Air Void Analysis (AVA) were repeated three times for each mix and the results averaged. An additional batch was tested to determine the change in volume and size distribution of entrained air bubbles over time. Every batch of mortar was rested after the tests at 5 and 20 minutes. During these periods, the mortar was also covered with a moist towel to prevent loss of moisture. AVA was carried out at 5 minutes and 120 minutes to clarify the effects of entrained air size distribution on the volumetric stability of the entrained air in fresh SCC mortar.

Table 5.1
Test procedure

Type	Procedure		
	5 minutes	20 minutes	At 120 minutes
Mortar	- Mortar flow test - Mortar funnel test - Air measurement (gravimetric method and AVA)	- Remix for 5 sec. - Mortar flow test - Mortar funnel test - Air measurement (gravimetric method)	- Remix for 5 sec. - Mortar flow test - Mortar funnel test - Air measurement (gravimetric method and AVA)

5.2.2 MORTAR MIX PROPORTIONS AND FRESH PROPERTIES

The mortar mixes tested in this series of experiments are shown in **Table 5.2**. The water-to-powder ratio (w/p) was adjusted such that the relative funnel speed (Rm) of every batch of mortar was in the range 1.30 to 1.40 (**Table 5.3**). The relative flow area (Γm) of every batch of mortar was also controlled, by altering the dosage of the superplasticiser (SP/P), to be in the range 5.5 to 6.6. Furthermore, the target was to achieve an air content in entrained-air mortars of 10% to 12% by changing the dosage of air-entraining agent (AEA). Thus, for all mix proportions with entrained air, s/m (where the total mortar quantity includes the air) was between 0.49 and 0.50. Two ratios of fly ash to mortar, including air, (fa/m) were considered in the series of mortar mixes: 0.04 and 0.10.

Various types of AEA were used to study the effects of air size distribution on volumetric stability of entrained air, AEA1, AEA2, AEA3 and AEA4 (Table 5.2). Several mixing methods were tested with the aim of enhancing the entrainment of fine air bubbles. The differences in these mixing methods mainly consist of different sequences of admixture additions. A defoaming agent (DA) was also employed in mortar mixes MA6, MA9, MAF6, MAF7, MAF10 and MAF11. The dosages of DA tested in the experiment were 0.05% and 0.10% by total weight of powder.

Table 5.2
Mortar mix proportions

Mix	Mix proportion (kg/m³)									SP/P (%)	F.M. of S	fa/m* including air	Mixing method	s/m* including air
	C*	Fly ash	W*	S*	AEA 1	AEA 2	AEA 3	AEA 4	DA					
MA2	636	-	248	1474	0.04	-	-	-	-	1.30		0.00		
MA3	641	-	246	1474	-	0.39	-	-	-	1.22		0.00		
MA4	633	-	249	1474	-	-	0.10	-	-	1.24		0.00	B	
MA5	619	-	253	1474	-	-	-	0.173	-	1.27	2.8	0.00		0.50
MA6	627	-	251	1474	-	6.77	-	-	0.63	1.15		0.00		
MA7	636	-	248	1474	0.07	-	-	-	-	1.35		0.00	A	
MA8	644	-	245	1474	-	-	0.26	-	-	1.35		0.00		
MA9	653	-	243	1474	-	-	2.29	-	0.65	1.30		0.00	C	
MAF3	672	-	237	1474	-	0.05	-		-	1.65		0.00		0.50
MAF4	562	107	227	1474	-	0.08	-		-	1.55		0.04		0.50
MAF5	355	267	226	1474	-	0.12	-		-	0.84		0.10		0.50
MAF6	338	267	242	1474	-	0.42	-		0.30	0.82		0.10		0.50
MAF7	341	267	230	1474	-	1.10	-		0.61	0.99		0.10		0.50
MAF8	656	-	242	1474	-	-	0.53		-	1.20		0.00		0.50
MAF9	341	267	230	1474	-	-	3.16		-	0.65		0.10		0.50
MAF10	331	267	234	1474	-	-	5.74		0.30	0.56		0.10		0.50
MAF11	338	267	232	1474	-	-	7.26		0.60	0.58	2.9	0.10	A	0.50

*C: Cement; W: Water; S: fine aggregate; fa/m: volume of fly ash in mortar; s/m: fine aggregate to mortar volumetric ratio

Table 5.3
Measured properties of fresh mortar

Mix	Air content by gravimetric method (%)	Γ_m	R_m
MA2	11.22	6.0	1.36
MA3	10.39	5.9	1.37
MA4	11.24	5.8	1.32
MA5	10.82	5.8	1.37
MA6	10.35	6.4	1.36
MA7	10.16	6.1	1.35
MA8	10.01	5.7	1.40
MA9	10.31	5.7	1.39
MAF3	10.70	5.7	1.36
MAF4	10.13	5.5	1.40
MAF5	10.94	5.7	1.36
MAF6	10.50	5.6	1.38
MAF7	10.67	5.5	1.36
MAF8	10.46	5.7	1.39
MAF9	10.86	5.8	1.39
MAF10	10.03	5.8	1.37
MAF11	10.73	6.1	1.35

5.3 EFFECTS OF ENTRAINED AIR SIZE DISTRIBUTION ON VOLUMETRIC STABILIY OF AIR IN SCC MORTAR

5.3.1 EFFECTS OF AEA TYPE ON VOLUMETRIC STABILITY OF ENTRAINED AIR BUBBLES IN SCC MORTAR

Mortar mixes MA2, MA3, MA4 and MA5 were tested to clarify the effects of AEA type on the volumetric stability of entrained air bubbles in SCC mortar. As explained in **Section 1.3.2**, the volumetric stability of entrained air bubbles is quantified in terms of changes in the air content over a period of 120 minutes after mixing. Thee size distributions of the entrained air bubbles, obtained from AVA, were used to evaluate the effects of entrained air size distribution on the volumetric stability of air in the fresh mortar.

Rath et al (2017a) suggested that the volumetric stability of the air bubbles tends to decreases with the higher content of larger air bubbles with a size over 1500μm. However, the results from this research indicate that air entrained in fresh mortar with AEA1 has equivalent volumetric stability to that with AEA2 and AEA3 even when there is a significantly higher content of large air bubbles (>1500μm), as illustrated in **Fig. 5.1** and **Fig. 5.2**. Further, AEA4 tends to produce entrained air bubbles with slightly higher stability as compared to AEA1, AEA2 and AEA3, as highlighted in **Fig. 5.2**, despite the higher proportion of large air bubbles (>1500μm). These results imply that the volumetric stability of entrained air bubbles may depend on differences in the coalescence rate of finer air bubbles (<1500μm) with different AEAs, in addition to the content of large air bubbles (>1500μm). Past research indicates that this may be attributable to differences in the physical and chemical characteristics of the shells of the entrained air bubbles (Ley et al, 2009a and 2009b).
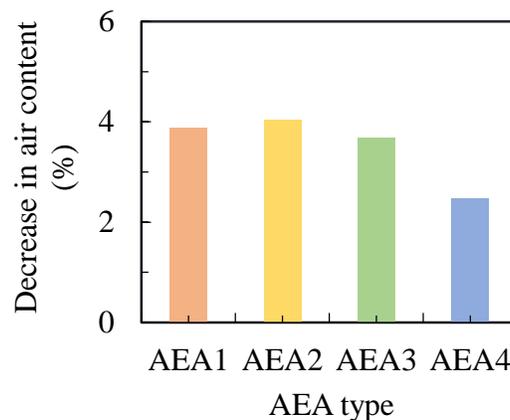
Fig. 5.1 Equivalent Volumetric stability of entrained air bubbles in fresh mortar with AEA1, AEA2 and AEA3 and slightly higher volumetric stability of entrained air bubbles in fresh mortar with AEA4
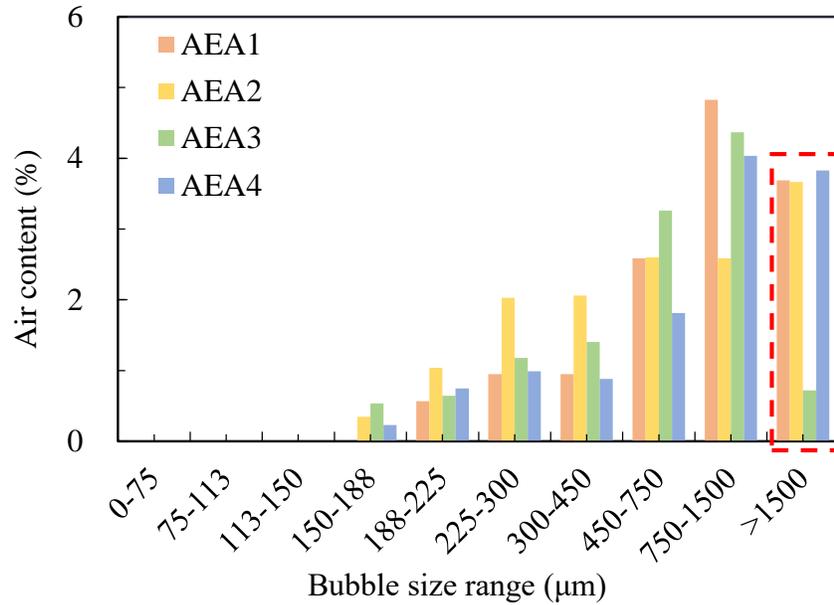
Fig. 5.2 Lower proportion of large entrained air bubbles (>1500µm) in fresh mortar with AEA2 and AEA3 as compared to that with AEA1 and AEA4 at time 5 minutes after mortar mixing

5.3.2 EFFECTS OF MIXING METHOD ON VOLUMETRIC STABILITY OF ENTRAINED AIR BUBBLES IN SCC MORTAR

The change in air content over a period of 120 minutes after mixing of mortars MA2, MA4, MA7 and MA8 was investigated to evaluate any effect the mixing method has on the volumetric stability of entrained air bubbles. The size distribution of entrained air bubbles in the mortar in the fresh state, which are used to clarify the results, were determined by AVA.

The results demonstrate that air bubbles entrained in the fresh mortar with mixing method A tend to be more stable as compared to mixing method B, whatever the AEA type (**Fig. 5.3**). This suggests that the volumetric stability of entrained air bubbles can be improved by adding the

superplasticiser to the mix with the fresh mortar prior to the addition of the AEA. **Figure 5.4** shows that this may be mainly attributable to the lower content of large and unstable air bubbles (>1500μm) in fresh mortar mixed using method A.
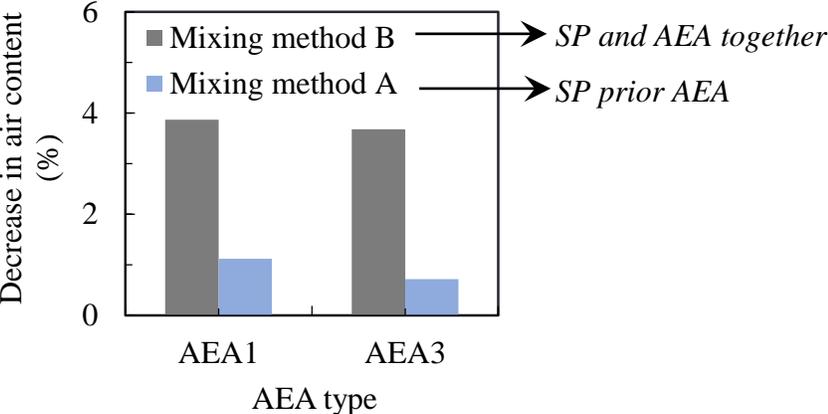
Fig. 5.3 Improvement in volumetric stability of entrained air bubbles in fresh mortar whatever the AEA type with mixing method A
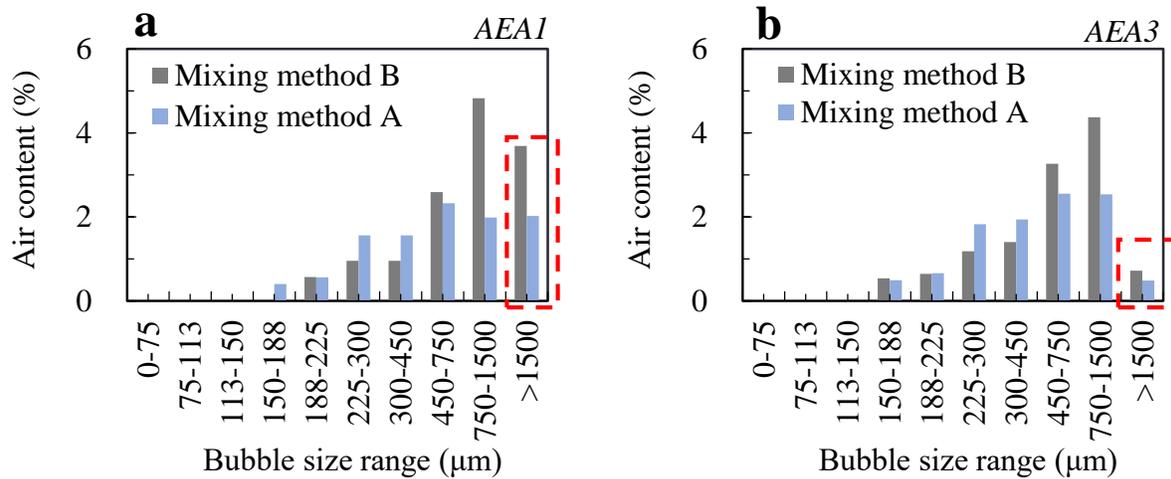
Fig. 5.4 Lower content of large and unstable entrained air bubbles (>1500) in fresh mortar with mixing method A, as compared to that with mixing method B, in mortars with both AEA1 (a) and AEA3 (b) 5 minutes after mortar mixing

5.3.3 USE OF DEFOAMING AGENT TO IMPROVE VOLUMETRICT STABILITY OF ENTRAINED AIR BUBBLES IN SCC MORTAR

Mortar mixes MA3 and MA6 were tested to investigate any improvement in the volumetric stability of entrained air in fresh mortar when a DA is used. The volumetric stability of the entrained air was quantified in terms of the change in air content over a period of 120 minutes after mortar mixing. Air Void Analysis (AVA) was also carried out to determine the size distribution of entrained air bubbles in the fresh mortar.

Figure 5.5 shows that, when the DA is used, the loss of air content from mortar containing AEA2 after 120 minutes is reduced. This suggests that the volumetric stability of entrained air bubbles is improved by the DA. **Figure 5.6** illustrates that this may be mainly attributable to the ability of the DA to eliminate large and unstable air bubbles with a size over 1500μm.
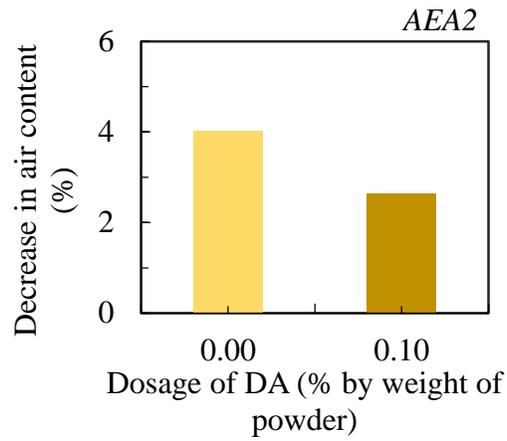
Fig. 5.5 Improvement in volumetric stability of entrained air bubbles in mortar with AEA2 when DA is used
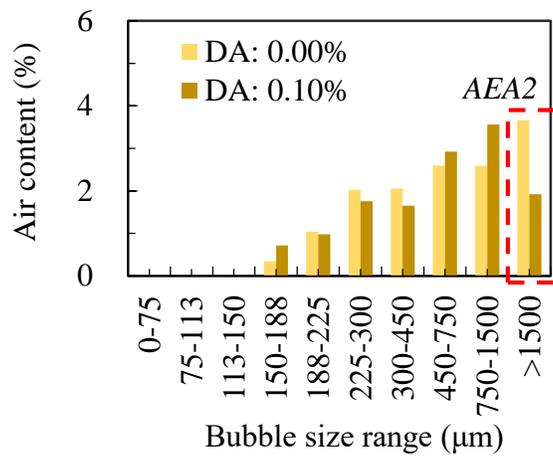
Fig. 5.6 Lower content of large and unstable entrained air bubbles (>1500μm) in fresh mortar with DA 5 minutes after mixing

5.3.4 RELATIONSHIP BETWEEN ENTRAINED-AIR SIZE DISTRIBUTION AND VOLUMETRIC STABILITY OF ENTRAINED AIR BUBBLES

The volumetric stability and size distribution of entrained air bubbles in all mortar mixes, MA2, MA3, MA4, MA5, MA6, MA7, MA8, MA9, were analyzed in order to clarify the relationship between entrained air size distribution and volumetric stability of entrained air. Volumetric stability is determined in terms of the change in air content of the mortar between mixing and 120 minutes. The size distribution of the entrained air bubbles was obtained both in the initial state and at 120 minutes by AVA. These air size distributions also made it possible to take coalescence of air bubbles into account when evaluating the results.

Rath et al (2017b) suggested that the volumetric stability of the entrained air tends to fall as the proportion of large and unstable air bubbles (>1500µm) increases. However, in this research, the relationship between large air bubbles (>1500µm) and volumetric stability is not clear (**Fig. 5.7**).
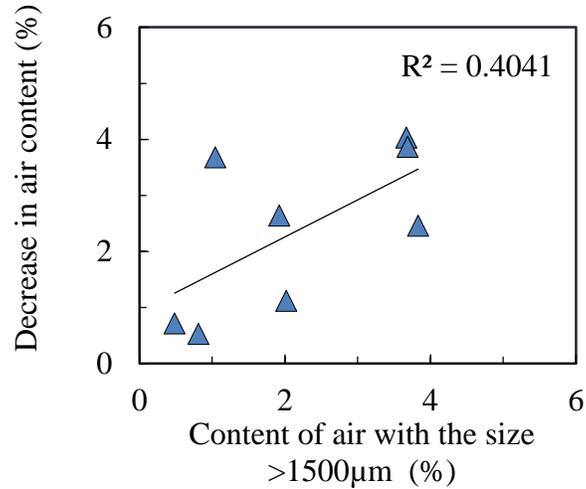
Fig. 5.7 Unclear relationship between volumetric stability of entrained air and content of

large air bubbles (>1500μm)

Analysis shows that the proportion of fine air bubbles (<1500μm) falls in all mortar mixes (MA2, MA3, MA4, MA5, MA6, MA7, MA8, MA9) as shown in **Figs. 5.8, 5.9, 5.10**, **and 5.11**, respectively. This suggests that these fine air bubbles (<1500μm) might coalesce to form larger and more unstable air bubbles (>1500μm). Another possibility is that that small entrained air bubbles might escape from the mortar. Nonetheless, in order to investigate the loss of small entrained air bubbles, it was assumed that coalescence was the cause. This assumption was used to adjust the amount of large entrained air bubbles (>1500μm) according to the loss of fine air bubbles (<1500μm). This was done by summing the reduction in the content of all fine entrained air bubbles (<1500μm) over the 120 minute interval, and adding this quantity of air in the form of 1500μm air bubbles, as illustrated in **Fig. 5.12**. A linear relationship between the reduction in volume of entrained air bubbles over 120 minutes and the adjusted volume of large entrained air bubbles is found (**Fig. 5.13**). This implies that the reduction in content of fine entrained air bubbles

(<1500μm) may be mainly a result of coalescence. It also suggests differences in coalescence rate in mortars with various mix proportions. The coalescence rate may vary according to different physical and chemical characteristics of the shells of the entrained air bubbles with the various types of AEA used (Ley et al 2009a and 2009b), as well as the use of a DA. The use of a superplasticiser and the timing of its addition on air entrainment (Plante et al, 1989, Barfield and Ghafoori, 2012, Łaz´niewska-Piekarczyk, 2013 and Rath et al, 2017b) may also affect the coalescence of fine air bubbles.
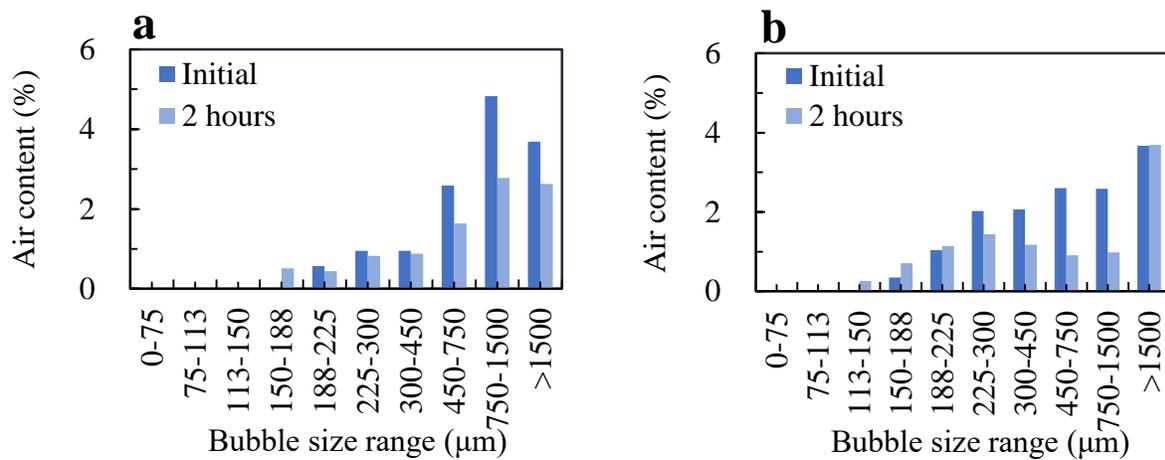
Fig. 5.8 Reduction in content of fine air bubbles (<1500μm) during 120 minutes after mixing in fresh mortars MA2 and MA3
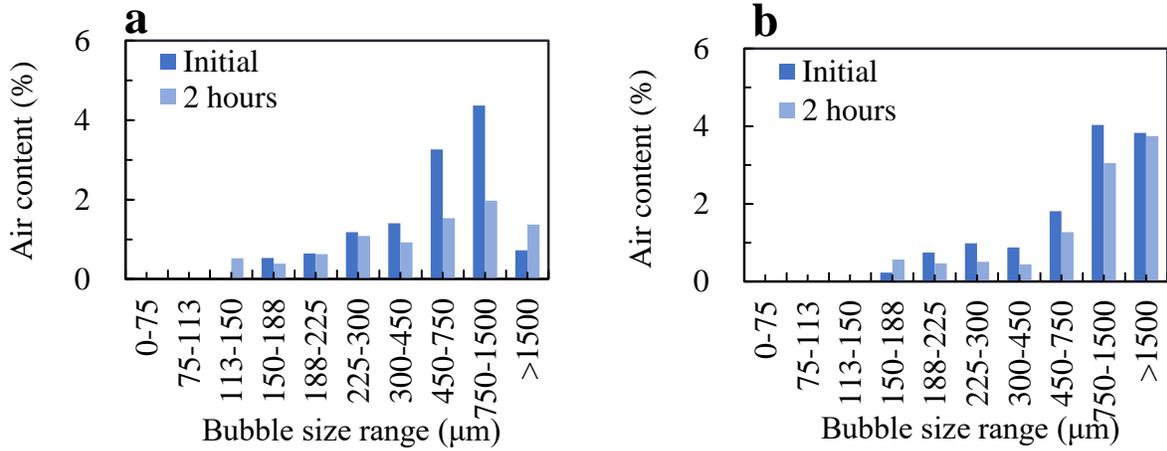
Fig. 5.9 Reduction in content of fine air bubbles (<1500µm) during 120 minutes after mixing in fresh mortars MA4 (a) and MA5 (b)
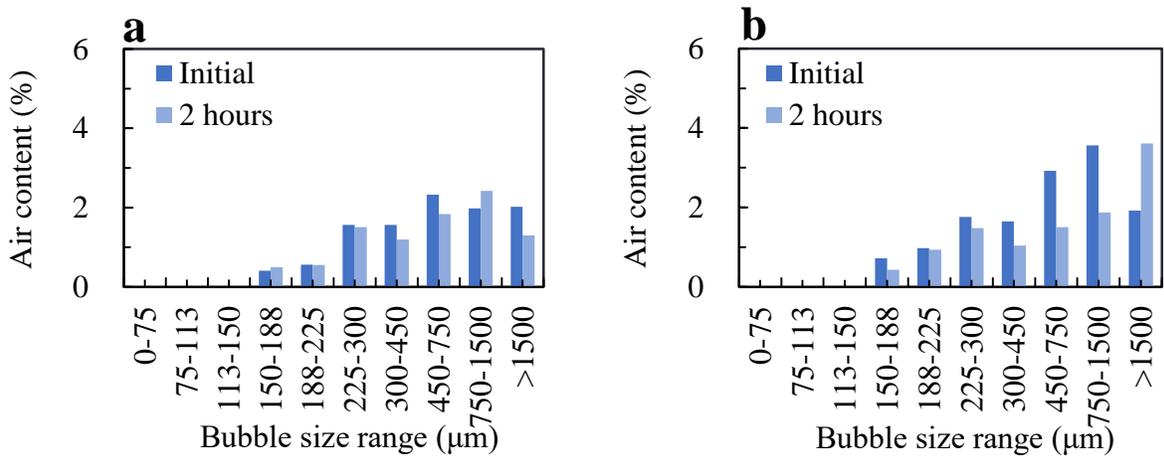
Fig. 5.10 Reduction in content of fine air bubbles (<1500µm) during 120 minutes after mixing in fresh mortars MA6 (a) and MA7 (b)
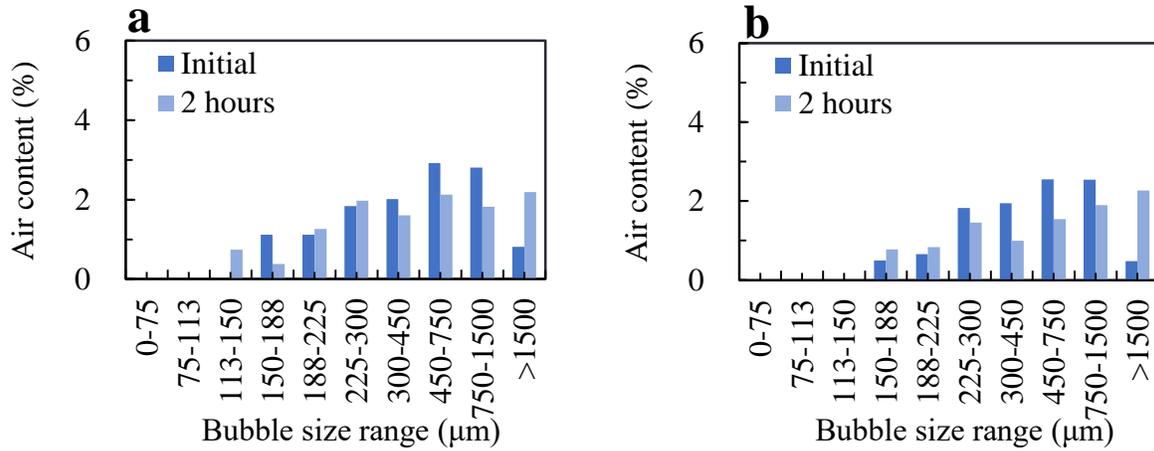
Fig. 5.11 Reduction in content of fine air bubbles (<1500μm) during 120 minutes after mixing in fresh mortars MA8 (a) and MA9 (b)
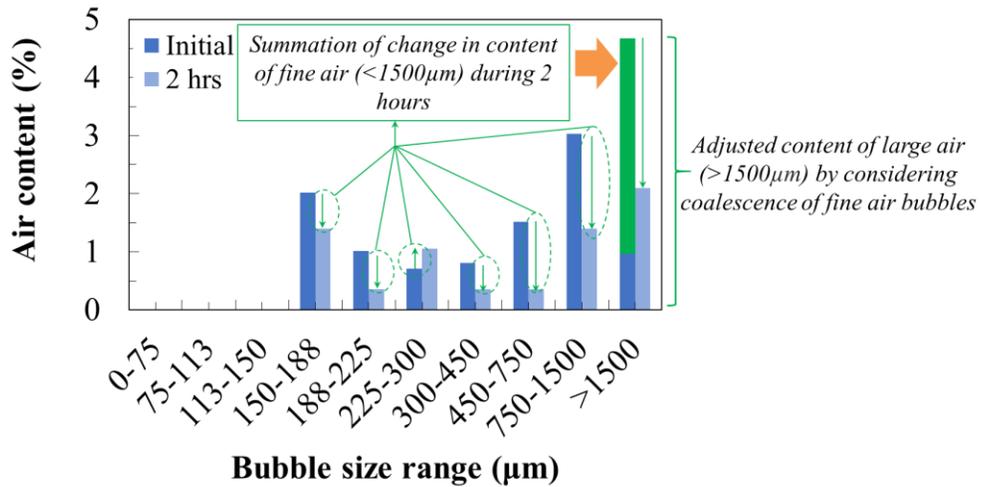
Fig. 5.12 Adjustment of content of large entrained air bubbles (>1500μm) assuming coalescence of small entrained air bubbles
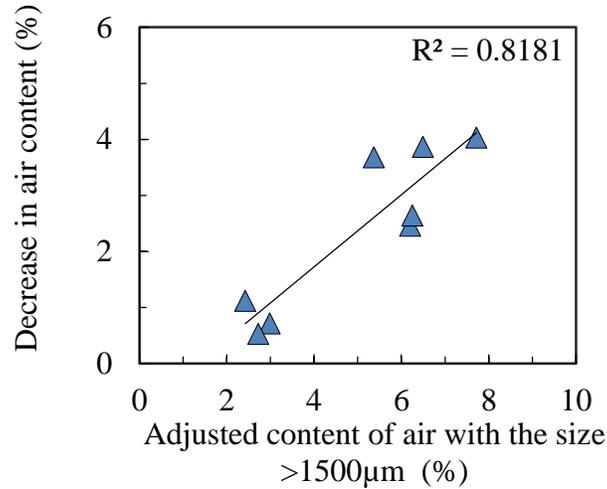
Fig. 5.13 Relation between decrease in air content and volume of large air bubbles (>1500μm) after the coalescence of fine entrained air bubbles (<1500μm) is taken into account

5.4 ENTRAINMENT OF FINE AIR BUBBLES FOR ENHANCED VOLUMETRIC STABILITY OF ENTRAINED AIR IN SCC MORTAR WITH FLY ASH

5.4.1 REDUCTION IN THE VOLUMETRIC STABILITY OF ENTRAINED AIR BUBBLES IN SCC MORTAR DUE TO USE OF FLY ASH

Mortar mixes MAF3, MAF4, MAF5, MAF8 and MAF9 were tested to clarify the effects of fly ash on the volumetric stability of entrained air bubbles in fresh SCC mortar. The volumetric stability of entrained air bubbles is quantified in terms of changes in the air content over a period of 120 minutes after mixing. The size distribution of entrained air bubbles in the mortar in its fresh state and 120 minutes after mixing was determined using AVA to help with evaluation of the results.

The results obtained show that, with either AEA1 or AEA2, the stability of entrained air bubbles tended to fall as the fly ash to mortar volumetric ratio (*fa/m*) increased (**Fig. 5.14**). This

may be due to the higher proportion of large entrained air bubbles, with a diameter over 1500μm, that results from a higher *fa/m* (**Fig. 5.15**). Since larger entrained air bubbles tend to escape through the mortar matrix easier than the smaller ones, as suggested by Rath et al (2017a), it is likely that the reduction in air volume is explained by the escape of these larger bubbles.

These results suggest that, with a particular AEA, a higher fly ash content leads to more loss of air as a result of a higher proportion of large entrained air bubbles (**Fig. 5.16**). However, the relationship between the change in volume of entrained air bubbles over 120 minutes and the proportion of bubbles over 1500μm in diameter is not unique. This may be attributable to the various mix proportions of fresh mortar, which may lead to different degrees of coalescence of fine bubbles into larger bubbles that can escape, as well as to the direct escape of some fine bubbles.
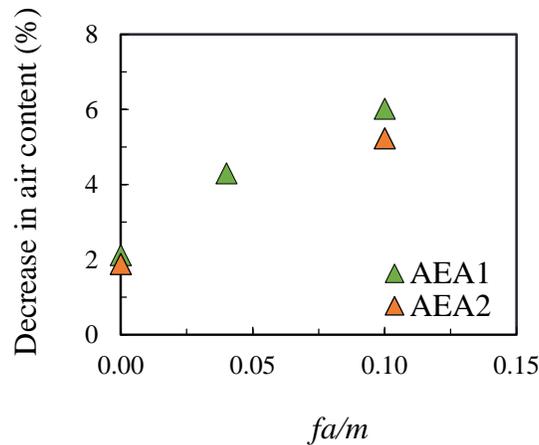
Fig. 5.14 Reduction in volumetric stability of entrained air bubbles with respect to higher fly ash to mortar volumetric ratio (*fa/m*) over 120 minutes with constant Rm
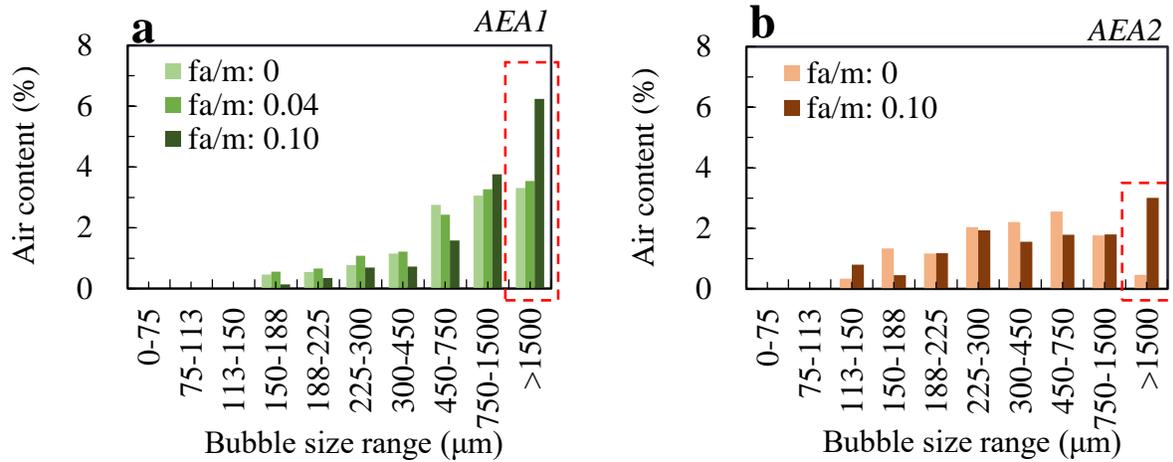
Fig. 5.15 Higher content of large entrained air bubbles (>1500μm) produced in mortar with fly ash as comparing with mortar without fly ash with AEA1 (a) and AEA2 (b) 5 minutes after mixing
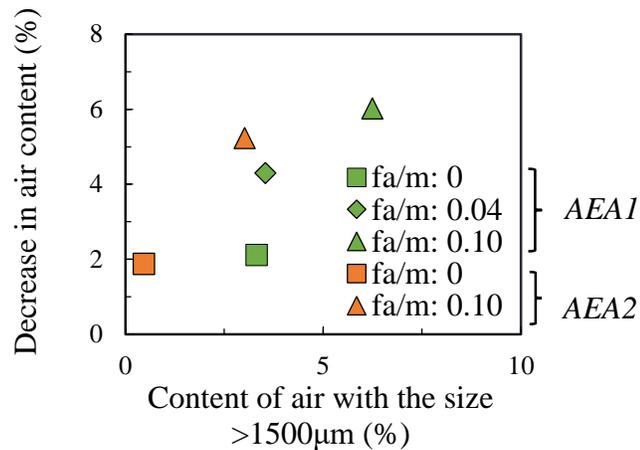
Fig. 5.16 Fly ash content and types of AEA dependent relationship between the stability in volume of entrained air bubbles and content of large air bubbles (>1500μm)

The results show also that, apparently, the volume of fine entrained air bubbles (<1500μm) decreases over the 120 minute period (**Figs. 5.17**, **5.18**, and **5.19**). This suggests that entrained air

97

bubbles with a diameter below 1500μm might coalesce to form larger bubbles (>1500μm). Another possibility is that that small entrained air bubbles might escape from the mortar. However, in order to investigate the loss of small entrained air bubbles, it was assumed that coalescence was the cause. This assumption was used to adjust the amount of large entrained air bubbles (>1500μm), as detailed in **Section 5.3.4 (Fig. 5.12)**. The results suggest a linear relationship between the reduction in volume of entrained air bubbles over 120 minutes and the adjusted volume of large entrained air bubbles (**Fig. 5.20**). This implies that the reduction in content of fine entrained air bubbles (<1500μm) may be mainly a result of coalescence. Also, a different degree of coalescence of fine entrained air bubbles in various mix proportions of fresh mortar is implied (**Fig. 5.20**). This may be attributed to variations in the shell characteristics of entrained air bubbles with different types of AEA (Ley et al 2009a and 2009b). Furthermore, when considering mortars with a particular AEA, since fly ash has a spherical shape, it has less effective area to restrain the movement of entrained air bubbles, as simply explained by **Fig. 5.21**. This might lead to the faster movement of entrained air bubbles in mortar with fly ash than in mortar without fly ash.
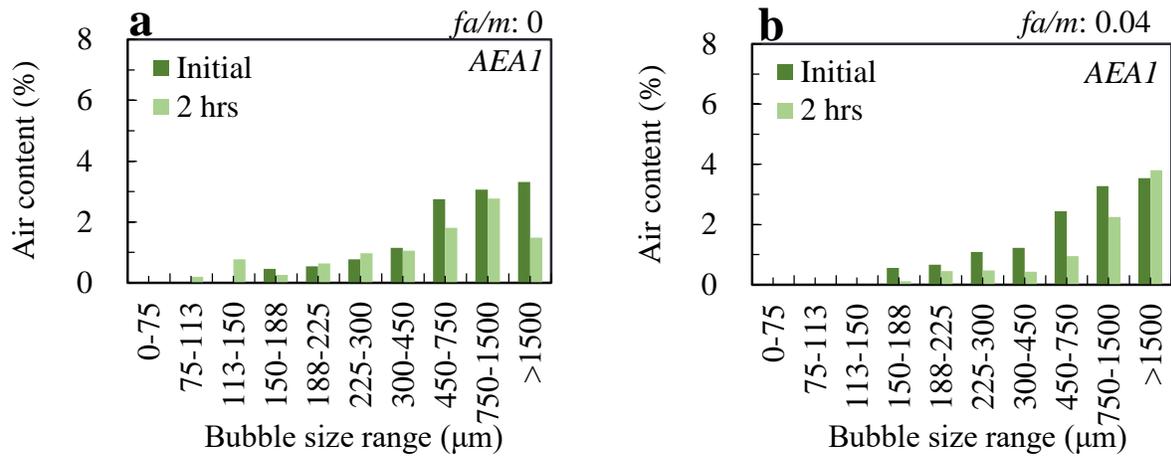
Fig. 5.17 Reduction of fine entrained air bubbles over 120 minutes in mortar with AEA1 without fly ash (a) and with fly ash at mortar ratio (*fa/m*) of 0.04 (b)
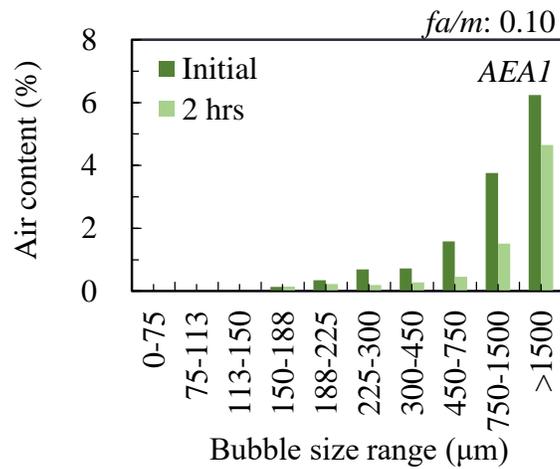
Fig. 5.18 Reduction in fine entrained air bubbles over 120 minutes in mortar with AEA1 and fly ash at a mortar ratio (*fa/m*) of 0.10
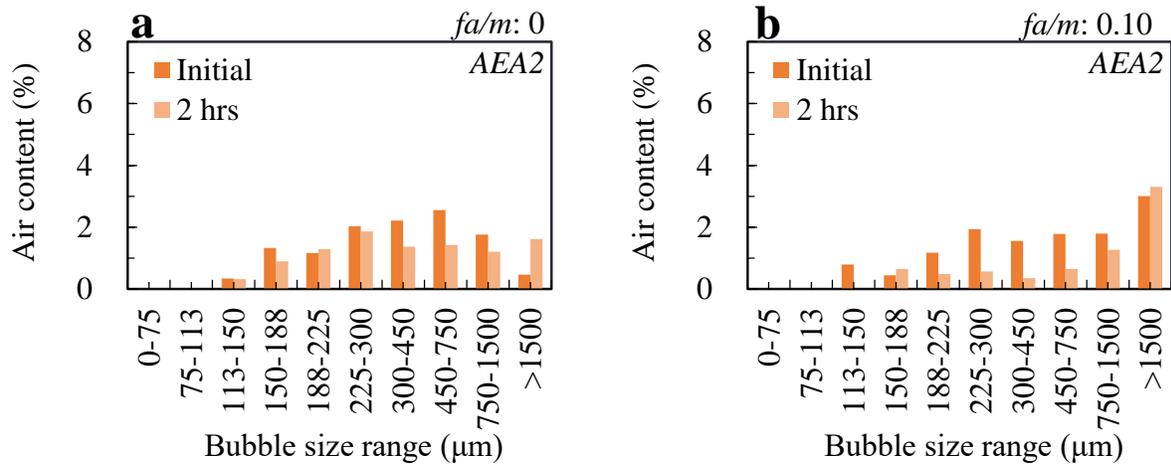
Fig. 5.19 Reduction in fine entrained air bubbles over 120 minutes in mortar with AEA2 without fly ash (a) and with fly ash at a mortar ratio (*fa/m*) of 0.10 (b)
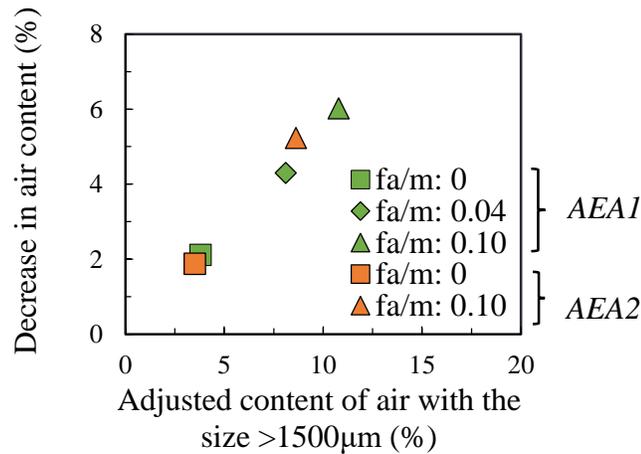
Fig. 5.20 Linear relationship between reduction in volumetric stability of entrained air bubbles with respect to increase in the content of large air bubbles (>1500μm) with different fly ash contents after considering coalescence of fine entrained air bubbles
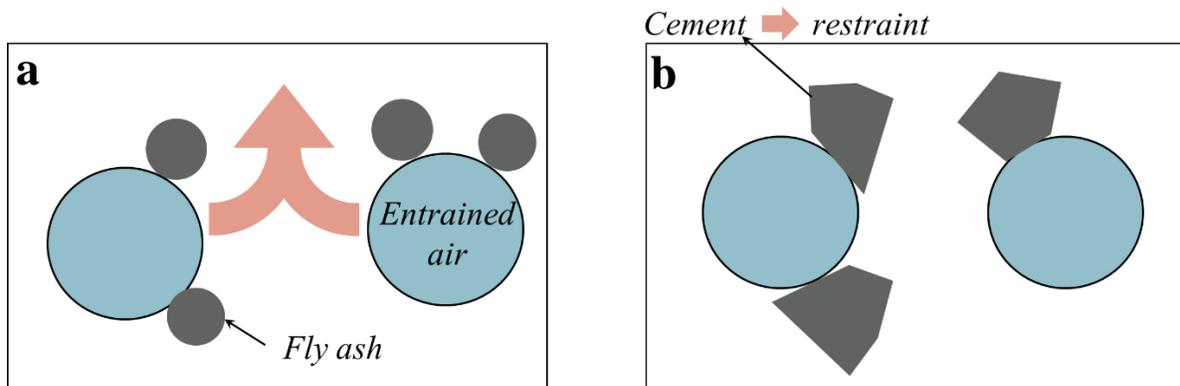
Fig. 5.21 Higher degree of coalescence of fine entrained air bubbles due to the spherical shape of fly ash (a) as compared to cement acting as restraint (b)

5.4.2 USE OF DEFOAMING AGENT TO ENHANCE ENTRAINMENT OF FINE AIR BUBBLES AND STABILITY OF ENTRAINED AIR IN SCC MORTAR WITH FLY ASH

Certain experiments were conducted on mortar mixes MAF3, MAF5, MAF6, MAF7, MAF8, MAF9, MAF10 and MAF11 to investigate the effect of a defoaming agent (DA) on the entrainment of fine air bubbles with the aim of improving the volumetric stability of entrained air.

The results, shown in **Figure 5.22**, suggest generally that less air is lost from mortar with fly ash when a higher dosage of DA is used. In fact, use of a DA is found to enhance the stability of entrained air bubbles in mortar with fly ash to the same level as in mortar without fly ash (**Fig. 5.22**). The stability of entrained air bubbles in mortar depends mainly on the proportion of large air bubbles with the size over 1500µm (Rath et al 2017a). This means that the improvement in stability brought by the DA may be attributed to the reduced volume of large entrained air bubbles (>1500µm) when DA is included in the mix (**Fig. 5.23**). Further, similarly to the results presented in **Section 5.4.1**, there is a linear relationship between the content of air bubbles with the size over 1500µm and the stability of entrained air when the coalescence of small bubbles is taken into

account, as illustrated in **Fig. 5.24**. This figure also implies an increased content of large entrained air bubbles in the mortar with *fa/m* = 0.10, AEA1 and DA = 0.10%, indicated as a slight increase in air content over 120 minutes. This might be caused by re-entrainment of air bubbles during testing and re-mixing.
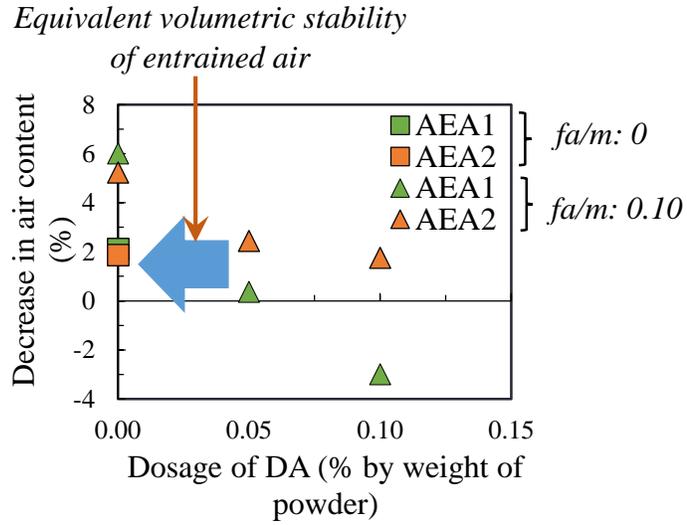
Fig. 5.22 Enhancement in volumetric stability of entrained air bubbles in fresh mortar with fly ash resulting from higher dosage of DA, making it comparable to that in fresh mortar without fly ash
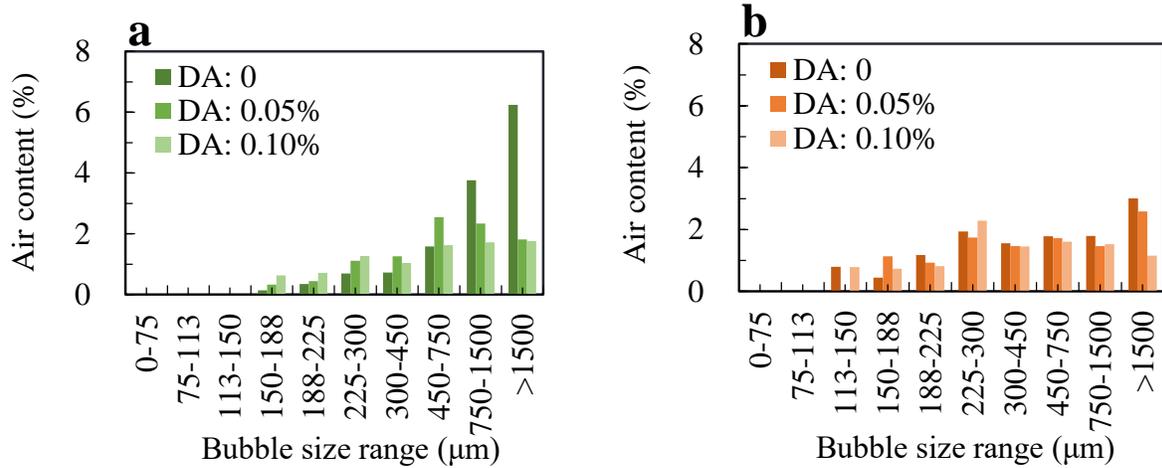
Fig. 5.23 Reduction in content of large air bubbles (>1500μm) with higher dosage of defoaming agent with *fa/m* = 0.10 for AEA1 (a) and AEA2 (b) 5 minutes after mixing
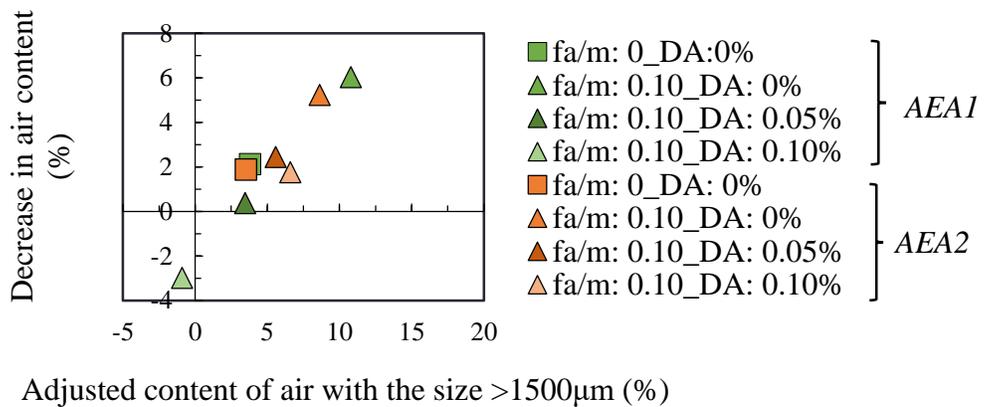
Fig. 5.24 Linear relation between volumetric stability of entrained air bubbles and content of large air bubbles (>1500μm) after coalescence of fine air bubbles (<1500μm) is taken into account

5.6 CONCLUDING REMARKS

In this chapter, a series of mortar mix proportions were tested to investigate the effects of air size distribution on the volumetric stability of entrained air. Various methods for enhancing the entrainment of fine air bubbles in the fresh mortar were tried. The reduction in entrained air stability resulting from the use of fly ash was also clarified. Further, the ability of a defoaming agent to enhance the entrainment of fine air bubbles and thereby improve entrained air stability in mortar with fly ash was studied. The following conclusions can be drawn from the evaluated results:

1) The volumetric stability of entrained air bubbles may fall with time mainly as a result of the escape of larger and more unstable air bubbles (>1500μm). Also, fine entrained air bubbles (<1500μm) are found to coalesce into larger air bubbles, which are then more likely to escape from the fresh mortar.

2) The reduction in fine entrained air bubbles (<1500μm) in the 120-minute period after mixing may primarily be attributable to their coalescence into larger bubbles.

3) A linear relationship is suggested between the decrease in air content and the volume of large air bubbles (>1500μm) after the coalescence of fine entrained air bubbles (<1500μm) is taken into account.

4) An increasing fly ash content results in a higher proportion of large entrained air bubbles (>1500μm). These bubbles can escape, which leads to a greater reduction in volume of entrained air bubbles over time as compared with mortar without fly ash.

5) The spherical shape of fly ash is the likely cause of reduced volumetric stability of the entrained air bubbles, as the coalescence and escape of fine entrained air bubbles (<1500μm) is promoted.

6). The stability of entrained air bubbles in fresh mortar of self-compacting concrete with fly ash,

is enhanced by the use of a defoaming agent, owing to reduced proportion of large air bubbles with a size of over 1500µm. With a suitable dosage of defoaming agent, the same level of stability as in mortar without fly ash can be achieved.

These conclusions are simply summarised in **Fig. 5.25** and **Fig. 5.26.**
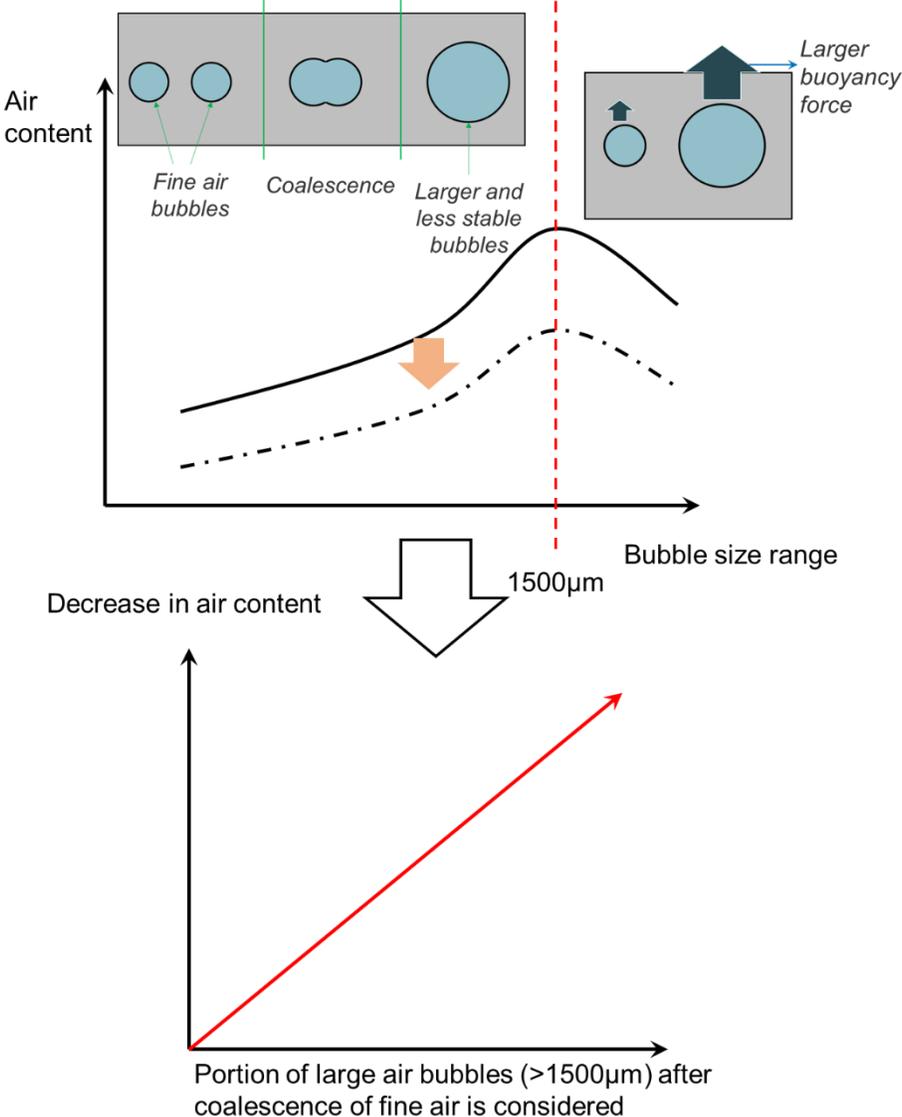
Fig. 5.25 Summary on the effects of air size distribution on volumetric stability of entrained air bubbles
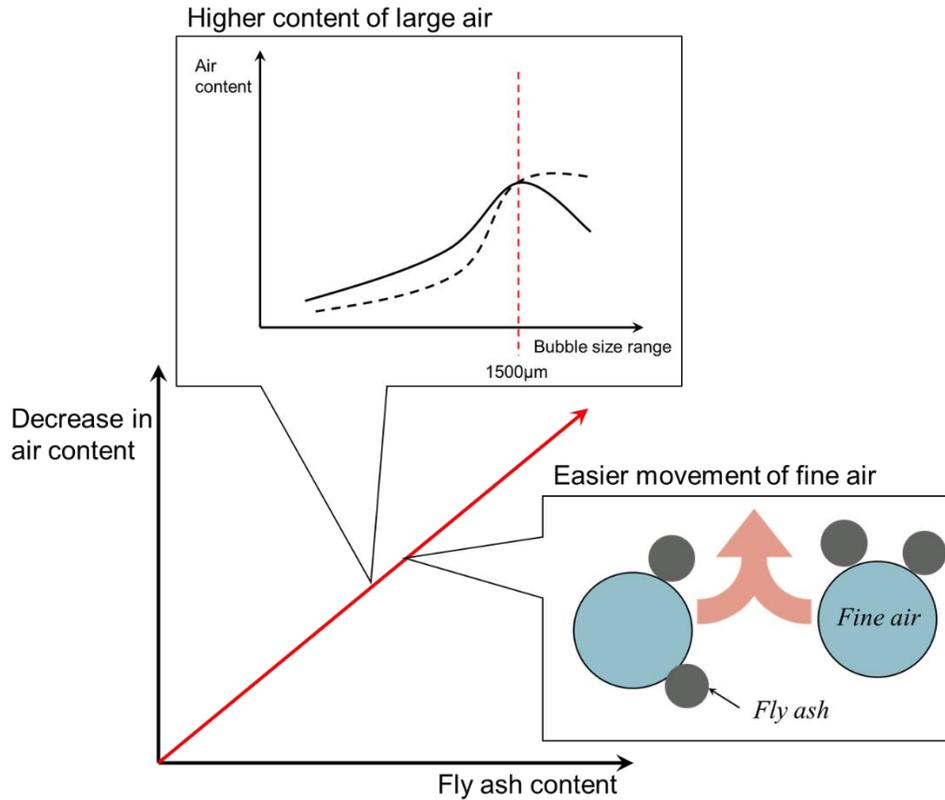
Fig. 5.26 Summary of effects of fly ash on air stability

REFERENCES

Barfield, M. and Ghafoori, N. (2012) Air-entrained self-consolidating concrete: A study of admixture sources. *Construction and Building Materials*. 26: 490-496.

Freeman, E., Gao, Y.M., Hurt, R. and Suuberg, E. (1997) Interactions of carbon-containing fly ash with commercial air-entraining admixtures for concrete. *Fuel*. 76(8): 761-765.

Gebler, S. and Klieger, P. (1983) Effects of fly ash on the air-void stability of concrete. *Proceedings of the CANMET/ACI First Conference on the Use of Fly Ash, Silica Fume, Slag and Other Mineral By-Products in Concrete*. 79: 103-120.

Hill, R.L., Sarkar, S.L., Rathbone, R.F. and Hower, J.C. (1997) An examination of fly ash carbon and its interactions with air entraining agent. *Cement and Concrete Research*. 27(2): 193-204.

Ley, M.T., Folliard, K.J. and Hover, K.C. (2009a) Observations of air-bubbles escaped from fresh cement paste. *Cement and Concrete Research*. 39 (5): 409-416.

Łaz´niewska-Piekarczyk, B. (2013) The influence of admixtures type on the air-voids of non-air-entrained and air-entrained high performance SCC. *Construction and Building Materials*. 41: 109-124.

Ley, M.T., Chancey, R., Juenger, M.C.G. and Folliard, K.J. (2009b) The physical and chemical characteristics of the shell of entrained air bubbles in cement paste. *Cement and Concrete Research*. 39 (5): 417-425.

Plante, P., Pigeon, M. and Foy, C. (1989) The influence of water-reducers on the production and stability of the air void system in concrete. *Cement and Concrete Research*. 19: 621-633.

Rath, S., Attachaiyawuth, A. and Ouchi, M. (2015) An effective and efficient mixing method for controlling initial air content for stability of entrained air in fresh mortar of self-compacting concrete. *Proceedings of the Japan Concrete Institute*. 37: 1447-1452.

Rath, S., Attachaiyawuth, A. and Ouchi, M. (2016) Fineness of air bubbles affected by mixing procedure in mortar in self-compacting concrete. *Proceedings of the Japan Concrete Institute*. 38: 1413-1418.

Rath, S., Puthipad, N., Attachaiyawuth, A. and Ouchi, M. (2017a) Critical size of entrained air for stability of air volume in mortar of self-compacting concrete in fresh state. *Journal of Advanced Concrete Technology*. 15: 29-37.

Rath, S., Ouchi, M., Puthipad, N. and Attachaiyawuth, A. (2017b) Improving the stability of entrained air in self-compacting concrete by optimizing the mix viscosity and air entraining agent dosage. *Construction and Building Materials*. 148: 531-537.

CHAPTER 6 CONCLUSIONS AND SUGGESTIONS FOR FURTHER RESEARCH

In this research, various mortar and concrete mix proportions were tested to investigate the effects of fly ash and entrained air bubbles on the self-compactability of fresh concrete. This is expected to reduce the proportion of cement required in SCC and, therefore, reduce the cost and environmental impact of SCC. The effects of air size distribution on the volumetric stability of entrained air in self-compacting concrete were also investigated. The following conclusions can be drawn, based on the analysis of the results from **Chapters 2 to 5**:

1) A satisfactory procedure was developed for correcting air size distributions obtained using air void analysis (AVA), which were shown to differ from those obtained by the gravimetric method.

2) Fine entrained air bubbles (<450μm) are found to reduce the friction between mortar and model coarse aggregate. This might attributable mainly to the relatively free motion in shear between mortar and model coarse aggregate with fine air bubbles acting as compressible bearings. On the other hand, larger air bubbles (>450μm) tend to increase the friction between mortar and model coarse aggregate. This is because they may be subjected to larger deformation under compression imposed by the aggregate. This leads to smaller spacing between aggregate particles acting as restraints to the mortar matrix.

3) The spherical shape of fly ash particles helps reduce friction between mortar and model coarse aggregate. This influence of fly ash may result from the ball-bearing effect and a reduction in contact area between solid particles.

4) Friction between mortar and model coarse aggregate tends to be more sensitive to air size distribution than that to the fly ash content. This may be attributed to relatively free motion in shear of between mortar and model coarse aggregate with fine entrained air bubbles acting as

compressible bearings, while fly ash may lead to adhesion between mortar and aggregate. Furthermore, large air bubbles may be subjected to large deformed. This results in shorter distance between aggregate acting as restraints to the mortar matrix, whereas fly ash is solid and does not deform.

5) The combined effects of fly ash and fine entrained air bubbles can further reduce friction between mortar and model coarse aggregate. However, the reduction in friction between model coarse aggregate and mortar with fly ash tends to be less sensitive to air size distribution, as compared to that in mortar without fly ash. Owing to the spherical shape of fly ash, lower friction are created between fly ash, as compared to cement, and other solid particles. This may result in lower effectiveness of fine entrained air bubbles, acting as compressible bearings for reducing friction between finer particles of fly ash, as compared to cement, with other solid particles. Besides, the increase in friction may be lower when the aggregate moves toward each other due to the large deformation of large air bubbles.

6) Reductions in friction between mortar and model coarse aggregate, obtained through the combined effects of fly ash and fine entrained air bubbles, enhance the self-compactability of the fresh concrete. This enhancement in self-compactability suggests that a combination of fly ash and fine air entrainment can be used to increase the aggregate content of self-compacting concrete.

7) The volumetric stability of entrained air bubbles depends mainly on the escape of large and unstable air bubbles (>1500μm) and the coalescence of fine entrained air bubbles (<1500μm) into larger ones, that can then escape. An observed fall in the proportion of fine entrained air bubbles (<1500μm) in fresh mortar over 120 minutes after mixing may be mainly attributable to the coalescence of fine air bubbles into larger ones.

8) Fly ash is found to reduce the stability of entrained air in the fresh mortar. This can be attributed

to the higher amount of large entrained air bubbles (>1500μm) being entrained. The spherical shape of fly ash particles can also result in greater air volume loss, as the coalescence and escape of fine entrained air bubbles (<1500μm) can readily occur.

9) The enhance entrainment of fine air bubbles can improve the volumetric stability of entrained air bubbles in both fresh mortar with and without fly ash.

This research has clarified the effects of fly ash and entrained air bubbles on the self-compactability of fresh concrete. However, although mechanisms for these effects have been suggested, there is no theoretical proof for them. To obtain evidence that will help prove the validity of these suggested mechanisms, the behavior of fly ash and entrained air bubbles in fresh concrete during flow have to be further observed and clarified.

APPENDIX A: RESULTS EVALUATION BY USING ADJUSTED AIR SIZE DISTRIBUTIONS TOWARDS LTM
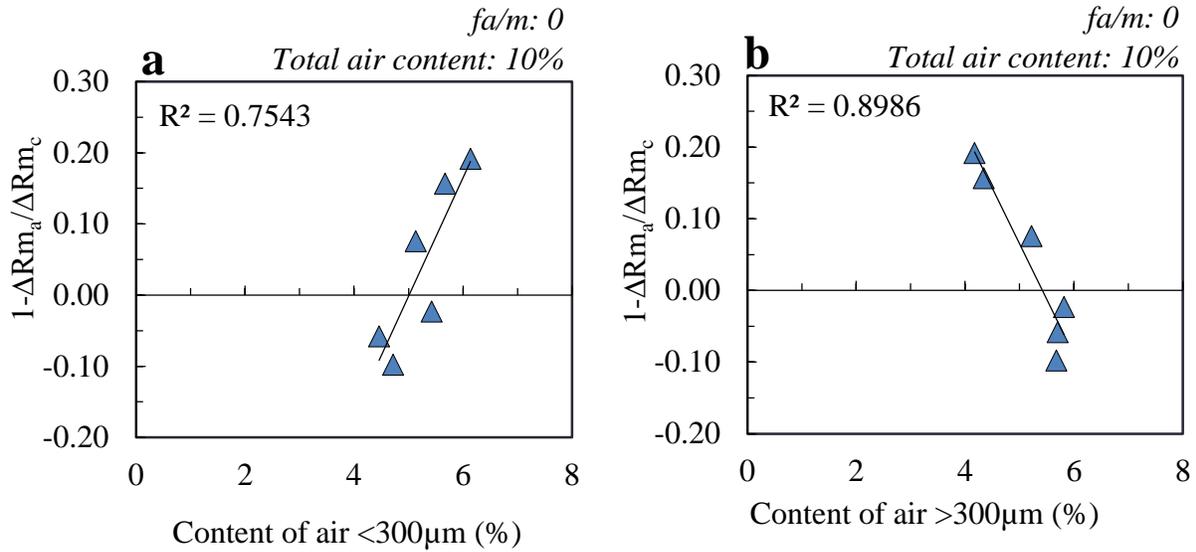
Fig. A1 Positive (a) and negative (b) of fine and large air bubbles, respectively, on the increase in 1-$\Delta Rm_a/\Delta Rm_c$
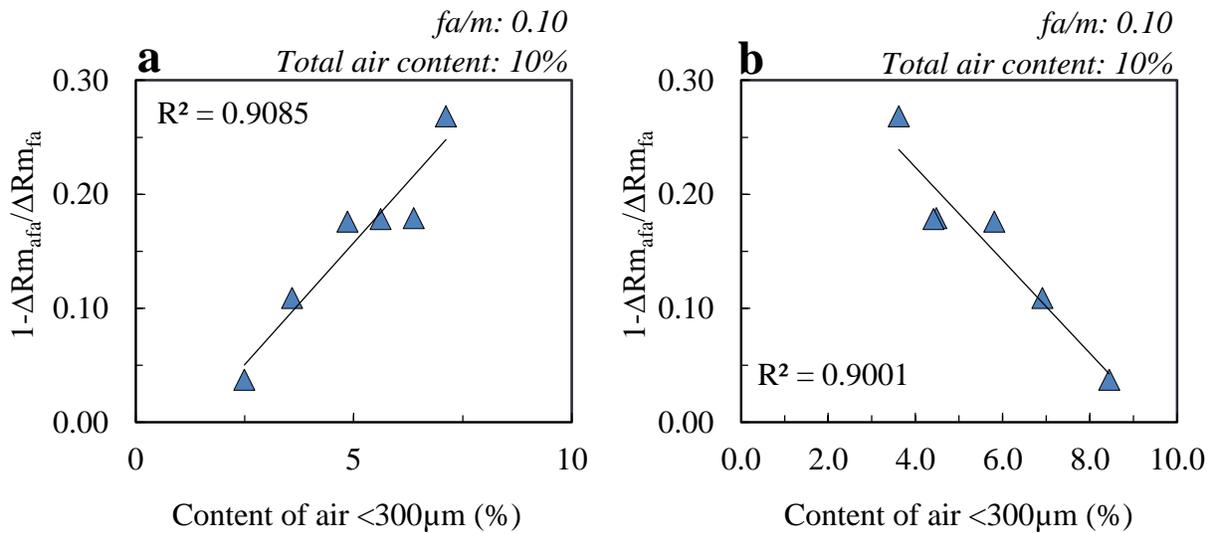
Fig. A2 Positive (a) and negative (b) of fine and large air bubbles, respectively, on the increase in 1-$\Delta Rm_{afa}/\Delta Rm_{fa}$
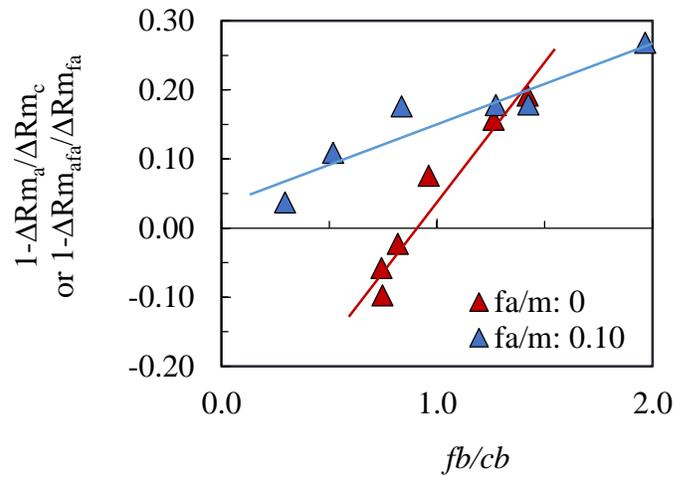
Fig. A3 Comparison between effects of entrained air bubbles on the reduction in friction between model coarse aggregate and mortar with and without fly ash, in terms of 1-$\Delta Rm_{afa}/\Delta Rm_{fa}$ and 1-$\Delta Rm_a/\Delta Rm_c$, respectively
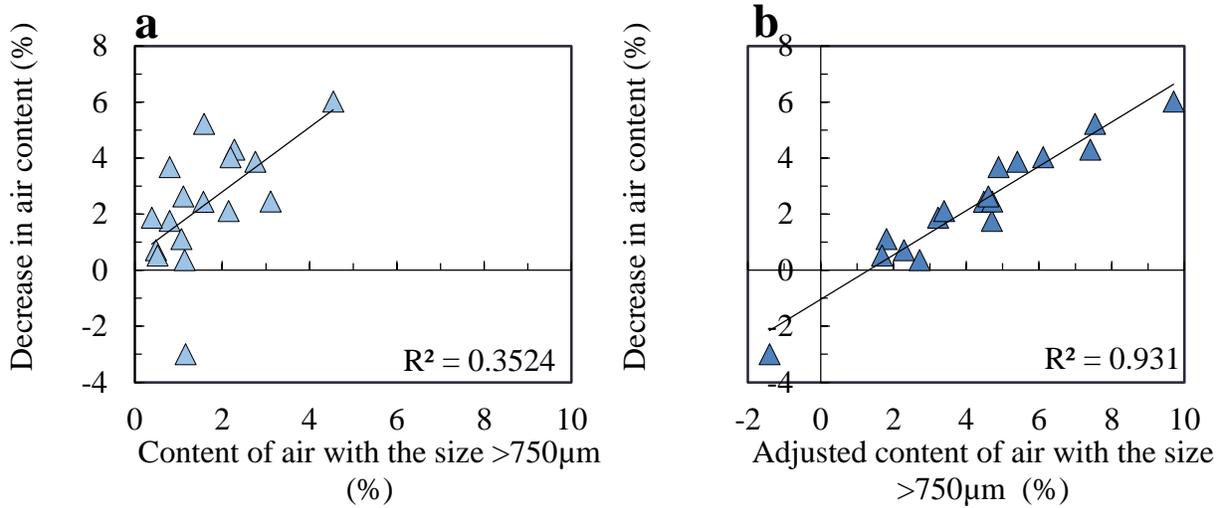
Fig. A4 Relationship between decrease in air content and volume of large air bubbles (>750μm) before (a) and after (b) the coalescence of fine entrained air bubbles (<750μm) is taken into account
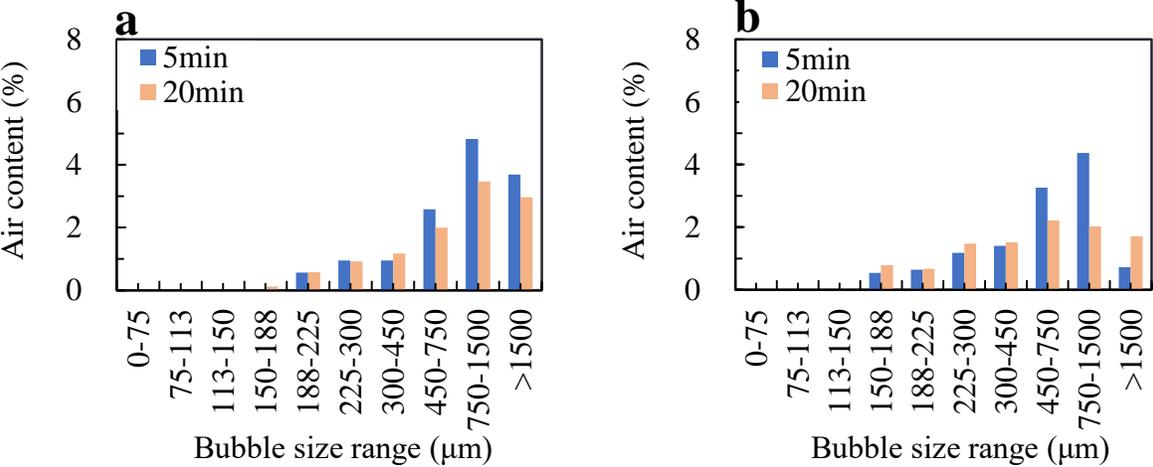
Fig. B1 Reduction in content of large air bubbles (>450μm) during 5min to 20min, in mortar mix proportion MA2 (a) and MA3 (b)
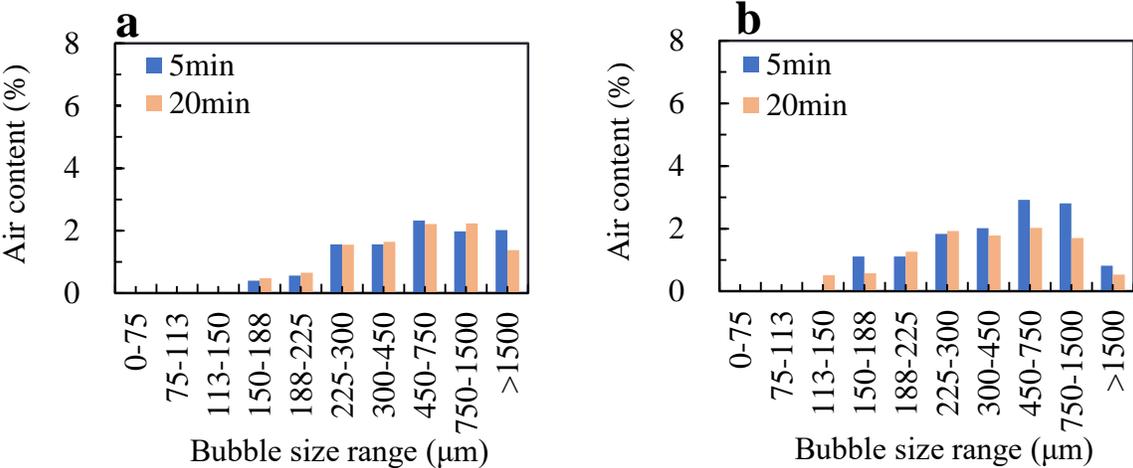
Fig. B2 Reduction in content of large air bubbles (>450μm) during 5min to 20min, in mortar mix proportion MA4 (a) and MA5 (b)
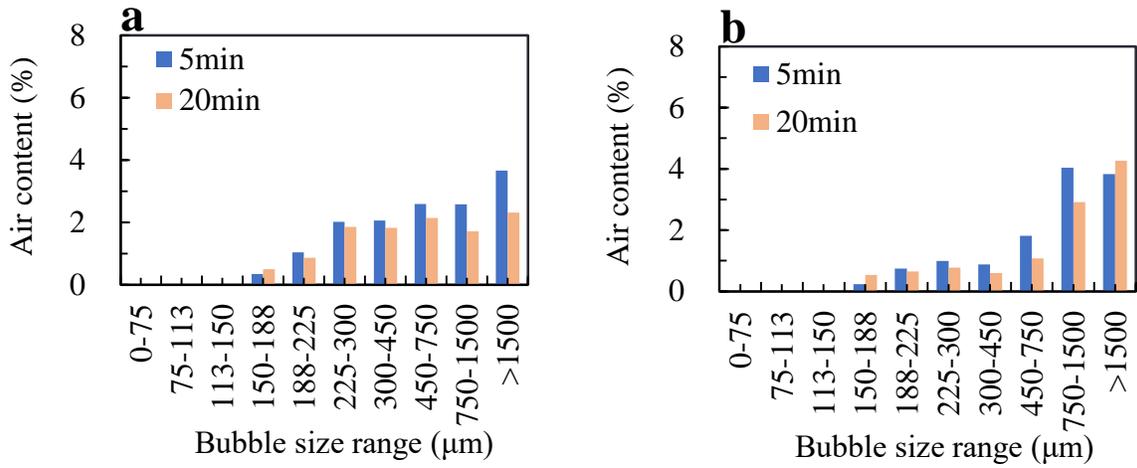
Fig. B3 Reduction in content of large air bubbles (>450μm) during 5min to 20min, in mortar mix proportion MA6 (a) and MA7 (b)
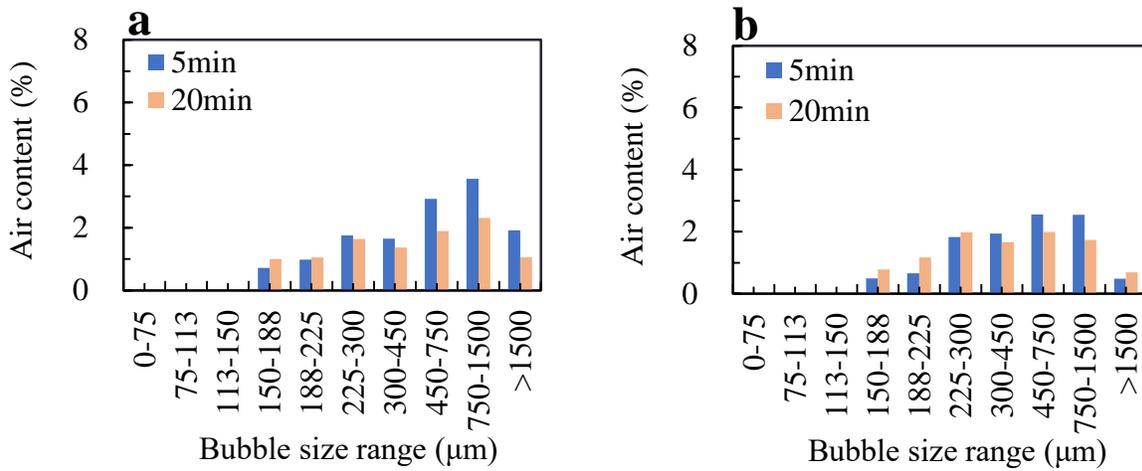
Fig. B4 Reduction in content of large air bubbles (>450μm) during 5min to 20min, in mortar mix proportion MA8 (a) and MA9 (b)